THE STRENGTH OF BONDED WOOD STRAND COMPOSITES

By

Edward Donald Higgins

B.Sc., The University of British Columbia, 1966
M.S., State University of New York 1970

A THESIS SUBMITTED IN PARTIAL FULFILLMENT OF

THE REQUIREMENTS FOR THE DEGREE OF

DOCTOR OF PHILOSOPHY

in

THE FACULTY OF GRADUATE STUDIES

Forestry

Department of Harvesting and Wood Science

We accept this thesis as conforming

to the required standard

THE UNIVERSITY OF BRITISH COLUMBIA

August 1990

In presenting this thesis in partial fulfilment of the requirements for an advanced degree at the University of British Columbia, I agree that the Library shall make it freely available for reference and study. I further agree that permission for extensive copying of this thesis for scholarly purposes may be granted by the head of my department or by his or her representatives. It is understood that copying or publication of this thesis for financial gain shall not be allowed without my written permission.

Department of Forestry

The University of British Columbia
Vancouver, Canada

Date Aug 8/90

ABSTRACT

A method for modelling the strength of bonded wood strands which are oriented principally in one direction is proposed. The hypothesis tested was that strand grain orientation data, fitted to a von Mises probability distribution, could be used in an analysis for estimating the potential tensile strength of an ideally bonded composite. The strand strength, resolved at any loading angle with respect to the principal composite strand orientation axis, was multiplied by the distribution probability at that angle. When integrated over all angles, this product yielded the mathematical expectation of strength for the composite. The model predicted composite strength at off-orientation axis angles and represented the material in two dimensions in an orthotropic fashion. A feature of this research is the use of a parametrically quantified strand orientation level in an algorithm developed to estimate composite strength.

A practical number of strand angle readings (100) were taken to characterize each composite. These angle readings defined orientation in terms of a parameter which described composites ranging from random to highly oriented. The model input also required microtensile strength means from samples of strands tested in the longitudinal and radial or tangential directions.

Comparisons between the model and actual specific strengths were made at five equally spaced composite principal axis load angles from 0 to 90 degrees. Both tensile and flexural tests were performed to evaluate the model. The evaluations were designated in terms of resin content, distribution, and droplet

size. These variables were studied using colorimetry and computerized image analysis. Composite density profiles through the specimens' thickness were obtained from direct reading x-ray densitometry. Composites made of juvenile trembling aspen, red alder, red cedar, mature lodgepole pine and yellow birch were studied.

Assumptions concerning wood shear strength and strand length/thickness ratio were discussed in the interpretation of an overlapping strand stress-transfer model. This led to the definition of failure criteria based on stress transfer. A trial of orientation modelling in elasticity estimation was made and a random function model of composite elasticity based on laminated plate theory is outlined in a supplementary proposal for further research.

The simplified algorithm for the strength of aligned wood strand composites provides design targets for reconstituted high strength strand lumber and panel products of the future.

TABLE OF CONTENTS

LIST OF TABLES

LIST OF FIGURES

ACKNOWLEDGEMENT

The writer would like to acknowledge the helpful and innovative suggestions offered by the numerous contributors to this research. Physical offerings of materials and equipment as well as expertise were made by the following organizations and individuals. Special thanks are extended to my family and to my thesis committee.

ORGANIZATIONS

Canadian Forest Service
Weldwood of Canada
Alberta Research Council
McMillan Bloedel Research
Borden Chemical Ltd.
Reichhold Ltd.
Forintek Canada
C.A.E. Machinery Ltd.
Paperboard Corp.
Econotech Services Ltd.
UBC Research Forest
UBC Metallurgy Dept.
Pulp and Paper Res. Inst. of Canada
Simon Fraser Univ. Statistics Dept.

INDIVIDUALS

J. Arden
G. Stout
M. Stout
B. Stroud
P. Crammond
C. Mierau
W. Ainsley
B. Scott
L. Josza
N. Sargent
K. Bartczak
E.W. Higgins and family
L.A. Fry
G. Eaton
J. Cook
D. Nguyen
G. Bohnenkamp
L. Bach
D. Seabrook
R. Knudson
H. Ehrenfeller
R. Kerekes
M. Stephens

COMMITTEE MEMBERS

L. Paszner
P. Steiner
D. Barrett
R. Foschi
D. Tait
J. Nadeau
E. Teghtsoonian

1. INTRODUCTION

Oriented strand board is one of the fastest growing segments of the forest products industry. Approximately fifty North American mills now produce waferboard or oriented board and it is projected that by 1993 oriented strand board will reach over 50 percent of total structural panel consumption. In Canada, this means that 63 million square meters per year, 9.5 mm basis, will be produced (18).

An improvement in composite strength parallel to the major panel axis is obtained if the strands are aligned with their longitudinal grain direction parallel to the panel axis. Alignment is normally done in three multiple layers of strands, with the center layer cross-plied. The term, oriented strand board (OSB) is used to describe a composite made of oriented grain elements, which have length-to-width ratios greater than 3. All new mills have the capability to orient the inner and outer layers of strands.

Fundamental understanding is needed about the orientation effect on the strength of the single unidirectional layers forming typical three-layer OSB. This is also critical to the development of reconstituted strand lumber. A theoretical model which predicts the effect of strand alignment changes on strength would be a valuable research and engineering tool. The creation and evaluation of such a model was the aim of this research. Engineering process consultants and standards committees have had few theoretical targets for the design of OSB layers or high strength reconstituted strand lumber. This model is intended to provide an awareness of an idealized, theoretical maximum strength of these products. Then product designers can

set strength targets, compare test results, and alter variables more knowledgeably. It is also intended to evaluate the potential capability of these products where high strength is required or where they are placed as natural wood substitutes.

In wood composite modelling, the variability of wood has historically favoured simple models that input only the major factors influencing a result. For example, in plywood flexural strength estimation, the cross band veneers are often assigned zero modulus in transformed moment of inertia elastic analyses, leaving only the contributions of parallel-grain laminae to be considered.

1.1 Objectives

While recognizing the variability of wood, the objective is to prepare a strength algorithm for describing single direction wood strand composites. The model is based on an assessment of the degree of orientation of the strands and their strengths in two planar directions. The hypothesis is that such a model is accurate in assessing the strength of existing and proposed strand composite products. The test of this hypothesis is made with a variety of species, adhesive levels, and orientation levels in the test composites.

The objective requires:

- Creation of a network analysis method of modelling oriented strand composite tensile and flexural strength,
- determination of the conditions of stress transfer between strands, under which the model is valid. This includes resin level and strand dimensions,

- qualification of another important strength determinant, adhesive deposition,
- trial application of network analysis to modulus of elasticity.

The objectives were to further ascertain:

- the ability of the model to predict the surface specific MOR at any angle of composite loading with respect to the principal axis of orientation,
- the effect of resin level and species on flexural strength,
- comparison of the specific tensile strength of the composites to the specific tensile strength of the strands themselves.

In short, the research focuses on modelling unidirectional wood composites that are similar to contemporary OSB layers or reconstituted strand lumber. The result is an analytical tool for guiding forethought in the setting of product strength expectations. It provides fundamental knowledge on the manipulation of orientation, strand configuration, and resin level in achieving optimal strength to weight ratio.

2. REVIEW OF THE LITERATURE

2.1 Orientation

There are several experimental studies in the literature concerned with the effect of strand orientation on strength. For example, Post (71), Gatchell et al. (23) and Geimer (24, 25, 26) deal with strand orientation effects on board strength. One of the difficulties in using and comparing these studies is the non-uniformity and differing interactions of variables other than orientation. Only a few of these studies have used a probability distribution function (pdf) to describe the orientation. The merit of the pdf is that it can be exploited to give a mathematical expectation of strength. To do this, the pdf is used as a factor which is integrated with an expression for the off-axis strength of solid wood. Until the present time, this approach has been taken only with the randomly oriented board where the pdf is uniform (72).

The investigations of Harris and Johnson (33) provide background for the present research. They suggest a probability distribution having a concentration parameter, k, which describes the dispersion of strand grain angles about the most probable orientation angle. Harris and Johnson's work refers to biometric applications of circular pdfs. described by Batschelet (11), and Mardia (58). The work of Harris (34) emphasized the methodology of orientation measurement. He then modelled the tensile elasticity of a strand composite by considering variously oriented strand units in the form of sequential strips of segments.

Less detailed methods of describing orientation have been used. Geimer (25) defined the percent of wafers having angles falling within ± 20 degrees of the most probable direction of alignment, and later devised a weighted average of angles from an orientation histogram. The absolute mean angle, ϕ, was calculated by Geimer (26) as the average of the measured angles ($-90° < \phi < +90°$), without regard to sign. The percent alignment was then defined as:

$$\text{percent alignment} = \frac{| 45° - \phi |}{45°} \qquad [1]$$

Lau (48) fitted a normal distribution based on the above absolute mean angle and its standard deviation. Numerical integration with an elasticity factor led to a regression relationship between density and modulus of elasticity.

Paper physics offers network analyses based on scanning sheets at angular intervals over zero to 360 degrees with respect to the machine direction. The number of fibers crossing the scan lines are counted. Corte and Kallmes (15) showed the scan data to define a Fourier series which they related to a pdf. This fiber crossing method was not suited to OSB where the strand width requires excessively large sample boards to achieve the necessary data collection. Experimental determination of fiber orientation in paper by various methods ranges from use of colored fibers, Danielson et al. (16) to submillimeter laser, by Boulay et al. (13). Change in dielectric properties with grain orientation have been exploited in lumber grading sensors by

Samson (75). The attenuation of microwaves has been studied by Musial (61) to determine the degree of strand orientation. Musial's instrumental methods were used to characterize another parametric pdf describing strand orientation.

Reviews of the Fourier series distribution, the von Mises distribution, and their interrelation, as used to describe orientation in paper sheets, were published by Perkins and Mark et al. (68). Advanced instrumental methods of quantifying fiber orientation in paper were presented in a critical evaluation by Niskanen and Sadowski (62). A review of methods used in high performance (glass, carbon) fiber composites was included in a study of continuous fiber reinforcement (98). The existing strength theories based on network analysis, both in paper and glass filament composites usually assign zero transverse strength to the fibers. In wood strand composites, the present thesis offers research in which the transverse strength of the wood strand is included.

2.2 Macroscopic Strength Theories for Wood

Macroscopic strength theories for wood are important because solid wood strands are elements of the model and their specific strengths are model inputs. Wood strength models were discussed by Perkins (69), Kaminski et al. (41), Bodig and Jayne (12), and Easterling et al. (19). A distortional energy theory was offered by Norris (65) for combined stress (off grain axis) prediction of wood strength. A similar, more general expression for glass fiber composites, was developed by Tsai-Hill (91). The Hankinson

wood strength formula and the more general Osgood formula were compared by Kim (46). Hankinson's formula provides a single expression for strength that approximates other more refined analyses, for example the maximum stress strength theory, (12). It was chosen because it develops off-axis strength estimates of strand strength from two basic inputs, and has proven satisfactory in previous strand composite studies (72). The Hankinson formula was developed experimentally in 1921 and is a practical description of the strength of wood as a function of grain angle. It can be used to describe not only strength but also proportional limit stresses in both tension and compression.

An effect of lamination of planar components can be to disperse flaws in the laminate, resulting in a narrower distribution of specimen strengths, and an increase in average strength. This effect was demonstrated in a statistical theory of laminated glass sheets, by Scop et al. (78). Occurrence of a critical flaw is related to specimen size and is known to affect strength tests as shown by Barrett (10) and Price (72). In recognition of these effects, any strands of differing species which are compared should be of the same nominal size distribution.

Relative bonded area as a strength factor was studied by Suchsland (88), also by Lyon (55) in a three-part comprehensive model written for mainframe computers. Lyon's strength model employs a simulated orientation distribution and does a strand-by-strand analysis and search for local layer failure in the flexural strength estimation.

Laminated plate theory (LPT) was used in elastic analysis of plywood by Rautakorpi (74) and has merit as an element of a proposed Monte Carlo simulation of elasticity. This is discussed in Section 5.4.

2.3 Micro-Mechanical Strength Theories

An approximately 25 year span of literature exists on fracture-mechanical theories of wood strength. Some examples are presented by Porter (68), Schniewind et al. (76), Nadeau et al. (62) and Pellicane et al. (67). A collection was compiled by Forintek (1). Fracture in phenolic glue lines was studied by Ebewele et al. (20). Internal bond was investigated by Lei et al. (54) successfully using fracture mechanics. A choice was made, based on this literature, not to use a crack growth theory as an element of the orientation model for strength. The reason is that fracture toughness data, especially at varying grain orientation load angles are lacking in the broad variety of species under study.

2.4 Composite Density

Turner (92) and Klauditz (47) concluded that flexural strength was strongly influenced by the mean density of the board. They did not control the surface densification. The flexural strength, within the mean density range of 0.5 to 0.7 g/cm^3, formed a linear relation with density. No specification was given for the density gradient. Flexural modulus of rupture (MOR) is dependent on the through-thickness

density gradient and surface density produced by pressing and consolidation of strands. Such gradients have been measured using x-rays, by Steiner et al. (83, 84), and Winistorfer et al. (96), and modelled by Harless et al. (32). Josza et al. (40) developed x-ray densitometry methods useful for small wood specimens. The factors affecting the gradient in three-layer panel boards were reported by Geimer et al. (27). Composite surfaces are not necessarily densified to the same extent with all species under equal pressing conditions. Moisture, temperature and pressing rate are major factors affecting the gradient. If uncontrolled, these can confound the density gradient with the species or other independent variables when MOR is the dependent variable. Also, during the process of strand furnish layup, it is possible that fines and adhesive fall through to the caul plate side of the press charge. This can result in one surface being denser or stronger than the other (83, 84). The gradient can be partly eliminated by slow press closure, and partial surface removal by planing. The effect of gradient on the interpretation of the flexure formula is critical in the use of bending tests to estimate surface stress.

2.5 Adhesive Level, Distribution and Droplet Dispersion

The phenolic adhesive resins used in this research, both liquid and powder, are presently offered to the OSB industry. A review of literature which describes chemical and physical features of resins and their behavior with wood includes, Hse (37), Wilson (94), Gollob (30), Stephans et al. (85) and Go (28, 29). The influence of resin level on tensile strength of random

waferboard was described by Laufenberg (50). In aspen boards made with randomly oriented short strands, the MOR rose in a diminishing curvilinear relation to resin level. These boards achieved only small strength gains after 7 to 12 percent resin solids addition. This trend was also observed by Price (72) with sweetgum OSB and by Adams (4) with aspen, balsam fir, and northern white cedar unidirectional OSB laminated as power line crossarms. In 1961 Post (71) found very modest flexural MOR elevation caused by resin increase, when using randomly oriented strands of length/thickness ratios of 10 to 40.

The literature suggests two resin levels at which the orientation model should be evaluated. The first is the approximate level at which industry currently applies it's adhesive. This is in the range of 2 to 3 percent solids by weight (29). The second is near the upper limit of industrial application (4-8 percent), where the effects of higher wood failure result in higher strength in the parallel to grain direction. According to Laufenberg (50), this resin level can yield nearly zero disbonding of strands when used with length/ thickness ratios of 100 or more. The critical importance of wafer thickness on adhesive requirement in terms of surface spread of resin was studied by Post (71) and Gunn (31). The resin level interacts with the other strength factors to the extent that many studies are very limited in scope. The most pertinent are mentioned above, but many others are reviewed by Kelly (44).

The resin distribution is a critical factor in strength determination. The best review of this subject is given by

Maloney et al. (57). The definitive research on the effects of application of liquid resin was done by Meinecke and Klauditz in 1962 (60). The dispersion of droplets (specifically the droplet size distribution) on a strand surface and the distribution of resin among strands were studied as separate effects in Meinecke's and Klauditz's work. They concluded that strand to strand distribution of the resin is often more important than the droplet dispersion. The frequent association of better distribution with better droplet dispersion has sometimes caused the two factors to be confused by designers of resin blenders.

Kasper and Chow (42) recognized the importance of resin distribution and devised a simple criterion for defining good distribution. They showed that the median/mean ratio from the frequency histogram of resin pickup on a sample of wafers should be unity. Their x-ray fluorescence detection of bromine tagged resin was used for simultaneous resin assays of both, combined, sides of the wafer. In contrast to this, the theoretical potential of resolving individual sides is also useful. The resin status of both sides can be used in calculating the probability of a diminished resin interface zone in a model stack of strands.

2.6 Species

The manufacturer's choice of species is mainly governed by economic factors such as availability, size, concentration of trees, and transportation costs (36), (38), (77). Canadian hardwoods have been examined extensively from a general utilization viewpoint in symposia, by McIntosh and Carroll (59).

Populus tremuloides, the main Canadian wood for OSB, is well documented with regard to resource forestry and wood technology. A review of aspen utilization is offered by Pronin and Vaughan (73). Mixtures of white birch, balsam fir, red alder, balsam poplar, black spruce and aspen were evaluated in waferboard by Alexopoulos and Shields (6). Adams (4) provides some reference data for comparison in a study of OSB made from northern white cedar, balsam fir, and aspen. Lodgepole pine made a servicable OSB according to data presented by Maloney (56).

Low resin level when applied to softer, low density species, made stronger board than high density species at equivalent final board densities according to Stegmann and Durst (82), and Alexopoulos and Shields (6). This is because the softer woods consolidate better. Such strands easily articulate in the formation of more ideal bond interfaces. The variation of density in mature woods of northern species was reported by Singh (80).

Juvenile woods will have increased importance in strand composites in the future. In juvenile aspen, the age, density, genetic and growth factors were investigated by Dawson et al. (17) and Einsphar et. al (21). Juvenile black alder was found by Chow (14) to make superior OSB. In high resin composites, where bonding is maximized, the intrinsic weakness of juvenile wood could affect composite strength. These studies provide background for a wide choice of woods to test the applicability of the strength model.

2.7 Other Process Variables

There are numerous other variables that affect OSB strength. For example, moisture content, compaction ratio, and strand cutting angle must be considered. These and other variables were held constant, carefully specified, or randomized in the present research. The U.S. Forest Products Laboratory reviewed a variety of strength determinants in a report by Kelly (44), containing 163 references. A similar review was provided by the U.S.D.A. in 1981 (2). The multitude of factors and their interactions emphasize the need to organize the fundamental ones in models, for expression of their effect on composite properties.

3. METHODS AND MATERIALS

3.1 Directional Data Processing

The method of quantifying orientation by using the von Mises probability distribution function was developed for OSB by Harris (34). This measures strand orientation directly on the board surface as shown in Figure 1. The angles that strands make with the axis direction form a data set falling between 0 and 180 degrees, (alternatively -90 to 90 degrees). Data in the 0 to 180 degree interval is called axial data.

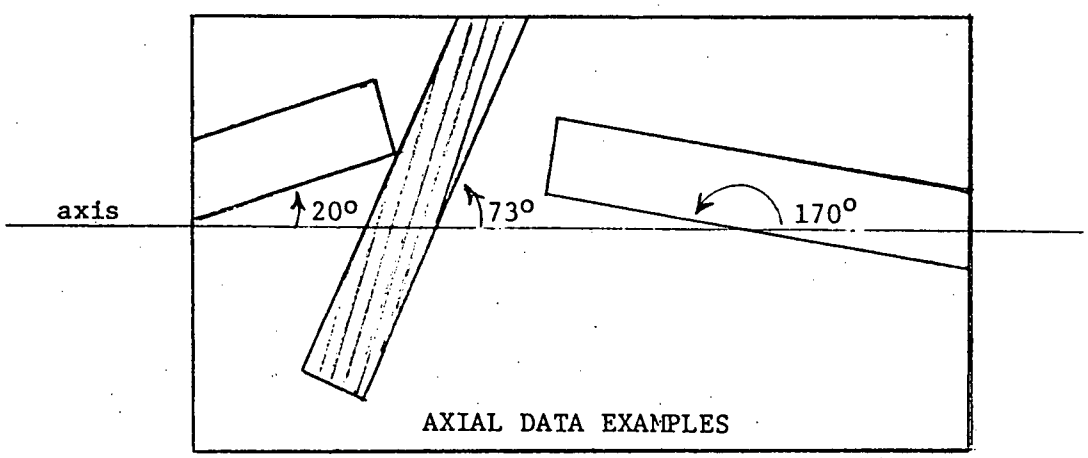

Figure 1. Angle measurement, θ

The angles themselves cannot be meaningfully averaged arithmetically but the set of associated complex points can be averaged. The set of points can be considered vectors with coordinates on the unit circle given by Fig. 2.

Harris and Johnson (33) stated, "the entire set of data can be characterized by an orientation vector, r, whose angular position relative to a preselected reference is given by a most probable angle, m, and whose length is related to the central

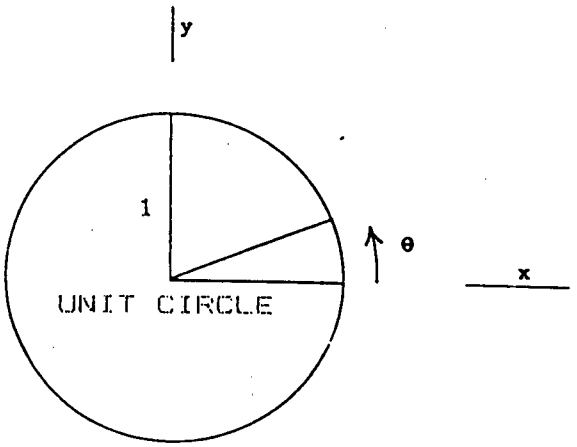

Figure 2. Components of the orientation vector.

tendency of the set." For large values of n, this is expressed mathematically as:

$$\text{mean } x, \quad x = \frac{1}{n} \sum_{i=1}^{n} \cos \theta_i = \overline{\cos\theta} \qquad [2]$$

$$\text{mean } y, \quad y = \frac{1}{n} \sum_{i=1}^{n} \sin \theta_i = \overline{\sin\theta} \qquad [3]$$

$$\text{orientation vector, (length) } r = (x^2 + y^2)^{1/2} \qquad [4]$$

$$\text{axis direction, (most probable angle) } m = \tan^{-1}\left[\frac{\overline{\sin\theta}}{\overline{\cos\theta}}\right] \qquad [5]$$

Angular data for these equations were collected as follows. A clear plastic grid was prepared by making horizontal slots on a X-Y coordinate plane of plexiglas. This was overlaid on the surface of the test specimens with the slots parallel to the specimen reference edge. Random points chosen as X-Y pairs defined angle measuring locations on the grid. These were pen-

marked through the slots, by means of dots and reference lines parallel to the slots.

Grain angles of marked strands were then measured using a hand protractor through a large viewing lens. The actual fiber directions, not strand edges, were measured as data. Angles were taken from each side of the five replicate test boards forming a treatment. The axial angle measurements thus collected were then doubled to form an ordinary angle set (0 to 360 degrees). This formed data usable in Equations [2], [3] and [4] for calculation (in radians) of the orientation vector length, r.

Usually, the resulting orientation angle, m, was calculated to be less than one degree. This means the orientation was centered parallel to the reference edge and walls of the orientation box. The orientation vector length, r, calculated using Equation [4], was between 0 and 0.85 in all test boards. This value indicates the degree of orientation. A value of r=0 is random and r=1 is perfectly aligned.

3.2 The von Mises Distribution

The von Mises probability distribution function (pdf) is given by:

$$g(\theta,m,k) = \frac{1}{\pi I_o(k)} e^{k\cos 2(\theta-m)} \qquad [6]$$

This pdf is applicable over the required finite interval of π radians, has equal, recurring end points, and is axially

symmetric about m. The parameters m and 1/k correspond to the mean and variance in the ordinary linear normal distribution.

$g(\theta,m,k)$ = grain angle pdf, a two parameter probability distribution function

m = angle between the board axis direction, set at zero degrees, and any chosen reference (e.g. axis angle of loading on bias cut test composites)

k = the orientation parameter of strand (grain) angular spread; this is a measure of angular concentration

θ = the individual strand grain angle, with respect to the board axis, Fig. 1.

$I_o(k)$ = modified Bessel function of order zero given by the polynomial approximation formula of Abramowitz and Stegan (3), page 378.

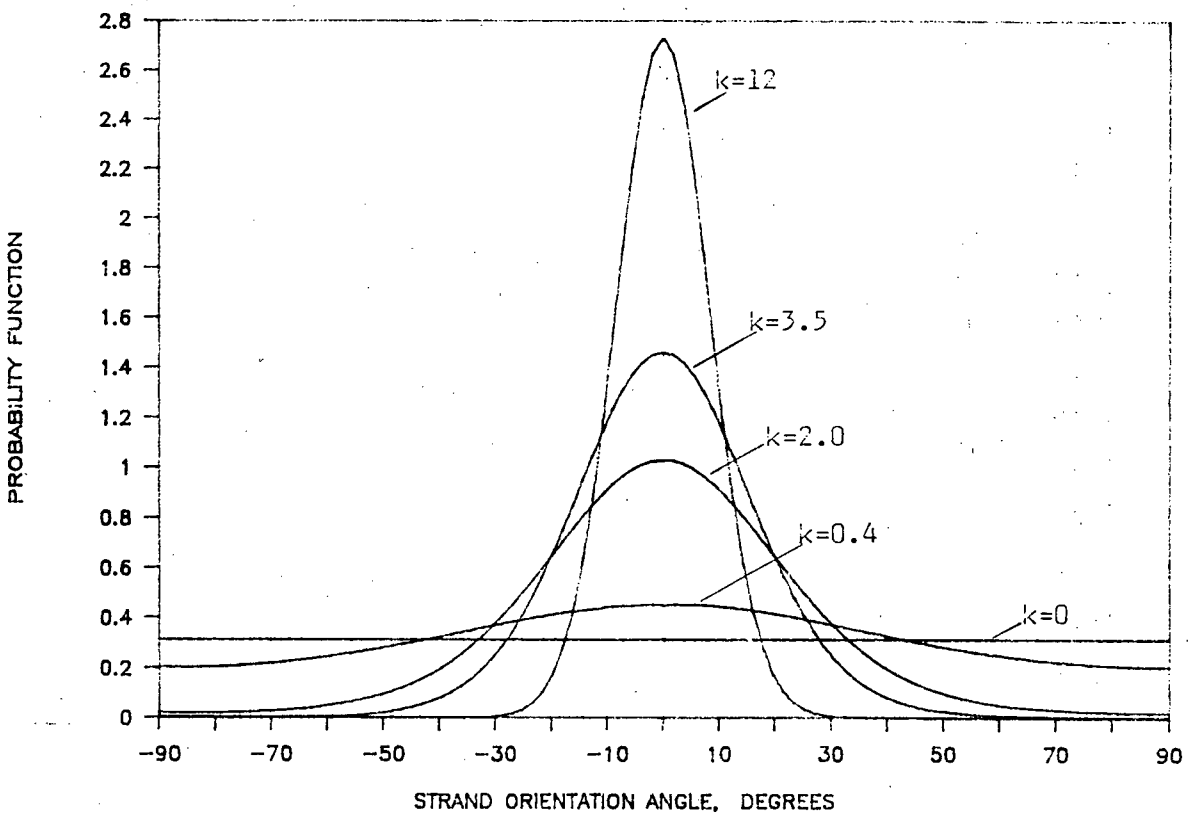

Figure 3. The von Mises pdf for some selected values of orientation parameter, k.

The orientation parameter is calculated using r, (Equation [4]). The ratio of the Bessel functions I_o and I_1, relates the orientation parameter, k, to the orientation vector, r, as shown in Equation [7].

$$r = A(k) = \frac{I_1(k)}{I_o(k)} \quad \text{and, inversely,} \quad k = A^{-1}(r) \qquad [7]$$

Batschelet (11) discussed the merits of k as a maximum likelihood estimate. An estimate of k is determined when r is known, from the tabulations of Mardia (58), in his appendix 2.2, or Table B, found in Batschelet (11). A polynomial regression of Mardia's table is presented in Fig. 4 and expressed algebraically in Equation [8].

$$k = 1.721 + 5.215r^2 - 31.96r^3 + 93.06r^4 - 120.9r^5 + 61.14r^6 \qquad [8]$$

A further approximation of k is given by Mardia (58)

$$k = [2(1-r) - (1-r)^2 - (1-r)^3]^{-1} \qquad [9]$$

Equation [9] yields three figure accuracy for r greater than 0.8.

3.3 Limits and Accuracy of Orientation Estimates

A result of the Harris (34) thesis on strand orientation was the conclusion that k values in the range of practical orientability, by hand or machine, could be specified by using a small, sample size of 100 strand angle measurements. To put this in perspective, an industrial OSB was later found to have a

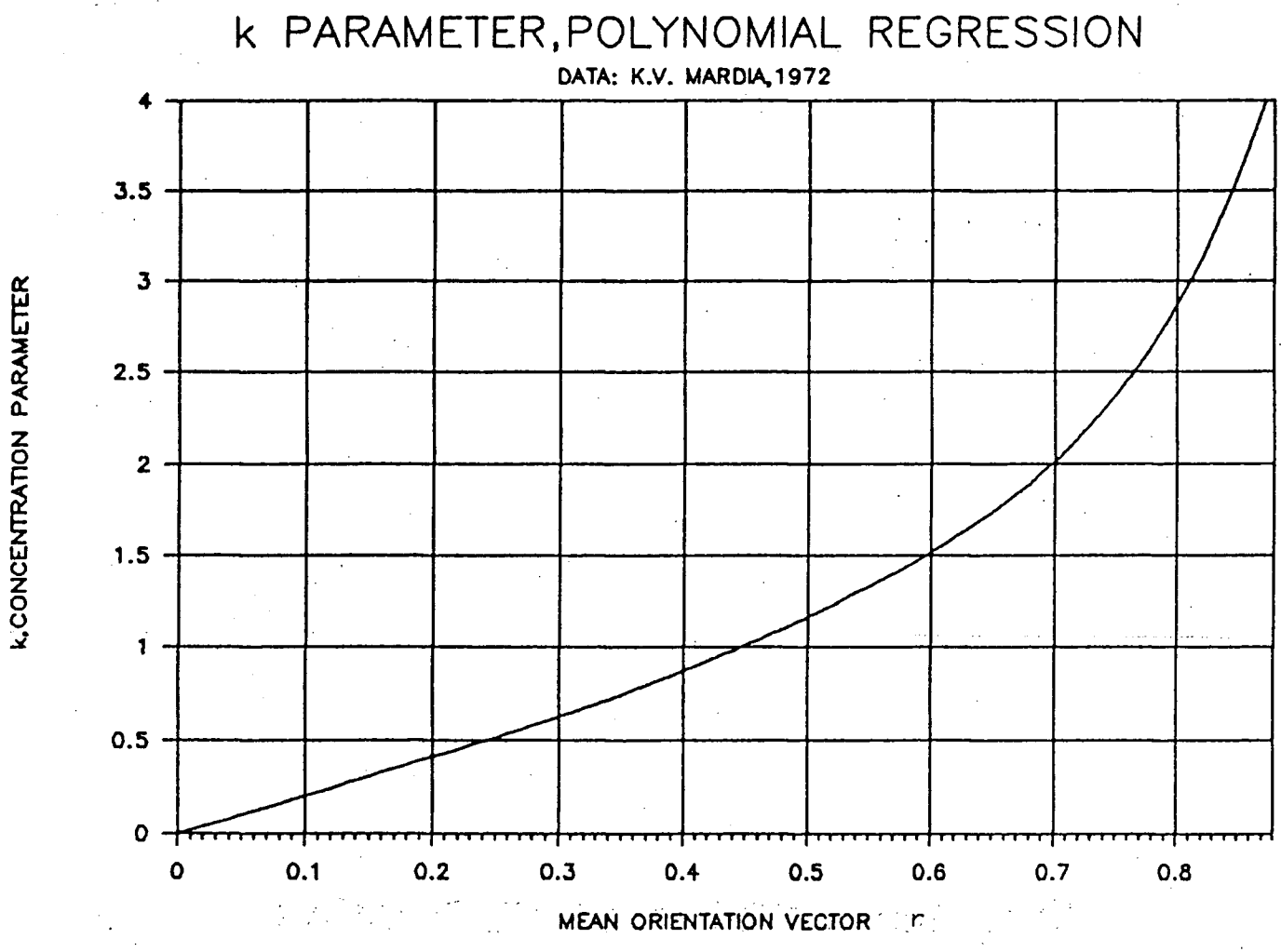

Figure 4 Regression of the orientation concentration parameter

value of k=1.1, and the most oriented lab board reached only k=9.0. Another important contribution of Harris was validation of the accuracy of his method of estimating m and k. He did this by use of specially made boards having calibrated k values, resulting from individually laid down strands. He found good agreement between calibrated and estimated values of k. Statistical t tests were made at the 0.05 level of significance.

Confidence limits for k values greater than k=5.0 can be obtained from an expression given by Batschelet (11).

$$\frac{X_1^2}{2n\ (1-r)} < k < \frac{X_\mu^2}{2n\ (1-r)} \qquad [10]$$

where X_1^2 = lower critical Chi-square value

X_μ^2 = upper critical chi-square value

n = number of trials

r = orientation vector length

The upper and lower critical chi-square values for n-1 degrees of freedom are found in the cumulative distribution of the C.R.C. Handbook of Probability and Statistics, published by the Chemical Rubber Company Press, 1966 edition. The probability columns headed by 5 percent and 95 percent give the X_1^2 and X_μ^2 values, respectively. Graphical plots published by Mardia (58), give 90% and 98% confidence limits for a fuller range of k values and were chosen for use because of their convenience. The confidence intervals can be made smaller by increasing the sample size at the researcher's discretion.

3.4 Roundwood

The five Western Canadian woods studied in this research all had good economic reasons for OSB candidacy, and had widely varying wood densities. The species were:

Trembling Aspen	(Populus tremuloides)
Red Alder	(Alnus rubra)
Western Red Cedar	(Thuja plicata)
Lodgepole Pine	(Pinus contorta)
Yellow Birch	(Betula alleghaniensis)

The aspen, alder, and cedar were mainly juvenile, cut from trees approximately 20 years old. Red alder and red cedar were cut at the Malcom Knapp University of B.C. research forest, Haney B.C. Aspen and lodgepole pine were cut in the Hope-Princeton region of southern B.C. With the exception of pine, all were cut from moist, open, fertile sites. Debarking was by hand. The industrial core aspen panel was from mature aspen cut in the Slave Lake, Alberta area. The mature yellow birch was from Quebec, and was received as thin veneer, (0.84 mm).

Table 1. Roundwood

Species		Age, years	Diameter cm	Average percent M.C.
R. Alder	tree 1	18	14.5	114
	2	24	16.0	
T. Aspen	tree 1	15	13.1	164
	2	21	20.0	
R. Cedar	tree 1	34	16.1	100
	2	21	16.5	
L. Pine	tree 1	68	17.0	51
	2	76	18.5	

3.5 Strand Waferizing and Drying

A 30 inch laboratory disc waferizer was used through the courtesy of C.A.E. Machinery Ltd., Vancouver. The roundwood was waferized in the green condition shortly after cutting. Moisture contents reported in Table 1 were taken from samples directly after waferizing. The waferizer knife settings were unchanged for all species except aspen where the higher moisture content made the wood so flexible that it didn't fracture on the counter knife to the desired width. This was improved by increasing the counter knife angle from 60 to 70 degrees. The low density cedar fractured into a greater number of under-width strands. This was the only species that required screen classification in order to maintain the same standard of strand dimensions in all the species.

The mechanical set-up of the waferizer is shown in Table 2. Whole 15 cm long bolts were fed tangentially so that a uniform distribution of ring angles was produced in the strands.

Table 2. Waferizer

Species	knife angle	knife projection	counter angle	knife position	reactor knife angle	speed R.P.M.
L. pine R. alder R. cedar	32 deg.	.635 mm	60 deg.	.762 mm	30 deg.	1300
T. aspen	32 deg.	.635 mm	70 deg.	.762 mm	30 deg.	1300

Strand drying was done through the cooperation of MacMillan Bloedel Research Laboratory where a one meter diameter by three

meter long rotary lab drier was used. Rotation was at 14 RPM and retention time was 7 to 9 minutes at a temperature of 160°C. The resident wet charge carried in the drier was 2 to 3 kg. Two to three passes of the furnish through the dryer were required to bring the moisture content to 3.7 to 4.9 percent. Losses as fines were about 10 percent.

3.6 Strand Properties

Dimensions were obtained under ambient conditions of 20°C and 50 percent R.H. on random samples of about 140 strands from each species. The distributions of these dimensions are shown in Fig. 5, for aspen. The exception was mature birch, which was cut from veneer using a "strander", fashioned by Durand-Raute Ltd. The strander is similar to a drum clipper. These were saw-cut to length and produced a highly uniform strand distribution.

Table 3. Strand description: 20°C and 50 percent R.H.

	R.Alder	T.Aspen	R.Cedar	L.Pine	Y.Birch
Ave. Length mm	57.8	59.0	59.5	58.9	113.5
Std. Dev.	13.6	13.1	13.2	13.0	1.5
Ave. Width mm	6.7	10.3	8.2	7.9	12.7
Std. Dev.	4.6	7.1	6.1	5.8	0.5
Ave. Thickness, mm	0.59	0.62	0.65	0.62	0.84
Std. Dev.	0.06	0.09	0.10	0.11	0.03
Length/Thickness, mm	98	95	96	95	135
Ave. Density, g/cm^3	0.34	0.35	0.31	0.39	0.62
Std. Dev.	0.04	0.02	0.05	0.04	0.04

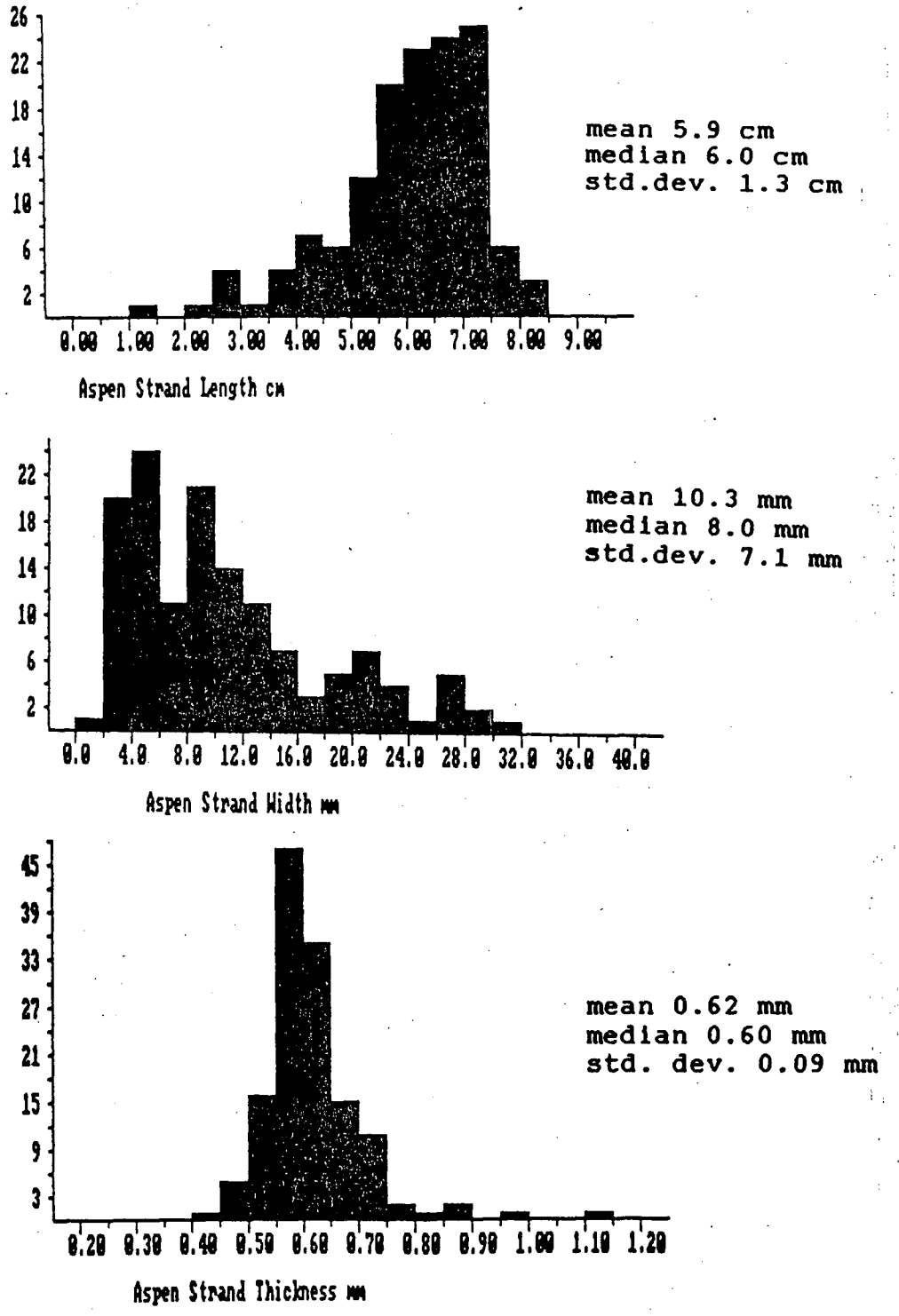

Figure 5. Distributions of aspen strand dimensions.

Random samples of 15-20 strands were selected from each species for density determination at 50 percent R.H. and 20°C. The results are reported in Table 3. The strand selection was randomized over earlywood and latewood, heart-and sapwood, ring angle, and vertical positioning in the two trees of each species. When the densities of Table 3 were adjusted to an oven-dry basis, the resulting averages were lower, but within one or two standard deviations of those expected by Jessome (39) of these woods in larger bulk. The low density exception was juvenile aspen, cut from a high growth site. Density for cultivated aspen as low as 0.299 g/cm^3 (oven dry basis) was reported by Einspahr et al. (21).

Specific tensile strength in each principal direction of the strands was important in this research because they were input variables to the strength model. Specimen size is an important consideration in measuring strand strength. The tensile strength typically decreases as the thickness or gage length increases. For example, Law et al. (52), (51), using zero span gage length, reported higher specific strengths in softwoods than Wilson (95) using extended microtensile specimens. Wellwood (93) reported specific strengths of necked micro-tensile specimens as being 23 to 27 percent higher than achieved with standard large size softwood tensile specimens. Acknowledging the size effects on strength, the zero span specimens were chosen explicitly as part of the model hypothesis as described in sections 3.10.1 and 3.10.3.

A Thwing-Albert QC-II electronic tensile tester was used at the campus facilities of the Pulp and Paper Res. Inst. of Canada. This 100 kg-force machine, was equipped with pneumatic grips and load break detector and was set in a test room at 22°C and 50 percent R.H.. The microspecimens were die-cut from strands. The die was aligned with the strand grain to produce rectangular specimens of 4.2 mm width. The thicker birch microspecimens were necked because the gripping length of the jaws was inadequate to prevent slippage. In this case the neck narrowed to 1.5 mm in width. The necked die was the same as used by Wellwood (93) with the grip tabs extended to take advantage of the full jaw length. The necked gage length was 12.7 mm on the birch specimens. A microscopic inspection of all parallel grain specimens insured that grain angle was zero or very small with respect to the parallel sides of the test zone. Perpendicular grain test specimens were die cut to nominal 15 mm wide by 30 mm long dimensions for zero span testing. The specimens are illustrated in Appendix iv. All tests were at a strain rate of 4 mm/min. Prior conditioning took place overnight in the test room at 22°C and 50 percent R.H. Approximately 12 zero span tests in parallel and 35 in the perpendicular grain direction were included in the data after culling misaligned specimens. Further details are provided in section 3.12.1. Results are presented in Table 7.

3.7 Adhesives Blending

A liquid phenolic resin of 45 percent total solids, designated as W31-54B, was provided by Borden Canada Ltd. Access to the Can-Car liquid blender at Borden Ltd. was also provided.

No wax was applied, because the boards were not to be tested for dimensional stability. The powder resin, BD-019 from Reichhold Ltd. was applied in a similar Can-Car blender at Forintek Corp., Vancouver. Both Can-Car blenders were rotating drums, 152.4 cm in diameter by 76.2 cm in length. A single inclined spinning disk atomizer of 25 cm diameter and rotation of 3600 RPM was used for liquid application. The liquid blender rotated at 34 RPM and the powder blender at 12 RPM. The powder resin was hand fed to the powder blender. The blending time for the powder application was based on industrial experience and is noted in Table 4.

The liquid resin application was based on the rationale that only surface strands held on the blender wall at the load surface were exposed to spraying. The spray which occurred during the random fall to the return point, was neglected. The result of this dynamic analysis of strand movement was a conservative estimate of the time required to properly blend a given amount of resin onto the strands. The blending was planned so that the probability of any strand not receiving adhesive spray exposure on at exactly one side was less than 0.05. The centrifugal blending time was extended directly as the amount of liquid resin applied increased. The rate of liquid delivery to the blender's atomizer was a constant 80 g/min.

The calculated liquid resin spreads were based on fixed strand thicknesses taken as the sample means. The spreads were later confirmed by colorimetric analysis. At the higher resin level, resin surface tackiness was beginning to affect the

Table 4. Resin blending.

Species	O.D. charge Size, kg	Blend time minutes	Calculated liquid spread mg/cm², O.D. wood basis	Total resin solids on O.D. wood percent
R. Alder	11.1	8.0	0.57	2.59
T. Aspen	11.0	7.5	0.57	2.44
R. Cedar	11.0	8.0	0.57	2.64
L. Pine	11.0	6.9	0.57	2.26
R. Alder	11.1	16.0	1.14	5.18
T. Aspen	11.0	14.9	1.14	4.90
R. Cedar	11.0	16.1	1.14	5.27
L. Pine	11.0	13.8	1.14	4.50
Y. Birch	7.5	6.0	1.76	2.87
T. Aspen	4.8	20.0	-	2.00 (powder)

dynamics of blending. This may favour the use of less tacky liquid adhesive in high resin content composites.

The colorimetric analysis was made by determination of the amount of resin deposited on the surfaces of vinyl tracer strands that were spray blended with the normal wood furnish. The tracers had weight length and width equal to the corresponding averages of the wood strands. They were prepared with removable, pressure sensitive tape on one side, so both sides could be analyzed. One half percent Rhodamine B dye, predissolved in methanol was dissolved in the Borden W31-54B phenolic resin. After spray blending, the plastic and tapes were separated and each washed into 25 mL aliquots of 15 percent NaOH water solution. Colorimetry was on a Pye-Unicam SP6-350 Visible Spectrophotometer at 555 nm, using a 5.0 cm cell length. Five standard solutions and a background blank were used for creation of the calibration curve. The lowest standard solution was 4.0 ppm. The resulting 95 percent confidence limits on the linear regression estimates of resin pickup were in the order of

± 0.2 mg/cm^2. These confidence limits were calculated according to Nalimov (63). The mode of operation of the blender was such that there was very little tendency for a strand to pick up the same amount of resin on both sides. The linear independence of the pickup on alternate strand sides was indicated by a low coefficient of determination (r^2=0.04 to 0.20) for each blender batch. This independence could not be known by methods of resin detection that ash, digest, or elute the whole strand for analysis of sodium or other resin tracer ions. Such methods were developed by Bacon et al. (7).

3.8 Forming Oriented Strand Board

An oscillating forming box, 43 cm long, 33 cm wide and 16 cm deep was the basis of the orientation device. A one cycle per second vibratory action of 2 cm amplitude was applied in the 33 cm direction. The forming box moved back and forth over the caul plate as pictured in Fig. 6. The thin alignment vanes sloped 60 degrees to the vertical and reached the full height of the furnish mat. After a 5 minute forming cycle, the vanes were removed and the top caul inserted into the forming box before prepressing. The air cylinder oscillator was controlled by means of input air pressure, exhaust metering, and the reset electronic timer. Microswitches controlled the stroke length.

The ability of this orienter to align to a chosen level was not as good as the more refined lab equipment of Geimer (26) which used vertical vibration similar to some industrial

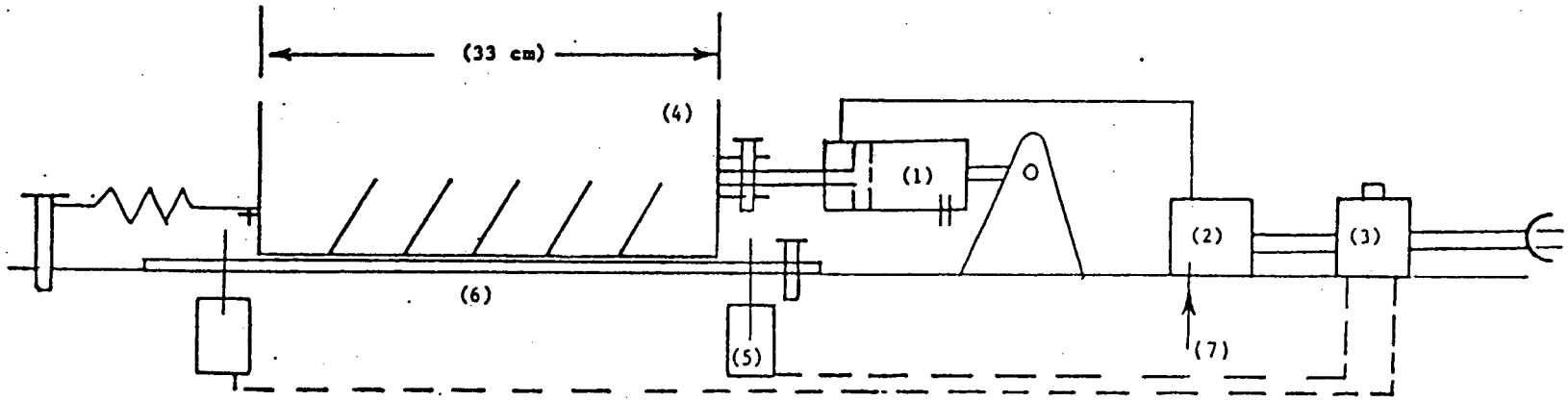

1. air cylinder
2. pilot valve
3. electronic auto reset timer
4. forming box and vanes
5. microswitch
6. caul
7. regulated air supply

Figure 6. Orienter.

equipment. An example of an industrial orienter is described in U.S. Patent 3,896,536 by Keller et al. (43).

Price (72) used a stationary box containing vanes as a gravity powered orienter. Better control of orientation in the laboratory was reported by Harris (34), using an electric field of intensity up to 6.7 Kv/inch. The electric field method was developed by Talbot et al. (90) but has found very limited use in industry because of its low efficiency on strands of 75 mm length and greater. A fundamental reason for this is that the aligning torque increases as the cube of the strand length but the strand rotational inertia increases as the fourth power of length. Also, the optimum moisture content for electric alignment is higher than that appropriate for adhesives. The strand fall distance in the electric orienter makes it very large in physical size, especially for larger strands.

In the present research, birch strands, 113.5 mm x 12.7 mm x 0.84 mm were oriented to a maximum k level of 9.0. By comparison, various lower levels of orientation up to k=2.59 were achieved electrically by Harris (34) on less dense, 38.1 mm x 9.4 mm x 0.38 mm Douglas fir strands.

In summary, the vibrating strand orienter performed well in providing a high level of orientation, but lacked the control of an electric orienter. The apparatus in Fig. 6 also caused strands to be laid down at an angle, (shingled). This promoted lay-up racking during press consolidation. Pre-pressing helped to control this.

3.9 Hot Pressing

Approximately 135 experimental panels were pressed to a thickness of 7.9 mm using stops. The same nominal weight of furnish was used for each test panel. Minor adjustments in weight provided a small range of densities within each set of five replicates. Minor mat weight adjustments also provided moisture content correction. Five replicates were made for each species - resin - orientation treatment. All pressing was done in a randomized sequence to conform with the completely randomized experimental design.

Consolidation pressure varied with species and orientation. Peak pressure varied from 2.0 to 3.4 MPa on the mat. A slow closing time of 1.0 to 1.5 minutes to the stops was maintained manually for all boards. Other press conditions were:

total mat moisture (including resin contribution)	7-11 percent
platen temperature	206°C
closed press time	5 min
time for board center to reach 100°C	0.5 min

A long press time was used to insure complete cure of the phenolic resin and minimize blows. The target density was calculated to be in the range of industrial boards currently made from aspen. This was from 0.59 g/cm^3 to 0.69 g/cm^3. Birch was the exception, where the specimens reached densities of 0.82 to 0.97 g/cm^3. These densities defined the compaction ratios which were calculated as the equilibrated board densities at 50 percent R.H. and 20°C, divided by the wood strand densities at the same condition. Mid-range estimates of these ratios are presented in Table 5.

Table 5. Compaction ratios

R. alder	1.83 : 1
T. aspen	1.77 : 1
R. cedar	2.10 : 1
L. pine	1.64 : 1
Y. birch	1.38 : 1
industrial core	1.37 : 1

These ratios are indicative of how much the original wood volume yielded in terms of pressed board volume, and together with the resin content, are important factors affecting the economics of board making.

3.10 Modelling Methods

3.10.1 Model Development

The major factors of longitudinal and transverse strand specific tensile strengths, together with the orientation level, drive the model as inputs. From these, the model can be used to predict the expected tensile strength of the composite, at any angle with respect to the principal axis of strand orientation. In this model, the strands are simplified as being transversely isotropic in strength.

Density is diminished as a tensile strength factor by the choice of specific strengths as inputs and outputs of the model. Accordingly, in comparisons of the test results, it is required that the tensile strength of the composites be divided by the composite densities. In the estimation of flexural strength, a density gradient through the thickness is adjusted for at the surface because the MOR is defined at the surface.

The strand's tensile strength is known to vary by a factor of 15 to 30 depending on the grain angle. The longitudinal versus cross-grain (axial) anisotropy of wood decreases as the density increases, according to Easterling et al. (19). It was observed by Bodig and Jayne (12) that the anisotropy of wood is unsurpassed even by glass-epoxy unidirectional lay-ups.

wood E_L/E_T	24:1
glass-epoxy E_L/E_T	4:1

This extreme anisotropy suggested the proposition that the specific strength of a well bonded wood strand composite could be modelled to a first approximation, based only on the strand orientation and strand principal strengths. The zero-span strand strengths were considered as model inputs because the strands have tensile load applied continuously over their length, except for end shear, in both the zero span test and in the ideally bonded board. This is discussed further in section 3.12.1.

The mathematical expectation of strength for a collection of n strands, each having orientation angle θ, relative to the (mean) principal axis direction, was hypothesized to be:

$$S_m(\theta) = \sum_{i=1}^{n} \left[\begin{array}{l}\text{probability of a strand}\\ \text{grain being at angle}\\ \theta_i \text{ to the reference axis}\end{array}\right] \left[\begin{array}{l}\text{strength of the strand}\\ \text{when loaded at angle}\\ \theta_i \text{ to the reference axis}\end{array}\right] \qquad [11]$$

The von Mises probability distribution was chosen as the first factor in Equation [11] for reasons discussed in Sections 3.1 to 3.3. The Hankinson formula was used to express the second factor, strand strength, taken at any plane angle to the principal axis. This choice is supported by Price's (72) study

of wood strand strength as used in composites. The more refined theories relating strength to grain angle that were discussed in the literature review offer only marginal improvement in accuracy. Other relationships which accurately resolve strength as a function of grain angle are adaptable, but the Hankinson formula was judged most practical because it requires only two input strengths.

The mathematical expectation of composite strength was therefore taken as:

$$S_m(\theta) = \int_{-\pi/2}^{\pi/2} g(m,k,\theta) \cdot s(\theta)\, d\theta \qquad [12]$$

$g(m,k,\theta)$ = von Mises pdf

m = angle between the principal orientation axis and the axis of load,

k = orientation parameter,

θ = individual strand grain angle with respect to the specimen's principal orientation axis,

$s(\theta)$ = Hankinson expression for the specific strength of a strand loaded at angle θ with respect to its grain.

The board orientation axis was defined as the most probable angle of strand orientation with respect to the board reference edge. The orientation axis and the specimen reference edge were adjusted to be parallel in all cases (zero degrees). Rewriting Equation [12] with substitution, yields the working Equation [13], where:

L = mean specific tensile strength of strands tested parallel to grain (zero-span)

T = mean specific tensile strength of strands tested perpendicular to grain (zero span)

$$S_m(\theta) = \int_{-\pi/2}^{\pi/2} \frac{1}{\pi I_o(k)} e^{k\cos 2(\theta - m)} \cdot \frac{L}{1 + ((L/T)-1)\sin^2\theta} \, d\theta \qquad [13]$$

The consideration of Equation [13] as an unbiased estimator of ultimate fiber stress in bending as well as tensile strength is discussed in section 3.10.5.

3.10.2 Weighted Average Criterion

The model simulates the two dimensional orthotropic board strength as the strand strength, resolved in the composite axis direction, and weighted by the strand angular directional distribution function. The board failure criterion is defined by the failure of a characteristic through-thickness set of strands taken at a random point on the specimen's surface. Innumerable characteristic stacked strand sets such as this are interlocked in the model composite structure. They are assumed perfectly bonded so that the strain in all strands in the set occurs equally. When the applied stress in the composite reaches the calculated failure stress of the characteristically oriented model set then the composite is assumed to fail.

The physical model of the multiple layered strand set fits well to the basic definition of the mathematical expectation of strength based on the orientation distribution. The mathematical expectation of a board's strength is defined as the arithmetic

mean of the estimates made from all possible strand samples; it is the sum of the estimates after weighting each by its' probability. Equation [11] approximates this expectation. As a further approximation, the input to the model Equation [13] uses arithmetically averaged values of strand principal strengths, L and T. These are far enough apart in value that their distributions do not overlap and they shall be considered as fixed variables (appendix iii). A further step in refining this model would be treatment of the L and T strengths as random variables with the model generating a random function (stochastic) prediction of strength.

The predicted variance associated with the single stacked strand set is given by:

$$v(\theta) = \left[\int_{-\pi/2}^{\pi/2} g(m,k,\theta) \cdot s^2(\theta)\, d\theta \right] - \left[S_m(\theta) \right]^2 \qquad [14]$$

Equation [14] refers to a single vertical stacked strand modelling unit, assumed to be the same at all planar locations in the composite. The actual composite consists of a multitude of such units, having unknown size, shape and number. This set of units has additional components of strength variance which are driven by such factors as local orientation and density variation in the plane. This limits the utility of Equation [14]. In a trial calculation, the variance of [14] was much larger than that estimated on the basis of 5 tensile specimens (ASTM D1037) cut from differing locations in the board plane.

3.10.3 Model Assumptions and Stress Transfer

The model makes assumptions about several co-determinants of strength and neglects others. For example, such factors as lamination micro-defects and duration of load are special topics and should be studied separately. Checks, knots, and grain imperfections are dispersed when wood is waferized and rebonded in a composite. The composite strengthening effect of this dispersion of flaws is acknowledged in the present model in which the input strand strengths were tested on small specimens that were clear of knots and checks. These strengths are generally accepted as being higher than large specimens containing such flaws. This further supports the choice of zero span testing of the strands.

The excessive complexity of detailed bond stress analysis led to the brick-lay model of Fig. 7. The strands are arranged in half-overlapping array with the grain angles represented by the von Mises probability distribution. This representation is assumed to model the mean results of a large number of stress transfer points in a composite. The strands themselves are considered transversely isotropic. Annual ring angle effects on strength were neglected because ring angles are uniformly distributed in the furnish and tensile strength differences from the radial to tangential directions are small.

All stresses engendered by Poisson effect interactions between strands and the failure criteria effects of them are neglected. The theory follows the concept of a continuous strand network which has been established in glass filament composite design and also paper physics. In the idealized network theory

enough bonding and strand length are assumed to permit maximum stress development along the full length of the strand. This is equivalent to assuming the strands are continuous through the composite material. The loaded strands are actually discontinuous in some cases and continuous in others, depending on resin level and strand shape.

Barnes in patents (8, 9), specified a minimum length to thickness ratio of 53 and discussed unidirectional composites having a slenderness ratio of 280 which had MOR approaching that of the original wood. Density gradients were not presented in Barnes' comparisons, and the patents also do not rigorously quantify orientation. The experimental strands for this thesis were cut at slenderness ratios near 100, except for birch where it was at 135. Limitations on material handling do not permit production of oriented panelboards having higher length slenderness ratios than about 160 in most 1989 OSB mills. The practical limitations of processing long strands are formidable.

Simpson (79) discussed strand length/thickness ratio (slenderness ratio) in a perfectly parallel orientation model. He indicated that ratios of 55 to 200 would lead to composite tensile strength that was 90 to 95 percent of the strand strength, depending on species. This was based on the limiting factor in stress transfer being the shear strength of the wood, not the adhesive bond.

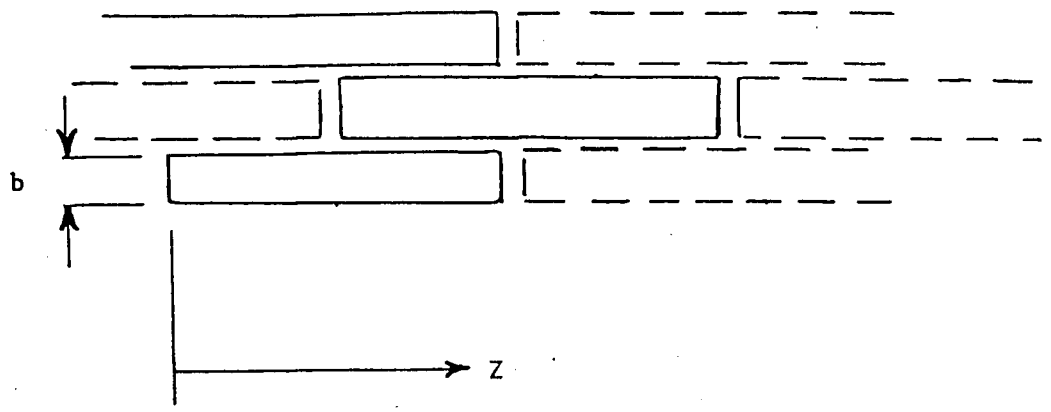

w = width of strand
b = thickness of strand
p = strand tensile stress
s = shear strength of the adhesive bond or strand, which ever is lowest

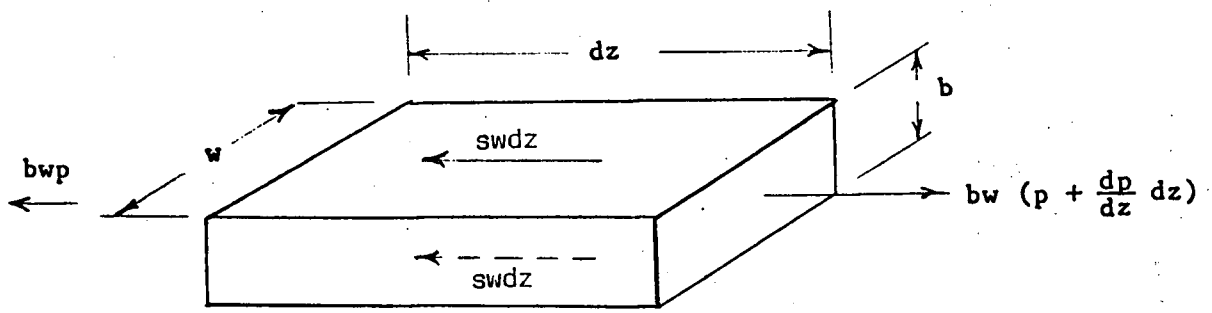

free body

Figure 7. Stress transfer

An expression for the tensile stress in strands within a composite is made with reference to Equation [15]. Only face adhesion is considered in the analysis because of the flat, thin strand shape. The sides and ends of the strands are assumed free of loads. Considering the equilibrium of the free-body diagram in Fig. 7,

$$2sw\ dz = bw\ \left(\frac{dp}{dz}\right) dz \qquad [15]$$

The tensile stresses, p, are hypothetically assumed to be as represented in Fig. 8. It follows from this assumption that the strand shear stresses are represented as in the second diagram of Fig. 8. Thus, the interface shear stress is assumed constant along the portion h at the end of the strand length. Either the shear yield strength of the wood or the adhesive bond can define the idealized shear stress in this simplified analysis. It is also possible that the material which is assumed subject to shear flow is more accurately considered as a resin-treated wood subzone, having properties different from either wood or adhesive. An elastic model analysis of double lap joint stresses can also provide theoretical estimates of the shear, s, and it's distribution over the length . (eg. Stresses in Adhesive Joints, H. Perry, Product Engineering, July 7, 1958). Further experimental research is needed to test the use of the shear flow hypothesis and to estimate h. Equation [15] is derived with reference to the critical fibre length estimate made for discontinuous fibres in polymer matrices (5).

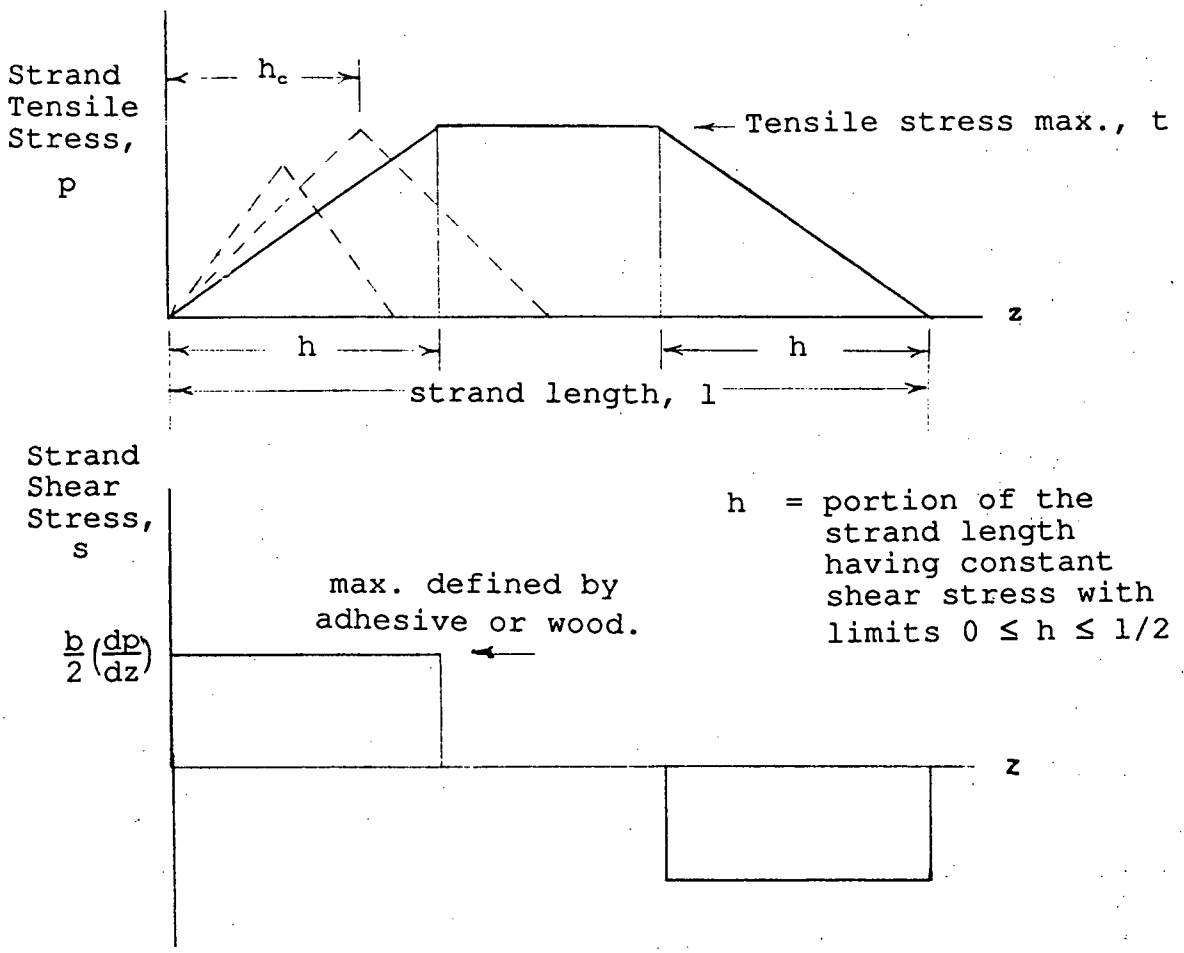

Figure 8. Strand stress.

The cancelling of opposing symmetric normal forces occurs in the model's double lap joint configuration. This simplifies the shear stress loading of perfectly oriented and lapped strands. But void gaps, multiple overlaps, and variation in strand elastic modulus with grain angle confound the true state of shear stress in the practical strand composite. More research on this is needed.

A critical constant shear length, h_c, is derived from Equation [15]. The peak tensile force applied to the strand is reached at dz = h_c and this substitution is made in Equation [15]. The peak tensile stress is equal to the ultimate tensile stress, t, of the strand at the critical constant shear length h_c. Therefore, strand tensile strength, t, is substituted for the strand stress dp in Equation [15] to complete the derivation of [16].

$$h_c = \frac{bt}{2s} \qquad [16]$$

For example, a critical constant shear length h_c for strand tensile failure can be estimated using the substitution of wood shear strength for the hypothesized constant value of s. Depending on bonding, s does not necessarily reach this wood shear strength level. Using Jessome (39) for an estimate of aspen parallel shear strength (6.8 MPa), the critical length, h_c is about 2.5 mm with the strand thickness, b, set at 0.6 mm. (Table 3) The definition of h_c allows shear, s, and strand thickness and length necessary for 2 types of failure to be designated. Both of these, tensile and shear failure, occur together when $h=h_c$ as in the example.

If:

constant shear length $h \geq h_c$, then the strand fails in tension,
constant shear length $h \leq h_c$, then the interface fails in shear.

According to the assumption of constant shear, the critical constant shear length is at h=l/2 (midlength).

Substituting:

$$l \geq bt/s \text{ : tensile failure,} \qquad [17]$$
$$l \leq bt/s \text{ : shear failure,} \qquad [18]$$

The strand length l_c=bt/s is termed the critical stress transfer length of strand. Thus, when using short strands or particles with $l<l_c$, strength gains are possible through increased adhesive shear bonding only up until s reaches the wood's shear strength. Composite strength increases with s until enough stress transfer is provided to cause tensile or shear failure (or both) in the wood. The analogous rationale applies to the strands that are stressed perpendicular to the grain (Section 5.2). The perpendicular tensile strength and rolling shear strength are then used in Equation [16] for h_c.

If the strand bonding length l were abundantly greater than the l_c, then the strength developed in the composite would be near that of the strands. This defines the perfectly bonded situation, where continuous strands are simulated. In glass fiber-epoxy composites this typically requires fiber length, $l > 50\ l_c$. A "strength factor" for glass fiber composites discussed by Agarwal et al. (5) provides an estimate of composite strength increase as the fibre length, l, becomes much longer than l_c. According to Simpson (79) the model composite of Fig. 7, should have parallel strength near that of the strand or perfectly oriented strand network when the expression [(l/b)+1]/[(l/b)+(t/s)] has a value close to 1. The variable l in Simpson's expression is the strand length. In the present analysis, as the fraction 1-(h/l) approaches 1, the full length of the strand is exposed to tensile failure stress. The expression 1-(h/l) is interpreted as the strand's length average relative tensile stress (strength factor). Thus, for the idealized composite strength to be achieved, the criteria of

$l >> l_c$ and $l >> h$ are required. It has been assumed (5) that this condition of maximum strand (length) tensile loading corresponds to maximum composite strength.

In summary, the target of efficient composite formation is represented by the continuous strand network model strength, (Equation [13]). This provides an idealization of the maximum attainable specific tensile strength when bonding is sufficient to cause tensile failure over most of the strand length.

3.10.4 Density Gradient Effect and Measurement

The density gradient effect is taken advantage of in industrial practice. Current OSB panels are produced with denser surface layers than core. This is done with the purpose of maximizing the bending strength while maintaining a core strength sufficient to survive the neutral axis shear stress and also pass the standard internal bond test.

The presence of a through-thickness density gradient was observed in both experimental and industrial boards. Consideration of the gradient effect on tensile strength was simplified by assuming both strand and composite strengths as linearly proportional to density, and choosing specific strength as the dependent variable. This general linearity changes only in extreme densification in the transverse grain direction, where (compressive) strength varies as the cube of density (19). The specific tensile strength was therefore approximated by dividing the ultimate strength of the test specimen by its specimen average density based on oven-dry weight and conditioned volume at 7 to 8 percent moisture content. This made the model, test

panel, and native wood strands, reasonably valid to compare in tension, despite the density inhomogeneity (gradient), and linearity approximation.

Density gradients affect flexural strength in a complex fashion. Flexural tests were concluded according to CAN3-0437-M85 and MOR was calculated using the elementary flexure formula:

$$MOR = \frac{Mc}{I} \qquad [19]$$

where:
MOR = ultimate (rupture) fiber stress at the surface
M = maximum bending moment
I = cross section moment of inertia
c = half thickness of the symetric specimen

The formula assumes each layer in a homogeneous test beam makes an elastic contribution to the internal resistive moment proportional to the layer's distance from the neutral axis. This is based on all layers having the same elastic modulus and the assumption of pure, geometrically defined bending strain. Because the density gradient contradicts the homogeneity assumption, the bending test results vary, depending on the gradient. The greater elastic modulus and strength of the surface layers is due to the higher surface density. In a strictly rigorous sense, this means that the comparisons of specific MOR of various different composites are valid only when the density gradients are the same.

The assumption is made that ultimate flexural failure is governed by first fiber failure at the tensile surface. The modulus of elasticity, E, and the bending (fiber) stress, $\sigma=E\varepsilon$, increase parabolically toward the test beam surface. Assuming

pure bending strain, the stress at the tensile surface is actually greater than the flexure formula, Equation [19] predicts on the basis of a constant or fixed average value of E. The division of this conservative surface stress by the increased surface density yields a conservative approximation of the specific fiber stress at the beam surface. Therefore the MOR test results used as data in Fig. 18 to 27 are thought to be low boundary limits of ultimate fiber stress, in tension, at the bottom surface of the test beam. This conclusion also accommodates any deviation from pure bending, such as fiber crushing, on the compression side.

An alternative transformed section approach to MOR of boards having density gradient requires calculation of the flexural elastic modulus followed by application of a strength criterion based on the maximum fiber strain at the surface. The MOR is estimated as:

σ = (calculated flexural modulus) x (surface failure strain)

In a trial calculation the above method yielded high MOR values. This was in the presence of the transformed moment of inertia analysis producing reasonably accurate estimates of flexural modulus as shown in Table [22]. The transformed section analysis was performed in section 5.4 using the Appendix ii program for flexural elasticity which is applicable to any parabolic density gradient in the strand laminate. The accuracy is similar to that of Geimer (27) who also used a transformed section approach. The details are discussed in Section 5.4. In the above formula, the

apparent flexural elasticity results from Appendix ii are multiplied by the failure strain of the composite. The surface failure strain was assumed to be similar to the tensile failure strain of the composites in the parallel to grain direction in the tensile tests (Table 10). Strains at failure of 3 to 7 percent were observed. The resulting estimates of MOR were at least 5 to 10 times larger than those observed in Figure 27 and Table 10, because of this excessive strain at failure. The 3 to 7 percent composite failure strain is above that expected of normal dry mature wood (about 1 percent). Bond creep and strand interlocking may be contributors to this high strain.

For these reasons, the previously described method of estimating specific MOR was used. This provided the advantage of being able to estimate a minimum MOR with knowledge only of the surface density while using a standard test procedure. The MOR test results, divided by their respective surface densities, provided the low bound experimental specific MOR data displayed in Fig. 18 to Fig. 27 and Fig. 29 to Fig. 33 (averages of nominal 5 replicates).

The method of measuring the density profile was direct reading x-ray densitometry. The equipment was developed by Forintek Canada Corp. for scanning tree increment cores. Therefore, small cross section specimens were required. The speed and accuracy of x-ray and higher frequency gamma radiation (Winistorfer (96), Laufenberg (49)) have made the gravimetric methods (86) obsolete. The Forintek procedure passed a 0.25 by 1.00 mm collimated x-ray beam having power of 2 mA by 15 to 20 kV through the specimens according to Fig. 9. Cold-set urea

formaldehyde resin was used to prebond the specimens before sawing to the test shape. The repeated glue line between samples had a lower mass attenuation coefficient and higher density than the adjacent strands. This separation was useful for identifying the samples to within one strand thickness. The x-ray detector resolution was 100 microns. Scanning was at air-dry ambient conditions and the resulting densities were adjusted to the same (50 percent R.H., 22°C) conditions as the mechanical test specimens.

The Lambert equation used for relating radiation attenuation to density is expressed as:

$$P = \frac{\ln\left(\frac{I_o}{I}\right)}{\left(\frac{a}{p}\right) t} \qquad [20]$$

where:

P = specimen point density, g/cm^3

I_o = unattenuated radiation intensity, counts

I = attenuated radiation intensity, counts

t = specimen thickness, cm

(a/p) = linear attenuation per unit density, (mass attenuation coefficient, cm^2/g)

Mass attenuation coefficients can be determined experimentally or calculated from constituent elemental analysis. The mass attenuation coefficients of adhesive resins and moisture are slightly higher than for wood. Therefore, a small error is caused by neglecting the resin and moisture attenuation in the

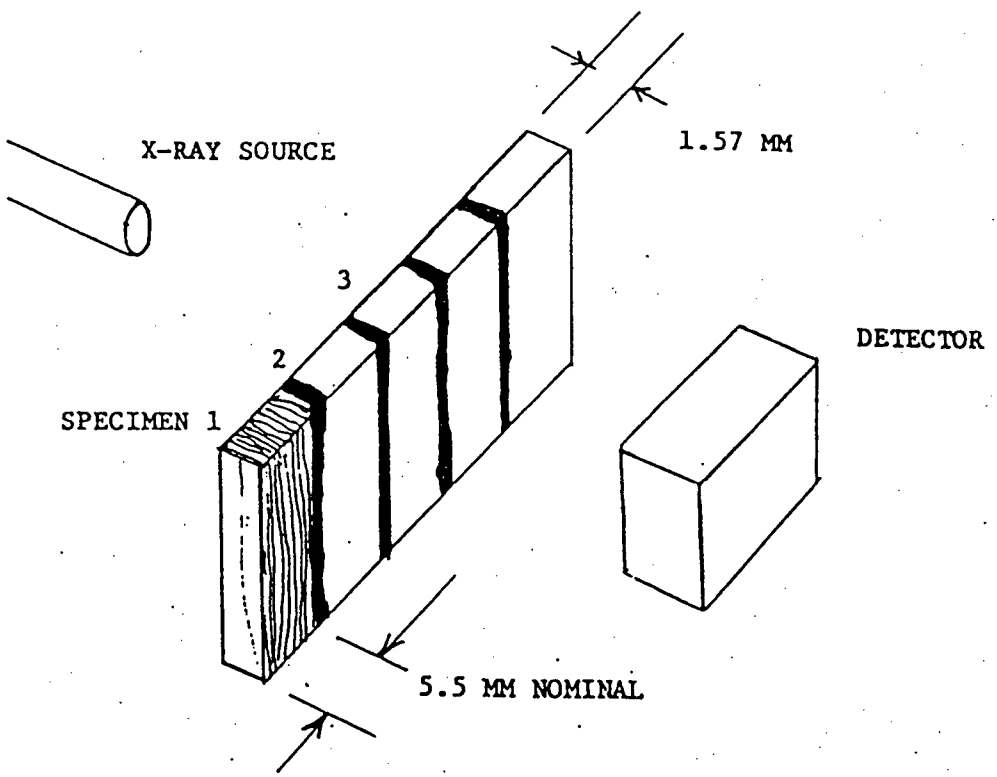

Figure 9. Densitometry specimen.

composite, but this underestimation of density was found negligible in Laufenberg's (49) study using gamma rays. Olson et al. (66) showed that mass-attenuation coefficients can vary with species and ash content when using gamma rays of less than 40 KeV. (Mid-range gamma rays have 10 times the energy of x-rays.) Forintek's x-ray mass-attenuation coefficient was common to the Delrin acetal plastic step wedge used for calibration, and to both hardwoods and softwoods (40). Extractives are said to decrease the x-ray mass attenuation coefficients slightly, and may cause overestimating the material density when not removed.

3.10.5 Model Structure and Programming

The model was based on Equation [13]. The program integration between o and π for the von Mises pdf was performed using Simpson's Rule for numerical integration, with 50 iterations. The angle of loading, m, was incremented in steps of 4.5 degrees within a computer program devised to calculate Equation [13]. In this way, a picture of strength was developed for a composite made from wood strands of specific longitudinal tensile strength, L, specific transverse tensile strength T, and having concentration parameter k, for orientation. The GWBASIC program for calculating Equation [13] is presented in Appendix i and produces results exemplified by Fig. 10, when plotted.

The program falters at orientations greater than k=80 where the ratio $e^{k\cos 2(\theta-m)}/I_o(k)$ became excessively large. At this level the orientation distribution (Fig. 3) tends to a spike configuration and for practical purposes the model represents

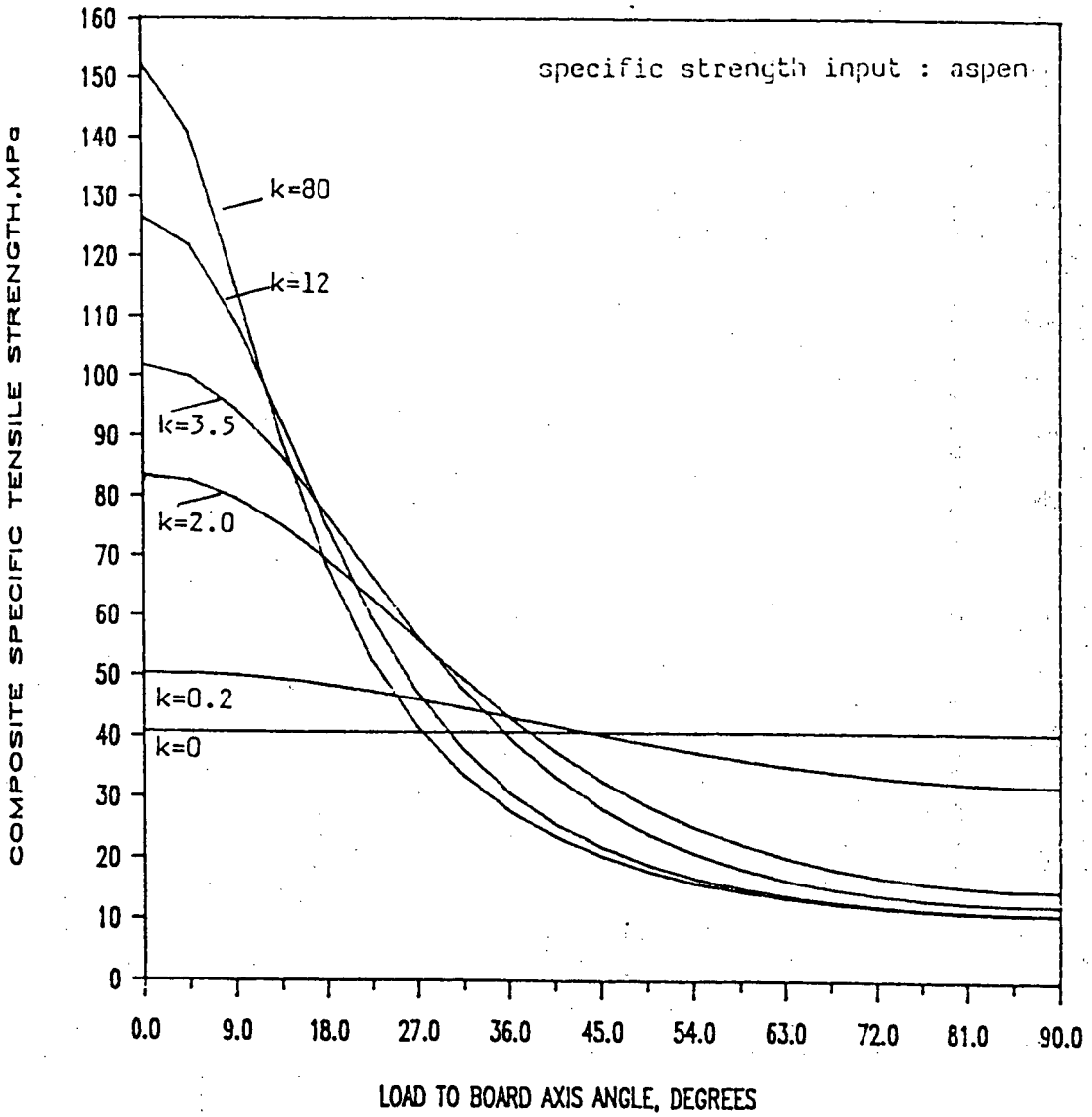

Figure 10. Orientation model output.

natural wood. Fig. 10 places the k value pdf's in a visual display of ranking. As the level of orientation is reduced, the composite strength is also reduced. At the k=12 level of orientation, for example, the computer model predicts a composite specific tensile strength parallel to the orientation axis of about 80 percent of the parallel grain wood strand strength tested at zero-span.

The theoretical tensile strength for random boards is given by Equation [21], as expressed by Price (72).

$$S_{\perp} = (LT)^{1/2} \qquad [21]$$

Equation [21] presents the value of the integral (Equation [13]) with k=0. The probability distribution function becomes uniform with value $1/\pi$ in the random case. At k=0, in random orientation, the model predicts a composite specific tensile strength of about 25 percent of the wood strand's specific tensile strength parallel to grain. It is obvious that much strength is lost when little or no orientation is present. This deficiency has traditionally been recovered by the panel industry by using surface densification to increase MOR.

3.11 Experimental Design

3.11.1 Composite Strength Comparisons

In comparing the strength results to those predicted by the model, it was chosen to evaluate the independent variables of resin level (2), species (5), and the orientation parameter, k, over its range between 0 and about 9. This approach

comprehensively tested the accuracy of the predictive strength algorithm in a wide range of wood strand composites. When one factor was manipulated, the others were held as constant as possible so that the effect could be observed in a rigorously selective fashion.

The completely randomized experimental design required that variables such as board pressing order and specimen cutting and testing sequence, in pattern and time, be randomized to minimize and diffuse any systematic effect on the dependent strength variable under study.

The strength data were presented in both tabular and graphical form with standard deviations. Where strength differences required statistical scrutiny, the null hypothesis that the model prediction was not a member of the population set represented by the test sample was tested. The student "t" statistic was used for this hypothesis test. The tests were normally made at the $p=0.05$ level of probability of falsely rejecting the null hypothesis. Species and resin level effects on strength were examined in (2-way) factorial analysis of variance in random orientation boards.

3.11.2 Repeatability of Orientation Parameter

The 95 percent confidence limits were calculated for evaluating the repeatability of the determination of the orientation parameter, k. The methodology is based on the chi-square distribution and was developed for this purpose by Batschelet (11). Results are discussed in Section 4.1.1.

A further verification and assessment of the goodness of fit of the orientation data to the von Mises distribution was made. The null hypothesis that the angular data did not contradict the estimation of parameter k, and that data fitting discrepancies could validly be explained by chance fluctuation was tested. The chi-square statistic was again used for this hypothesis test at the p=0.05 probability of false rejection. Graphic and statistical results are presented in Section 4.1.2.

3.11.3 Species Comparisons of Strength

The comprehensive direct comparison of species effects on strength in a factorial experiment was reserved for the randomly oriented case where orientation differences between various species and resin levels were negligible. In these direct comparisons, further resolution of species differences was possible in addition to comparing percentages of the model strengths that were achieved in each species. The factors were species (4) and resin level (2). The analysis of variance was repeated with both specific tensile strength and flexural strength as independent variables. The experimental design was completely randomized. Where significance was identified, Duncan's Multiple Range Test was used for grouping factors into further significant sub-ranges.

3.12 Test Procedures

3.12.1 Strand Testing, Strength

The strands in a perfectly articulated, bonded, and oriented composite are loaded in tension along their length continuously

except for small, randomly spaced discontinuities. The zero span test approximates this load condition more closely than extended gage length testing. In addition, the highest correlation coefficients between density and strength have been found when using this method in microtensile testing (52). This is important because such linearity is assumed in the present study. For these reasons, the following zero span procedure was adopted.

The parallel specimens were prepared using the same cutting dies as used in Wellwood's (93) and Wilson's (95) research. The specimen shape was nominally 0.42 X 6.0 cm; this was used for aspen, pine, cedar and alder. The exception was birch, because of grip pull-out on the thicker strands which were used. The birch shapes were changed to the necked-down configuration also specified in Wellwood's (93) work. These specimens were 9.0 X 0.42 cm with the critical necked zone having a gage length of 1.27 cm and neck width of 0.15 cm. Parallel grain specimens are pictured in Appendix iv.

The perpendicular to grain specimens were cut from randomly selected strands, to width of 1.5 cm by up to 3.0 cm in length across the grain. Both flat cut and quarter cut specimens were included in the random selection. All positions in the tree were represented by the random selection of test strands.

All specimen preparation and testing was as 20°C and 50 percent R.H. with corresponding equilibrium moisture content of the wood at 7 to 9 percent. The Thwing-Albert QCII electronic tensile tester provided by the Pulp and Paper Research Institute of Canada was equipped with pneumatic grips which were able to apply 4 MPa pressure on the specimens. This is near the

perpendicular compressive yield strength of the woods that were tested and is also close to the pressures used in pressing OSB industrially. The tensile strength was calculated as the load at failure divided by the uncompressed strand cross sectional area. The specific strength of a strand was obtained by dividing this strength by the specimen's density. Weights were at oven-dry and volumes were at 7 to 9 percent EMC in the density calculation. The dimensions of the strand blanks were measured by micrometer for density determination.

Alignment in the grips was critical, and specimens that were misaligned by more than 0.5 degrees from parallel to the test force axis were discarded. The speed of testing (0.45 cm/min) was the same as specified in the ASTM D1037-86 procedure which was later used for testing the composites in tension. Twelve parallel and 35 perpendicular specimens were included in the data for each species.

3.12.2 Composite Tensile Strength

The test procedure followed ASTM D1037-86 using necked specimens as diagrammed in Appendix iv. The rectangular dimensions of the specimen were 5.1 cm X 25.5 cm with a necked gage length of 5.1 cm. The test average moisture content was 7 to 8 percent as a result of preconditioning at 20°C and 50 percent R.H. for 6 weeks. Specimens of this shape were used to test the zero degree direction, parallel to the axis and also the perpendicular direction. The test specimens were cut from 5 pressed replicate panels, as shown in the Appendix iv. A clear plastic marking template was placed on either the face or back of

the panels randomly and also randomly with respect to the top and bottom parallel reference edges. The purpose of this was to randomize any systematic orientation or density gradient artifacts. The same procedure was applied to the randomly oriented boards. One tensile specimen for parallel and one for perpendicular testing was cut from each replicate.

The rate of extension was 0.45 cm/min on the Tinius Olsen universal testing machine used at the UBC Forestry Dept. Conditions in the test room were 20°C and 50 percent R.H.

Noting the effect of specimen size in brittle failure of wood perpendicular to grain (10) adds importance to the compromise of using a standardized ASTM D1037 composite specimen size. This test size included bonding effects, as opposed to a zero span test which would have made bond effects smaller. The size effects must be tolerated for the purpose of testing an actual bonded composite. Size effects are complicated by the strand wood having a different crack microstructure than the bonded composite.

3.12.3 Composite Flexural Strength

The flexural test method was Canadian Standards Assoc (CSA) CAN-0437-M85 which closely references ASTM standard D1037 on flexural strength (MOR). The specimens were rectangular with the width modified from the 7.5 cm specification to 5.0 cm to accommodate the 5 specimens per board cutting pattern shown in Appendix iv. The length was 18.0 cm, allowing the requirement that the span be at least 24 times the thickness (0.55 cm). Five replicate panels were cut using the angled template in a

randomized fashion to minimize any within-panel inhomogeneity. Conditioning of the panels was the same as for the tensile tests. The static bending tests were performed by the Alberta Research Council under the above standards and specimen preparation using the further specification of:

span	. . . . .	13.2 cm
crosshead speed	. . . . .	0.264 cm/min
conditioning	. . . . .	20°C, 50%, R.H. - 6 weeks

4. RESULTS

4.1 Strand Orientation

4.1.1 Concentration Parameter, k

The primary objective of Harris (34) was the establishment of an accurate, verified, sampling technique to estimate k. A feature of this was the limitation to a practical number of 100 strand angle measurements for each k parameter estimate. Using this guide for the present thesis, the following levels of orientation were obtained from composites formed in the laboratory and from an industrial board core. A description of the lab formation process is found in section 3.8. The concentration parameters were calculated using Equations [2], [3], [4] and [8]. The intent was to assign and measure, not assiduously control, orientation. The Table 6 confidence limits were based on the plots by Mardia (58).

Inspection of this data showed the tendency of identical furnish samples having equal formation treatments, to orient to higher k parameters when the liquid resin level was low or when powder resin was used. This effect was attributed to the higher tackiness that the high liquid resin levels produced, relative to the low liquid level and powder resin. This serendipitous finding led to the speculation that less tacky resins such as crude 4,4 diphenyl methane diisocyanate (MDI), may allow better orientation in some mechanical orienters. The revelation of this tackiness effect demonstrated the sensitivity of the k measurement very well.

Table 6. Orientation levels

Liquid Resin Level 0.57 g/cm²

Oriented Strands	k, concentration parameter	r	90 percent C.L. upper	lower
T. Aspen	3.2	0.828	4.0	2.6
R. Alder	4.9	0.892	5.5	3.7
R. Cedar	2.8	0.795	3.4	2.3
L. Pine	3.4	0.840	4.2	2.7

Liquid Resin Level 1.14 g/cm²

Oriented Strands	k, concentration parameter	r	90 percent C.L. upper	lower
T. Aspen	2.3	0.735	2.7	1.8
R. Alder	3.5	0.842	4.4	2.8
R. Cedar	2.1	0.704	2.5	1.7
L. Pine	3.4	0.840	4.2	2.7

Liquid Resin Level 1.76 g/cm²

Oriented Strands	k, concentration parameter	r	90 percent C.L. upper	lower
R. Cedar	1.9	0.689	2.3	1.6
Y. Birch	9.0	0.942	10.2	7.1

Powdered Resin Level 2.0%

Oriented Strands	k, concentration parameter	r	90 percent C.L. upper	lower
T. Aspen (lab)	2.4	0.754	2.8	1.9
T. Aspen (industrial)	1.1	0.471	1.3	0.8

(Data Combined) Liquid Resin Levels at both 0.57 and 1.14 g/cm²

Random Strands	k, concentration parameter	r	90 percent C.L. upper	lower
T. Aspen	0.01	0.004	0.0	0.0
R. Alder	0.02	0.009	0.0	0.0
R. Cedar	0.26	0.131	0.5	0.0
L. Pine	0.01	0.008	0.0	0.0
Y. Birch	0.15	0.073	0.2	0.0

4.1.2 Goodness of Fit

The choice of the von Mises distribution was taken under the assumption that the distribution of strand grain orientation would follow this form of continuous probability distribution. The goodness of fit test was to see if the observations contradicted the distribution and whether the discrepancies could be explained by either chance fluctuation or the wrong choice of distribution.

The Chi-square test statistic was as used. This is the same expression used for ordinary noncircular distributions.

$$X^2 = \sum_{i=1}^{p} \frac{(n_i - e_i)^2}{e_i} \qquad [22]$$

e_i = the frequency of observation expected on the basis of the von Mises pdf

n_i = the observed frequency of strand angles in a cell.

The axial strand angle data was sorted into p = 12 cells of 15 degree increments, this gave the observed frequency distribution of the 100 measured strands in each treatment. The expected frequency, e_i, of a cell was computed by integration of the von Mises pdf between the cell limits. The resulting fraction of the total sample size (100) gave the expected frequency. The null hypothesis was that the observed sample be consistent with the expected population curve. This was tested at the alpha level of p = 0.05 probability of false rejection. A frequency polygon of the data from a sample of industrial OSB core layer is shown in Fig. 11. The hypothesis test showed that

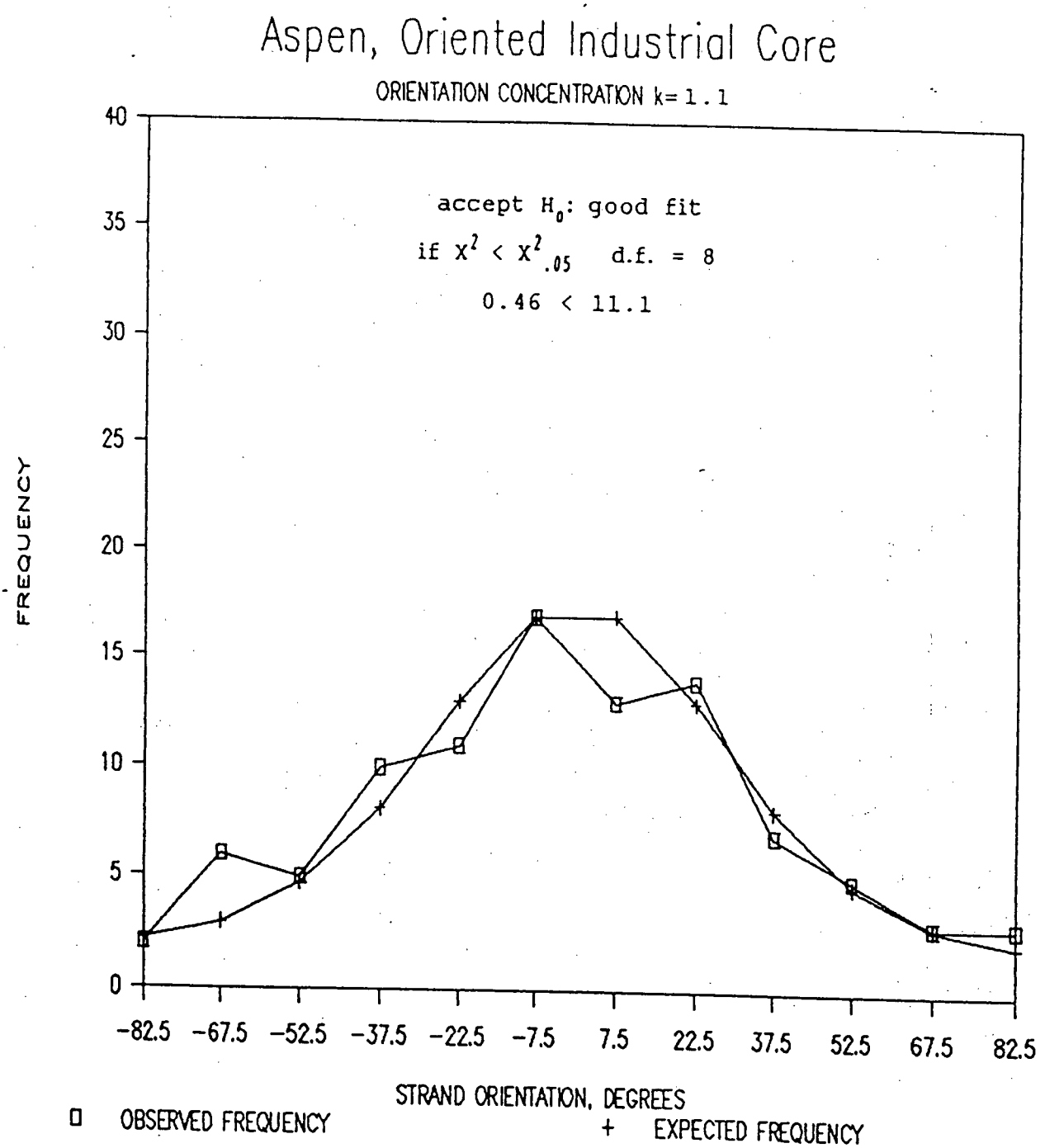

Figure 11. Curve fitting - aspen industrial oriented core

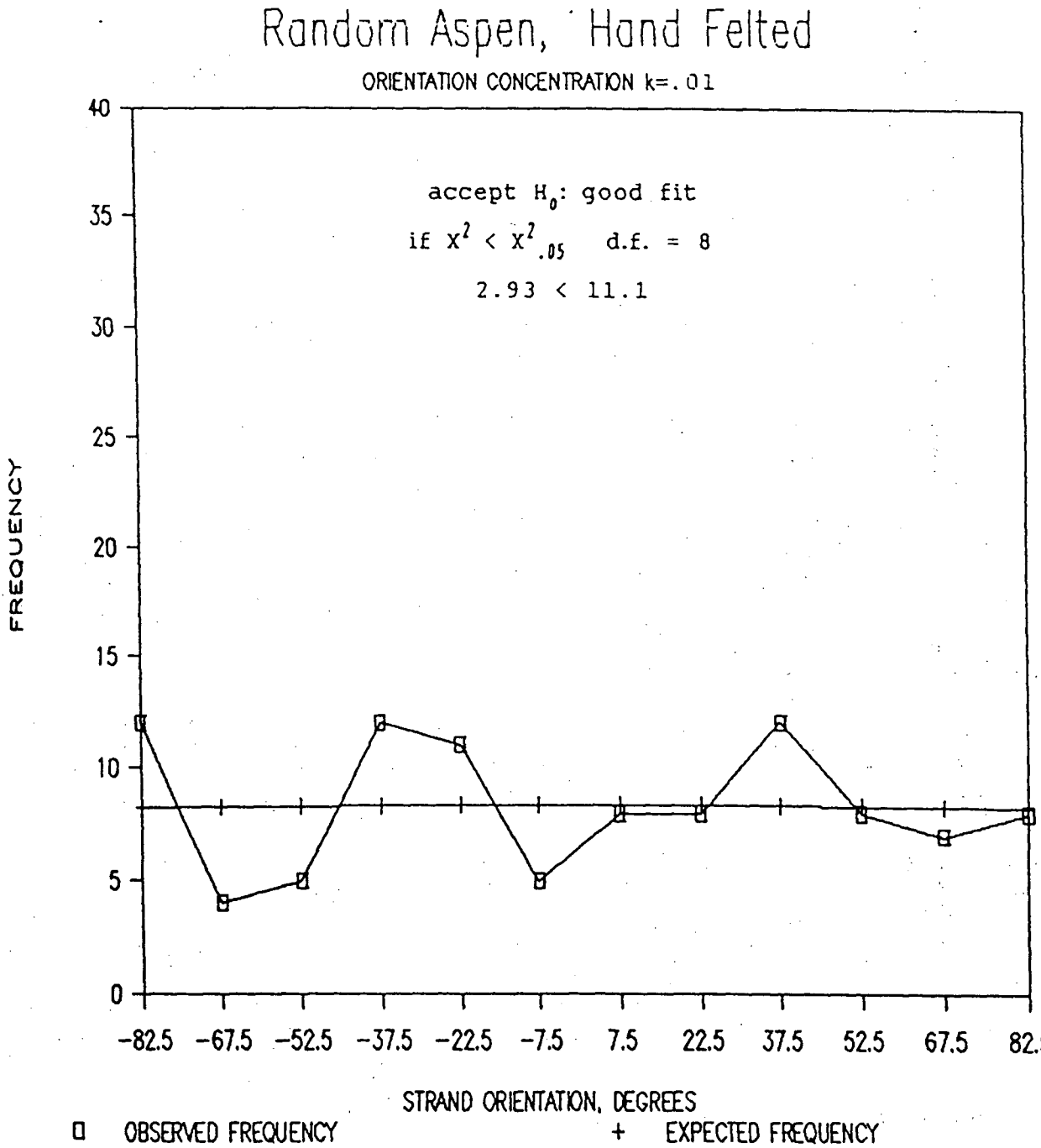

Figure 12. Curve fitting - random aspen, hand felted

the von Mises pdf fit the observed data satisfactorily. The null hypothesis of a good fit was not rejected at the p=0.05 level of error. The same applies to the random arrangement of the hand felted laboratory board orientation represented in Fig. 12. A summary of the results of the orientation k determination is provided in Table 6.

4.2 Process Variables

4.2.1 Strand Tensile Strength

The parallel to grain specific tensile strengths most closely resemble the specific MOR values calculated from the Wood Handbook (U.S.D.A., Madison) for each species at the 12 percent moisture condition. The Wood Handbook parallel MOR means were not significantly different from the strand tensile results presented in Table 7. The hypothesis of equality in this comparison was accepted at the p = 0.01 probability level of error. The perpendicular to grain strength comparison to the larger Wood Handbook tensile specimens indicates a possible specimen size effect on strength.

Table 7. Zero span, strand specific tensile strengths, MPa.

	R.Alder	T.Aspen	R.Cedar	L.Pine	Y.Birch
Parallel Grain, L					
Ave. Specific Strength, MPa	146.8	152.2	148.7	166.9	173.9
Std. Dev.	48.5	13.2	71.0	41.7	63.9
Perpendicular Grain, T					
Ave. Specific Strength, MPa	8.74	10.95	10.80	8.52	9.23
Std. Dev.	3.07	4.48	4.50	3.37	2.03
Wood Handbook, parallel grain MOR divided by density, 12% MC	164.8	152.4	160.9	158.6	184.6
Wood Handbook, perpendicular grain tensile strength, divided by density, 12% MC	7.1	4.7	4.6	4.9	10.2

Single factor (species) analyses of variance in completely randomized design were performed on the specific strength data summarized in Table 7. Sample size for the parallel grain analysis of variance was 12, and a minimum of 35 specimens of each species were analyzed in the perpendicular to grain direction. The null hypothesis that there is no difference between species specific tensile strength, parallel to grain, was accepted at the p=0.05 probability of false rejection. This was expected because of the uniform effects of cell wall material anticipated by the U.S.D.A. Wood Handbook (p.88). A cumulative probability distribution function plot of the parallel specific strength of the strands is presented in Appendix iii. Depending on specimen size, the parallel tensile strength of wood is usually larger than the corresponding bending strength and MOR's are often taken as conservative estimates of tensile strength. It is thought that the use of juvenile woods, or an artifact of the loading conditions, such as crushing in the test jaws, produced the unexpected lower tensile strengths and congruence with the Wood Handbook bending strengths for these species.

In testing perpendicular wood strength, the larger zero span results (relative to Wood Handbook values) are ascribed to specimen size effects. Birch was the only exception not showing this trend which is characteristic of brittle failure. Perpendicular to the grain, the species factor was significant at the p=0.05 level in the analysis of variance. A Duncan's multiple range test grouped the species as follows at a multiple range significance level of 0.01.

pine < aspen

alder < aspen

A typical cumulative distribution for the perpendicular specific tensile strength of cedar at zero span is plotted as an example in Appendix iii.

In summary, it should be noted that the strand specimen shape and loading conditions were chosen as part of the model hypothesis. They were contrived to approximate the condition of the strands in the composite, and served this primary purpose.

4.2.2 Resin Distribution: Spectrophotometry

Optimal resin distribution is the allotment of an equal and controlled amount of adhesive to each strand surface. For quality control or experimentation this should be extended over all batches processed. The random nature of blending means that optimal distribution is characterized by a narrow, symmetrically shaped histogram of resin take-up per strand. The blending process described in Section 3.7 achieved this in all species and with all resin levels blended. The desired symmetry was present in two trial widths of plastic tracer strands analyzed. A poor distribution histogram is marked by extreme skew to the left. This was the conclusion of Meinecke and Klauditz (60) and Kasper and Chow (42) who stressed the importance of strand-to-strand resin distribution.

Unpublished investigations by the author using a 90 to 120 micron droplet size, indicated that 25 to 30 percent of the strength perpendicular to the board surface (internal bond) was lost when random aspen board had as little as 10 percent of the

surfaces inadequately covered by adhesive. Minimal resin level was defined as the lowest spread required to cause wood shear failure. The minimum adhesive solids coverage was estimated to be in the order of 0.1 to 0.2 mg/cm^2, for resin in small droplets (10 micron) on ideally flat, dried, and pressed strands. These minimum spreads are extrapolations taken from the work of Suchsland (88), and Meinecke and Klauditz (60). Resin distribution in the present research is typified by Fig. 13 and 14, where virtually all strands received resin in a reasonably symmetrical distribution.

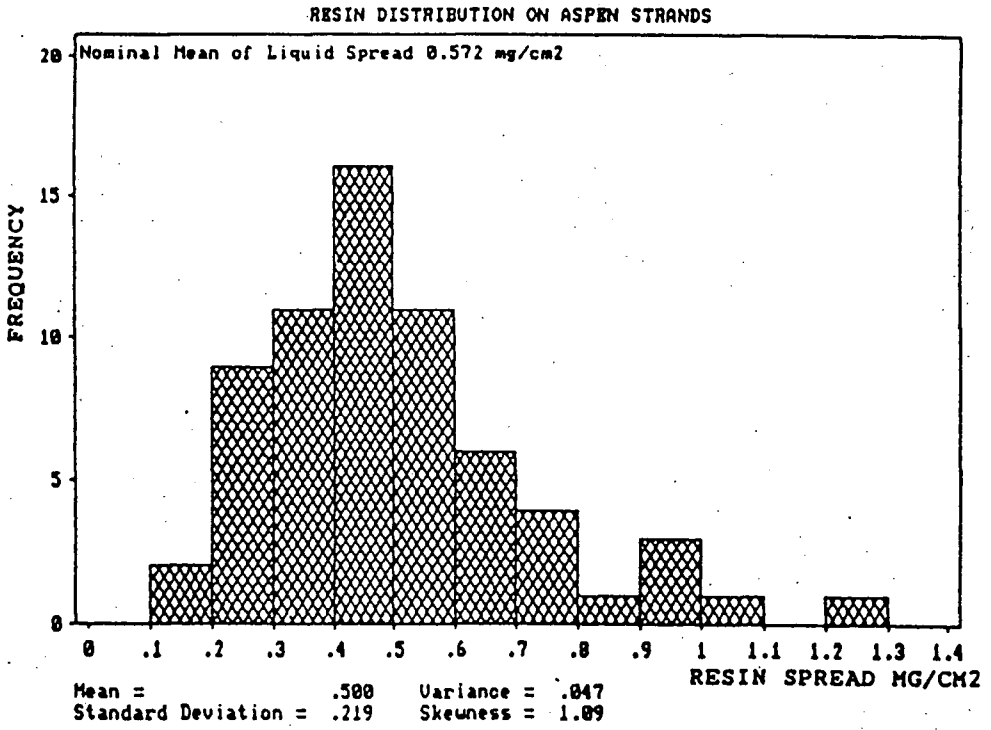

Figure 13. Resin distribution - aspen blending.

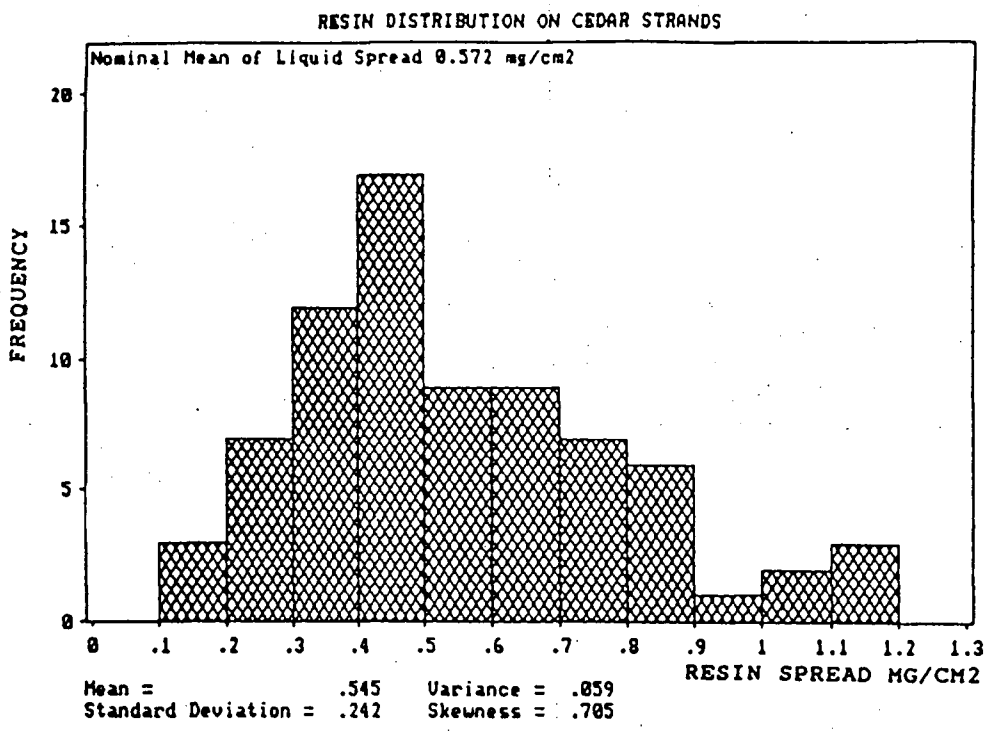

Figure 14. Resin distribution - cedar blending

Low blending rates usually favor good distribution, but expose large areas of blender wall surface to resin capture. Antagonistic to this, larger blender loads minimize resin losses to lab blender walls, but restrict good strand circulation in the blender. Losses of resin to the interior surfaces of the blender were estimated by resin recovery from test patches of vinyl sheeting which were taped to the ends and walls of the blender. When these losses were accounted for, the actual spread solids were only 4.7 to 12.7 percent under the nominal targets. Resin

material balance was correct when the total resin surface and blender interior were accounted for.

The histograms, Fig. 13 and 14, were made by determining the amounts of resin deposited on the surfaces of vinyl tracer strands that were spray blended with the normal wood furnish. The tracers had weight, length, and width equal to the corresponding averages of the wood strands. Fig. 13 and 14 typify results obtained as quality controls on all blender runs made in this research.

The most important advantage of determination of resin on separate sides of the strands is that it allows a probabalistic evaluation of bonding. The following derivation makes use of this distribution to assess the bonding potential of any vertical set of interface zones below an arbitrary location on the board surface. Considering a bonding zone of any area size between strands to be a bonding "interface cell" it is possible to estimate the probability, of at least one interface in a vertical stack sequence through the board thickness having no adhesive spray on either cell side. This is defined as a discontinous bond sequence with probability f. It is estimated on a randomly located vertical line through the thickness, disregarding voids. It is given by:

$$f = 1 - (1-p^2)^{M-1} \qquad [23]$$

where:

p = probability of zero or less than minimal resin spread on one side of a strand (exactly). This is termed a blank side.
M = the number of strands forming the thickness of the board.
The expression [23] is derived as follows:

Consider the interface as a binary cell of two sides with the restrictions:

a) probability of a blank on one side is independent of a blank being on the other side of the strands (or interface)

b) there is a random order of strands with respect to the stack (M) sequence

let p = prob [of exactly one side of interface blank]

then p^2 = prob [both sides of the interface blank], successively,

and $(1-p^2)$ = prob [not both sides of interface blank] = prob [of bond interface, with one or both sides sprayed]

In a stack of M strands there are M-1 interface cells. Therefore for M-1 successive bonded interfaces we have:

$$f = 1-(1-p^2)^{M-1} = \text{prob}[\underline{\text{not}}\ \text{M-1 successive bonded interfaces}] = \text{prob}[\text{at least one interface not bonded}]$$

Thus, "f" is defined, as the probability of there being a weak link of variable size, in the chain of strand bonds holding the board together.

The "f" defect criterion was experimentally related to internal bond strength in previous research at Borden Chemical Ltd. The result was a rapid loss of internal bond up to f=0.10 followed by a diminished rate of loss (slope) as f exceeded 0.10.

The probability, p, was also derived from the dynamics of the blender, as mentioned in Section 3.7.

In summary, all blending for this research was done at a bond defect probability, f, of less than 0.03. The manufacture of specimens in this fashion helped assure that bond defects did not confound the test of the orientation model. The strand-to-strand resin distribution was probably more uniform than produced by current industrial liquid resin blenders, but less than optimum.

4.2.3 Resin Dispersion: Image Analysis

Maloney et al. (57) emphasized that a near continuous film of resin be present between bonded strands for maximum and efficient strength development. This requires the dispersion of the resin into fine droplets or fragments that can flow into a film before or during board consolidation. Holding all other factors constant, droplet size alone, was shown by Meinecke and Klauditz (60) to have a significant range of influence over the internal bond and tensile strength of spruce strand boards. This range was secondary to that resulting from manipulation of strand-to-strand distribution. The droplet size (dispersion) effect on strength was found to vanish at a diminishing diameter size depending on the resin melt-flow properties, species, and pressing conditions. Strand surface roughness and drying history also play roles in glue line quality. The primary importance of glueline strength was emphasized by Simpson (79) in a tensile strength model for strandboard. In Simpson's model, the shear strength of the wood or the bond, whichever was lowest, limited

the tensile strength of the composite. This is common to the present research.

The merit of the examination of droplet size lay in placing in perspective its possible contribution to any shortfall in specific tensile strength relative to the expectation of the model. The documentation of the resin droplet histograms was also important for proper characterization of the composites and for control of the experimental comparisons.

A further objective was to explore the use of computerized image analysis in resin droplet and fragment size characterization. A Leitz instrument at the Department of Metallurgy, U.B.C. was used. In initial trials, it was seen that the method was practical if flat plastic tracer strands were used rather than wood strands. This was because optical microscopy was limited to picturing a field of 1 cm diameter containing perhaps 100 droplets. This lacked the depth of field to focus the height of grooves and roughness found on wood strands. Measurements were made of the major diameter of the irregular resin shapes. The volume of spheres and ellipsoids related to these diameters was shown by Lehman (53) to be proportional to the third power of the diameter. The meaning of this is that if the droplet diameter were reduced by one half; then the number of droplets dispersed over the same area would be increased by eight times. This explains how smaller droplet size promotes more continuous resin films by reducing the requirement for melt flow.

The use of extremely small particle or droplet size in adhesives has a limitation due to the surface roughness of the strands. Resin that is fragmented or sprayed small enough to

enter into fiber grooves, pits and wide cut lumen vessels is lost to the glue line, according to Meinecke and Klauditz (60). This is especially true of powdered resins where the particles are rubbed into grooves during blending and formation. In microscopic examination of the industrial powder resin, both spherical and irregular broken-shell shapes were observed. The irregular shapes are preferred because they have less tendency to migrate to grooves and to roll off the strands onto the cauls during mat formation. Examples of the liquid resin droplet sizes and powder particle sizes observed are presented in Fig. 15 and 16. The results are typical of blender runs on all the species in this thesis. The width of the plastic tracer strands made no observable difference to the results.

The interplay of droplet size and minimum spread was studied in detail by Meinecke and Klauditz (60). While assuming a good strand to strand distribution, they showed that reduction of droplet size from 100 microns to 50 microns resulted in an approximate 30 percent gain in tensile strength, parallel to the surface, in random flakeboard. The actual optimum droplet size is dependent on the resin, moisture content, temperature, species, board density, strand roughness and consolidation pressure.

Lehman (53) found bond improvement by merely reducing the variance of the droplet dispersion, using a phenol-formaldehyde (P.F.) resin having an average droplet diameter of 37 to 39 microns. The best available spinning disk atomizers are now claimed to operate in the 40 to 80 micron range. However application results vary with blender design, how fully the

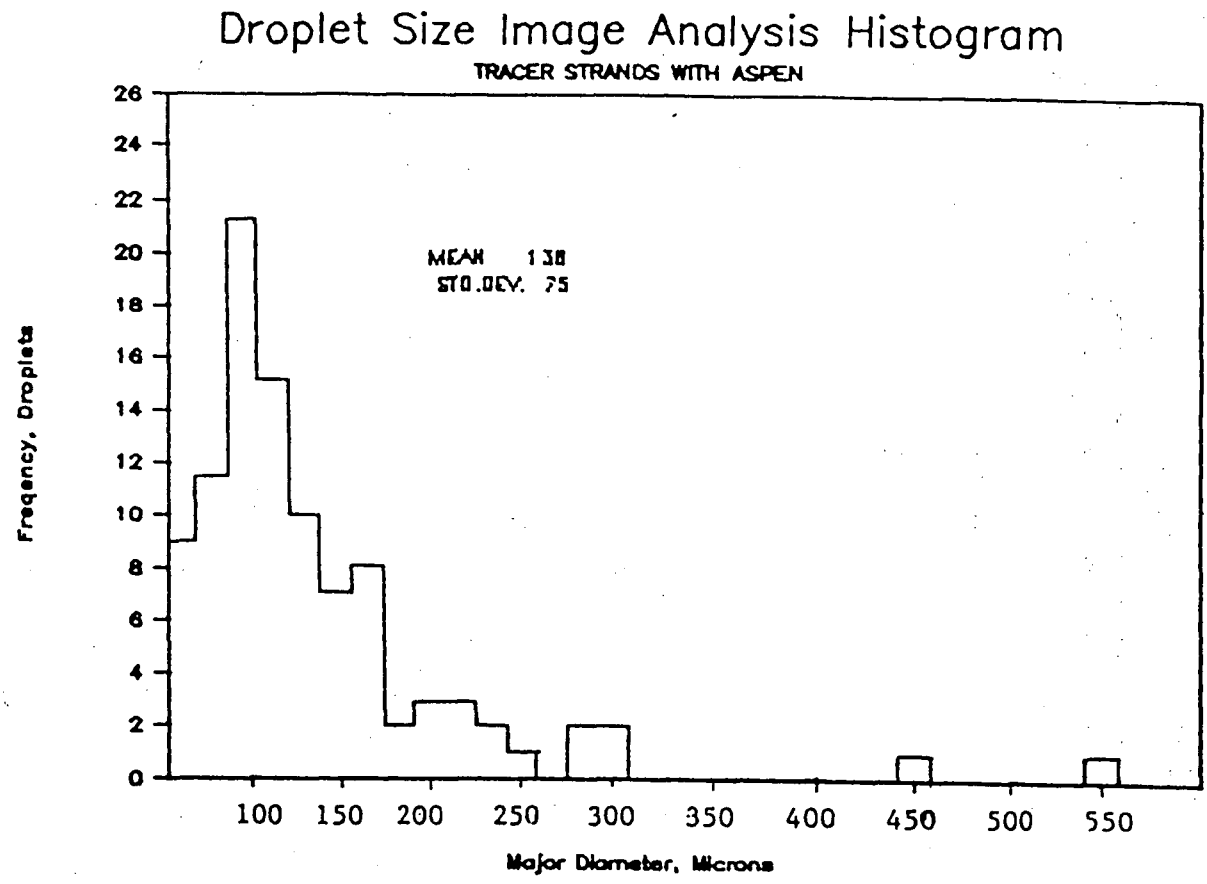

Figure 15. Resin dispersion - tracer strands with aspen.

blender is loaded, and how close the strands pass to the disk(s).

In summary, the experimental use of a relatively large average droplet size (138 micron) opened the question of ascribing small losses in tensile strength to the resulting possible lack of a continuous bonding film. The larger droplet ranges used in current industry and in this thesis were a concession to the limitations of currently available equipment.

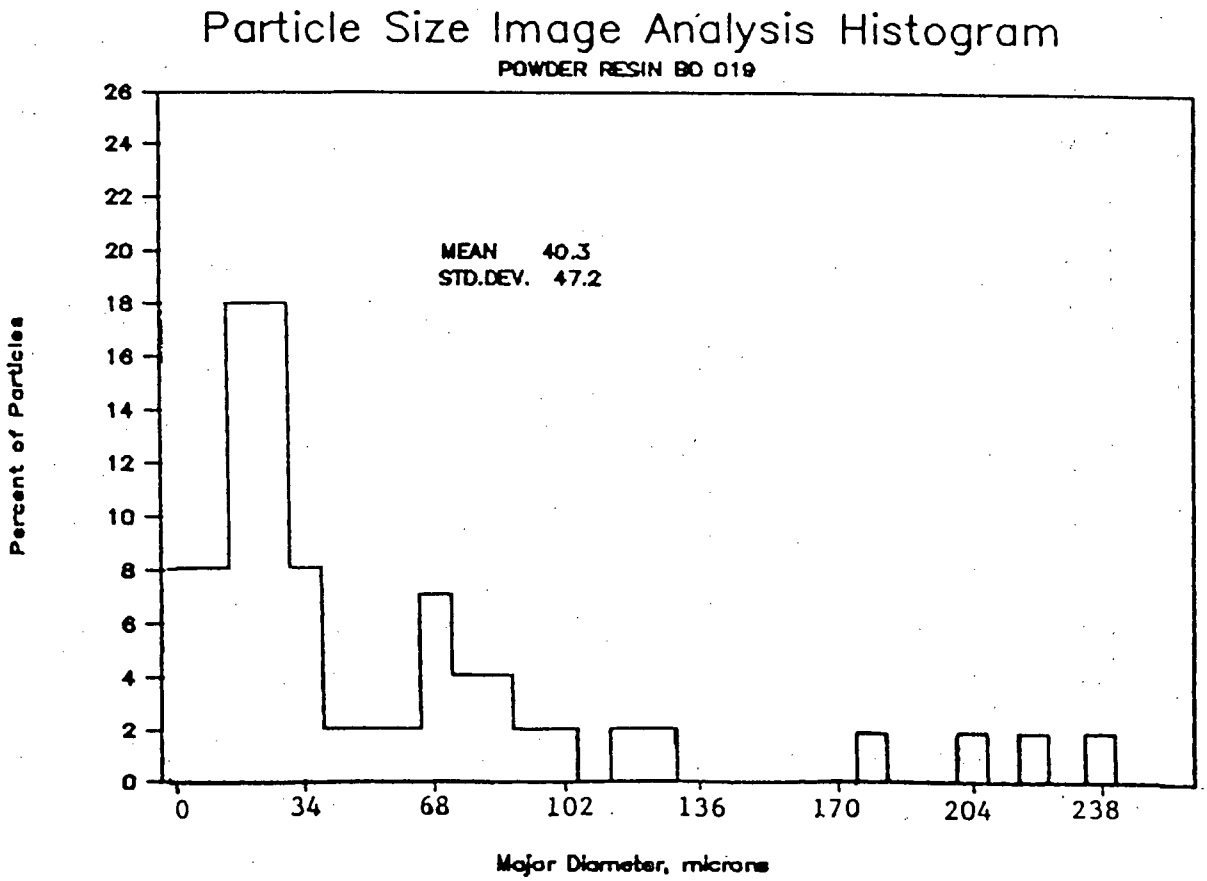

Figure 16. Resin dispersion - powder resin.

4.2.4 Composite Density Gradient

As discussed in Section 3.10.4 and 2.4, a density gradient, increasing toward the board surfaces, has a major effect on flexural specific MOR. Because strength comparisons to the model were to be made, it was required that the controlling surface density be known. Numerous factors affect the formation of a nonuniform density profile, such as:

- overall board density and compaction ratio,
- size, shape and orientation of strands,
- press closing rate, pressure-time profile,

- strand moisture content, steam injection,
- type of resin, wood species.

Some of these variables were investigated by Strickler (86), Steiner et al. (83), and Harless et al. (32).

The following considerations suggested that a thin layer be removed from the board surfaces after cooling from the press.

1. Resin precure can leave a densified but weakly bonded, thin, surface layer.

2. Higher densification of the immediate 2 or 3 strand layers beneath the pressed surface was observed by Strickler (86). These layers were found to be more critical determinants of MOR than the extreme surface densities.

Strickler (86) suggested the surface looseness was due to unrestricted spring back on short press cycles. Density profiles with this character were also reported by Kieser et al. (45) and are described fairly commonly in the literature.

For improved use of the MOR formula, it was decided that removing the surface layers to a depth of a few strands would avoid possible inaccuracies caused by not being able to assume first failure of the strongest strands at the surface. Moreover, removal of caul glaze and sizing to thickness by sanding is common to a large portion of industrial production. In this experimental work, it also allowed better inspection of strand angles for orientation measurements.

The results of the density scans are typified in Fig. 17. The numerically integrated average density was divided into the peak surface density to give a ratio used as a criterion of surface densification. This ratio varied with species, orientation, and resin level. The means of 5 scans of each

specimen type resulted in the data of Table 8. The results were randomized over test locations on the boards and over board replicates. Scanning through the radial, tangential and longitudinal direction of the strands was also randomized. The ratios were similar to those reported by Laufenberg (49).

The density ratios of Table 8 were used to adjust the gravimetric average densities to values representative of the surfaces of the specimens. The MOR values obtained from tests were then reported in terms of specific MOR, calculated as the maximum fiber stress (MOR) divided by the density of the specimen's surface.

Example:

MOR test result for a typical specimen, red alder, at resin level 0.57 mg/cm^2, orientation k=4.9, and tested in the parallel, 0°, direction . . . . . 63.45 MPa

Mean density of red alder specimen 0.59 . . . . . 0.59 g/cm^3

Ratio surface density/mean density, for red alder . . 1.36

Specific MOR (surface) is therefore:

63.45/0.59/1.36 = 79.1 MPa

Table 8. Density ratios, surface to mean

Species	Resin Level mg/cm²	k, orientation level	Surface/mean density ratio air dry
R. Alder	0.57 oriented	4.9	1.36
	1.14 oriented	3.5	1.43
	0.57 random	0.02	1.48
	1.14 random	0.02	1.52
T. Aspen	0.57 oriented	3.2	1.27
	1.14 oriented	2.3	1.37
	0.57 random	0.01	1.59
	1.14 random	0.01	1.63
R. Cedar	0.57 oriented	2.8	1.33
	1.14 oriented	2.1	1.43
	0.57 random	0.26	1.38
	1.14 random	0.26	1.41
L. Pine	0.57 oriented	3.4	1.27
	1.14 oriented	3.4	1.30
	0.57 random	0.14	1.35
	1.14 random	0.14	1.45
Y. Birch	1.76 oriented	9.0	1.10
	1.76 random	0.15	1.50
Industrial core, aspen	2.0 percent powder	1.1	1.10
Laboratory oriented aspen	2.0 percent powder	2.4	1.10
Laboratory random aspen	2.0 percent powder	0.4	1.60

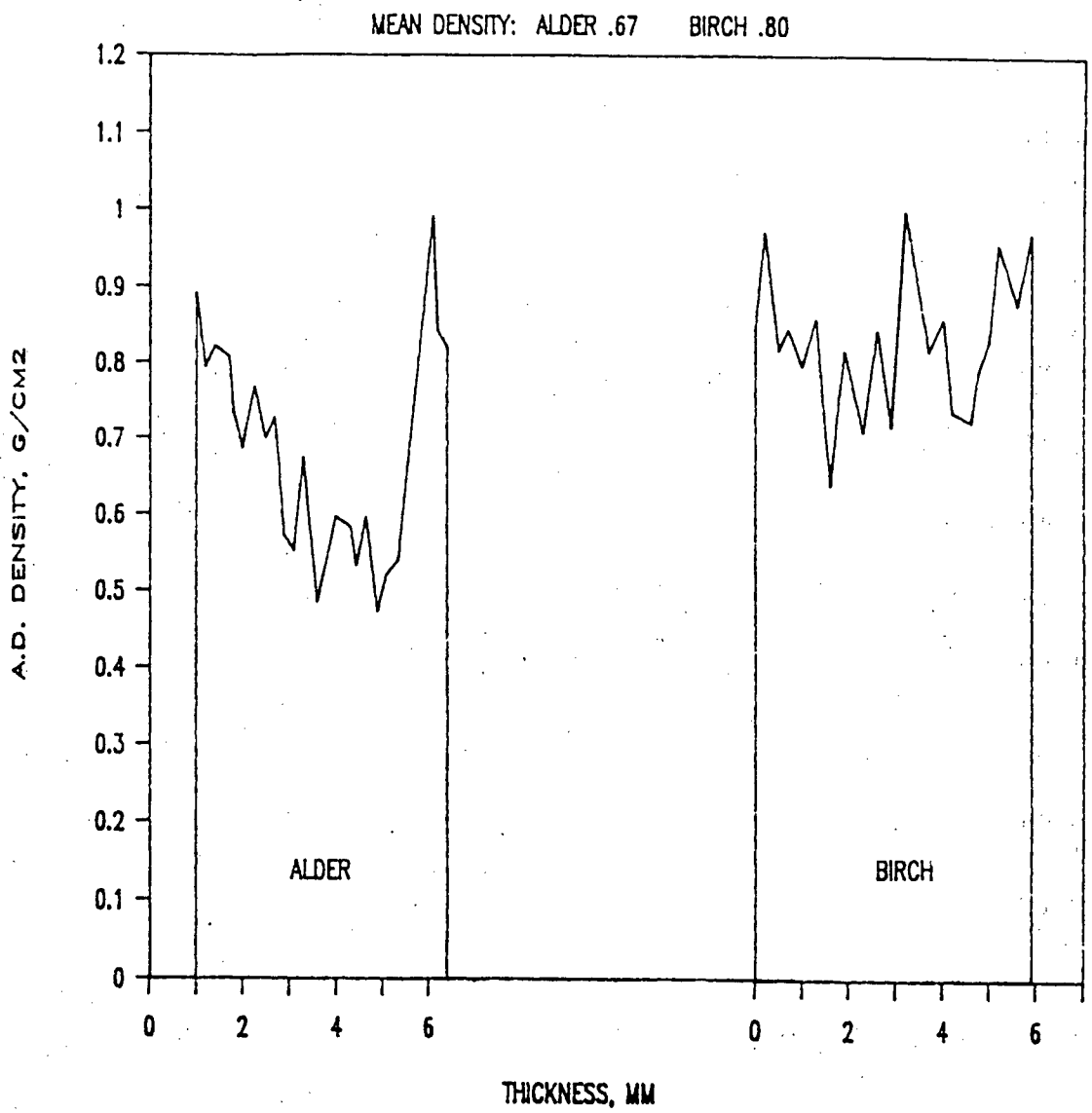

Figure 17. Typical density gradient profiles.

4.3 Results, Specific Tensile Strength

4.3.1 Tensile Strength, Oriented Composites

In the panelboard industry, oriented, one direction multiple strand layers have substantially replaced veneer as laminae in structural panels. Through the effects of higher surface density and higher overall density, it is possible for the non-veneer panels to gain equality with plywood in flexural strength. However, higher board density requires increased cost. A feature of the present specific tensile strength criterion is that it views comparisons on the basis of efficiency of wood usage (per unit weight). When this criterion is used, the effect of enhanced surface density is mostly eliminated. The level of performance that the non-veneer lamina achieves is put into an comparative perspective with veneer in Table 9.

In Table 9, much of the composite strength reduction relative to natural wood is attributable to imperfect orientation of the strands. Provision of adequate bonding and an orientation level of k=12 would yield a parallel-axis specific strength of about 80 percent of that of parallel-grain natural wood. An orientation level of k=9.0 was easily achieved with the long strand birch flexural specimens (Fig. 27) in this research. At k=9.0 the parallel-axis specific MOR of the composite was 66.6 percent of the parallel-grain specific strength of the wood strands. The continuous strand model was used for calculation of these mathematical expectations, (Equation [13]). Comparison of the experimental orientation levels to those present in industry (k=1.1) showed that the potentials of orientation are not fully exploited by OSB makers.

Table 9. Composite/wood specific strength comparison, MPa units

Species	Resin level mg/cm^2	Orientation Parameter k	(Source: Table 10) Parallel Specific Tensile Strength of composite	(Source: Table 7) Parallel grain Specific Tensile strength of strand	Percent composite/ strand
R. Alder	0.57	4.9	49.2	146.8	33.5
R. Cedar	0.57	2.8	36.3	148.7	24.4
L. Pine	0.57	3.4	47.5	166.9	28.5
T. Aspen	0.57	3.2	36.0	152.2	23.6
T. Aspen (industrial core)	2% powder	1.1	21.7	152.2	14.2
R. Alder	1.14	3.5	57.5	146.8	39.2
R. Cedar	1.14	2.1	46.8	148.7	31.5
L. Pine	1.14	3.4	52.8	166.9	31.6
T. Aspen	1.14	2.3	47.1	152.2	30.9
R. Cedar	1.76	1.9	54.5	148.7	36.6

An important feature of this research was the comparison of the actual ultimate strengths to the predictions of the model. These comparisons are presented in Tables 10 and 11. The results also permit species and resin effects to be evaluated, but with the restriction that those compared have similar (k) value of orientation. Tables 10 and 11 show that the strengths expected of continuous strand networks were not totally achieved in any species. These conclusions were made using individual "t" tests for the mean strengths against the model prediction. The tests were at the p=0.05 level of significance.

The test percentages of the theoretical model specific tensile strengths, parallel to orientation, increased with resin content, as seen in Table 11. The continuous strand model expectations of Table 11 are based on Equation [13]. Two opposing effects on the specific tensile strength are demonstrated in Table 10. The orientation parameters, k, in column D are less than or equal to the corresponding ones in column C. In the parallel to axis direction, increased k values imply higher expected theoretical strengths (see Fig. 10). Thus, we expect a strength decrease for column D relative to C, for any decreases in k. But in comparing D to C, we note a doubling of resin level. This overcomes the expected strength decline and replaces it with an increase in all species.

Table 10. Tensile strengths, tested parallel to the orientation direction, MPa.

	A	B	C	D	E	F
	Strength at 0.57 mg/cm² resin level	Strength at 1.14 mg/cm² resin level	Specific Strength at 0.57 mg/cm² resin level	Specific Strength at 1.14 mg/cm² resin level	Theoretical Specific Strength based on Orientation 0.57 mg/cm² resin level	Theoretical Specific Strength based on Orientation 1.14 mg/cm² resin level
Red Alder	(k=4.9)	(k=3.5)	(k=4.9)	(k=3.5)	(k=4.9)	(k=3.5)
Mean	32.8	37.1	49.2	57.5	100.1	93.7
Std. Dev.	5.3	6.7	5.4	8.6		
Red Cedar	(k=2.8)	(k=2.1)	(k=2.8)	(k=2.1)	(k=2.8)	(k=2.1)
Mean	21.5	32.5	36.3	46.8	92.1	83.4
Std. Dev.	4.4	1.6	7.3	0.9		
Lodgepole Pine	(k=3.4)	(k=3.4)	(k=3.4)	(k=3.4)	(k=3.4)	(k=3.4)
Mean	30.1	35.3	47.5	52.8	100.6	100.6
Std. Dev.	2.6	6.7	2.3	10.6		
Trembling Aspen	(k=3.2)	(k=2.3)	(k=3.2)	(k=2.3)	(k=3.2)	(k=2.3)
Mean	23.5	30.7	36.0	47.1	98.5	87.9
Std. Dev.	9.2	2.4	10.3	5.7		

	Strength	Specific Strength	Theoretical Specific Strength Based on Orientation
Trembling Aspen laboratory board 2% powder resin	(k=2.4)	(k=2.4)	(k=2.4)
Mean	22.7	36.8	89.2
Std. Dev.	4.9	8.5	
Trembling Aspen Industrial Core 2% powder resin	(k=1.1)	(k=1.1)	(k=1.1)
Mean	11.9	21.7	66.6
Std. Dev.	1.4	2.0	
Red Cedar 1.76 mg/cm², resin level	(k=1.9)	(k=1.9)	(k=1.9)
Mean	33.3	54.5	81.1
Std. Dev.	4.8	5.0	

Table 11. Parallel specific tensile strength

Species	Percent of Model Expectation	
	0.57 mg/cm² resin level	1.14 mg/cm² resin level
R. Alder	48.6	61.4
R. Cedar	39.4	56.1
C. Pine	47.2	52.2
T. Aspen	36.5	53.6

		Percent of Model Expectation
T. Aspen	Lab board, 2 percent powder resin	41.2
T. Aspen	Industrial core 2 percent, powder	32.6
R. Cedar	1.76 mg/cm² liquid phenolic	67.2

An example of Table 11 results are demonstrated for red alder by division of the test specific tensile strength (resin 0.57 mg/cm²) by the model specific strength. The GWBASIC program in Appendix i generates the strength model expectation.

red alder test specific tensile strength (k=4.9) ..... 49.2 MPa
red alder expected specific strength (k=4.9) ..... 100.1 MPa

$$\text{Therefore, percent of model expectation} = \frac{49.2}{100.1} = 49.1\ \%$$

Some unplanned direct comparisons of species were possible where the k parameters were similar in the oriented composites of Table 10. Three comparisons are presented in Table 12.

Table 12. Parallel specific tensile strength: species

Resin Level	Species Compared	Specific Tensile Strength
0.57 mg/cm²	Aspen vs. Pine	no sig. diff.
1.14 mg/cm²	Aspen vs. Cedar	no sig. diff.
1.14 mg/cm²	Alder vs. Pine	no sig. diff.

These results were valid at the p=0.05 confidence level in one tailed "t" tests, for ordinary tensile strength as well as specific strength. It was concluded that significant specific strength differences were not apparent between these composites of these particular species. No differences had been anticipated in the (Table 12) pairs because parallel specific strand strengths, resin levels, and orientation levels, were common within each set. A further discussion of parallel tensile species strength difference is presented in Section 5.1.

The perpendicular to orientation specific tensile strengths are presented in Table 13. Two reinforcing effects on perpendicular tensile strength are evident in Table 13. The orientation parameters, k, in column D are less than or equal to those of column C. Note that in the perpendicular to orientation direction a change to a lower k level of orientation logically necessitates an increase in expected or theoretical strength (see Fig. 10). Therefore in Fig. 13 the observed increase in strength from column C to D, and from E to F, is justified by both a resin increase and by an orientation change. The comparison of perpendicular specific tensile strength to the theoretical expectation is made in Table 14.

Table 13. Tensile strengths, tested perpendicular to the orientation direction, MPa.

	A	B	C	D	E	F
	Strength at 0.57 mg/cm² resin level	Strength at 1.14 mg/cm² resin level	Specific Strength at 0.57 mg/cm² resin level	Specific Strength at 1.14 mg/cm² resin level	Theoretical Specific Strength based on Orientation: 0.57 mg/cm² resin level	Theoretical Specific Strength based on Orientation: 1.14 mg/cm² resin level
Red Alder	(k=4.9)	(k=3.5)	(k=4.9)	(k=3.5)	(k=4.9)	(k=3.5)
Mean	2.9	4.7	5.0	7.3	9.3	10.0
Std. Dev.	0.6	0.6	1.2	0.9		
Red Cedar	(k=2.8)	(k=2.1)	(k=2.8)	(k=2.1)	(k=2.8)	(k=2.1)
Mean	2.9	5.9	5.4	9.6	12.8	14.3
Std. Dev.	0.6	1.3	1.2	2.0		
Lodgepole Pine	(k=3.4)	(k=3.4)	(k=3.4)	(k=3.4)	(k=3.4)	(k=3.4)
Mean	3.2	3.9	5.0	6.6	9.8	9.8
Std. Dev.	1.2	1.1	1.9	2.2		
Trembling Aspen	(k=3.2)	(k=2.3)	(k=3.2)	(k=2.3)	(k=3.2)	(k=2.3)
Mean	4.5	4.7	7.4	8.0	12.6	13.9
Std. Dev.	0.3	0.5	1.4	1.6		

	Strength	Specific Strength	Theoretical Specific Strength Based on Orientation
Trembling Aspen laboratory board 2% powder resin	(k=2.4)	(k=2.4)	(k=2.4)
Mean	4.5	7.4	13.7
Std. Dev.	1.3	1.6	
Trembling Aspen Industrial Core 2% powder resin	(k=1.1)	(k=1.1)	(k=1.1)
Mean	3.7	7.3	21.6
Std. Dev.	0.9	1.3	
Red Cedar 1.76 mg/cm², resin level	(k=1.9)	(k=1.9)	(k=1.9)
Mean	4.5	7.1	14.9
Std. Dev.	0.8	1.3	

Table 14. Perpendicular specific tensile strength

Species	Percent of Model Expectation	
	0.57 mg/cm² resin level	1.14 mg/cm² resin level
R. Alder	53.7	73.0
R. Cedar	42.2	67.1
L. Pine	51.0	67.3
T. Aspen	58.7	57.6

		Percent of Model Expectation
R. Aspen	lab board, 2 percent powder resin	54.0
T. Aspen	industrial core, 2 percent powder	33.8
R. Cedar	1.76 mg/cm² liquid phenolic resin	47.6

4.3.2 Tensile Strength, Random Orientation

The comprehensive comparison of species strength in a factorial analysis was reserved for the random case where the orientation parameter was near k=0 in the various species and resin level combinations. In these specimens, the orientation parameter, k, was slightly above the theoretical zero level because the random mat formation was dropped manually into a rectangular forming box. However, the edges were trimmed, and no significant directional strength bias appeared in the randomly oriented tensile specimens. The data summarized in Table 16 was

Table 15. Random orientation, specific tensile strength analysis of variance

Source	d.f.	S.S.	M.S.	F	$F_{.05}$	
species	3	411.829	137.276	7.085	3.01	sig.
resin	1	18.015	18.015	0.929	4.26	not sig.
s x r	3	17.979	5.989	0.309	3.01	not sig.
error	24	464.990	19.374			
totals	31	912.800				

analyzed in a completely randomized design with fixed factors and four replicates. The two main factors were species and resin level. The independent variable was specific tensile strength.

Species was a significant factor, and resin level and interaction were not significant in their effect on specific tensile strength as shown in Table 15. On the basis of Duncan's multiple range test at a significance level $p = 0.05$, the randomly oriented pine boards were found lower in specific tensile strength than the aspen, cedar and alder. No other differences were significant. Like the perpendicular to orientation case, the random case showed no increase in strength with escalation of resin levels.

The very few strands in panels having random orientation with grain direction near parallel to the stress axis are the only ones capable of carrying higher loads than the applied adhesive will bear. In a shorter strand random aspen waferboard of 5 percent resin content (approximately 1.14 mg/cm^2), Laufenberg (50) observed about 4 percent unfailed strand pull-outs in a microscopic study of failure surfaces. On this basis it was thought that strengths approaching that of the model prediction would be achieved at both resin levels. This is verified for alder in Tables 16 and 17. The theoretical values are based on Equation [21]. The theoretical predictions of Table 17 provide a reasonable first approximation of strength in 3 out of 5 species. The strengths in Table 17 were averaged over both liquid resin levels, because the analysis of variance (Table 15) indicated no strength effect ascribable to the resin level.

Table 16. Random orientation, specific tensile strength

(Means were taken from 5 specimens cut at 0, 22.5, 45, 67.5 and 90 degrees to the axis)

	A Strength 0.57 mg/cm² resin level MPa	B Strength 1.14 mg/cm² resin MPa	C Specific Strength 0.57 mg/cm² resin, MPa	D Specific Strength 1.14 mg/cm² resin, MPa	E F Theoretical Strength based on orientation, MPa
R. Alder					
Mean	21.62	21.4	33.3	32.7	35.7
Std. Dev.	3.03	5.6	5.21	5.58	(k=.02)
R. Cedar					
Mean	16.8	17.7	27.3	30.2	40.7
Std. Dev.	5.11	2.3	5.16	1.47	(k=.26)
L. Pine					
Mean	14.2	14.1	22.6	24.6	37.5
Std. Dev.	3.91	4.92	3.91	4.23	(k=.01)
T. Aspen					
Mean	16.7	17.3	30.2	33.1	40.8
Std. Dev.	4.09	4.65	3.1	1.6	(k=.01)

Trembling Aspen, laboratory board 2% Powder resin	Strength	Specific Strength	Theoretical Specific Strength, MPa
Mean	13.9	24.2	40.8
Std. Dev.	3.33	2.06	(k=.04)

Because slight alignment was measured in the random orientations, the tabulated specific strength ranges presented are averages. The theoretical effect of the slight orientation was a range of about ± 5 MPa from the parallel to cross orientation direction.

Table 17. Comparative tensile strength of random composites for both resin levels combined.

Species	Composite Specific Tensile Strength, MPa	Percent of Theoretical Specific Strength	Tensile Strength as a Percent of Parallel Grain Strand Strength
R. Alder	33.0	92.4	22.5
R. Cedar	28.8	70.7	19.4
L. Pine	23.6	62.9	14.1
T. Aspen	31.6	77.6	20.8
T. Aspen (2% powder) (laboratory)	24.2	59.3	15.9

The specific tensile strength of lodgepole pine random oriented composites was significantly lower than that of the other species. Pine had to be pressed at lower compaction ratios relative to the others in Tables 16 and 17, to achieve the same nominal density. This was necessary because of the higher density of the pine strands themselves. The lower compaction ratio means that the consolidation of the strands allows more internal voids, and less internal bonding area. The result is excessive shear stress levels within the strand bonding areas and inadequate stress transfer. This mechanism is thought to partly explain the failure of the lodgepole pine to reach a high level of specific tensile strength relative to the theoretical model.

4.4 Results, Flexural Strength

4.4.1 Introduction

Knowledge of the flexural strength of unidirectional layers is important in the design of three layer OSB and the oriented strand lumber products of the future. To review, the objective required determination of:

- the ability of the model to predict the specific MOR at any angle of composite loading with respect to the principal axis of orientation,
- the effect of resin level and species on flexural strength,
- comparison of the ultimate specific surface stress in flexure of the composites to the specific tensile strength of the strands themselves.

The limitation of the flexural test to assess the ultimate fiber stress of materials having elastic inhomogeneity (density gradient) was discussed in Sections 3.10.4 and 4.2.4. Despite the violation of an assumed constant material elasticity, the flexure formula is commonly used by engineers to calculate nominal MOR in wood panel composites. Further, it should be recognized that variation between compression and tensile properties within a specimen can alter the MOR to be different from the fiber stress estimate of Equation [19].

Fig. 18 to 27 show the anisotropy of the specific MOR in five species and at two resin levels of oriented strand composite. The orientation levels go from lowest, (k=1.1) in the industrial core, to highest (k=9.0), in the yellow birch specimens. The limit bars associated with the means represent the standard deviation bounds of the test data. The continuous

strand theory solid lines are the calculated results of Equation [13]. An efficient way to evaluate the research hypothesis (model accuracy) in the bending property, is to assess the fit of data in Fig.18 to Fig.33 by visual inspection.

Tendencies of the data to fall modestly short of the theoretical MOR represented by the solid lines in Fig. 18 to 27 were identified in most comparisons, particularly at load angles approaching parallel to the orientation. The surface specific MOR was predicted well by Equation [13], at off-axis angles. The model's specific MOR strength prediction was usually within one standard deviation of the test data mean. Discrepancies in the parallel direction are discussed in section 5.1.

The inputs to the model Equation [13] were the mean specific tensile strengths of the strands in the two principal grain directions, L and T, (Table 7). Although these inputs to the strength algorithm are random variables, the effects on predicted strength of variation within them are relatively small. This is because they are widely separated in strength and because the algorithm is very sensitive to orientation (k).

4.4.2 Flexural Strength, Parallel to Orientation

The specific MOR values parallel to orientation are presented as the zero degree strengths in Fig. 18 through 27. In parallel specific MOR, the composites ranged from 26.9 to 66.6 percent of the specific tensile strength of the wood strands, parallel to grain. These extremes are for the aspen industrial core and birch composites respectively.

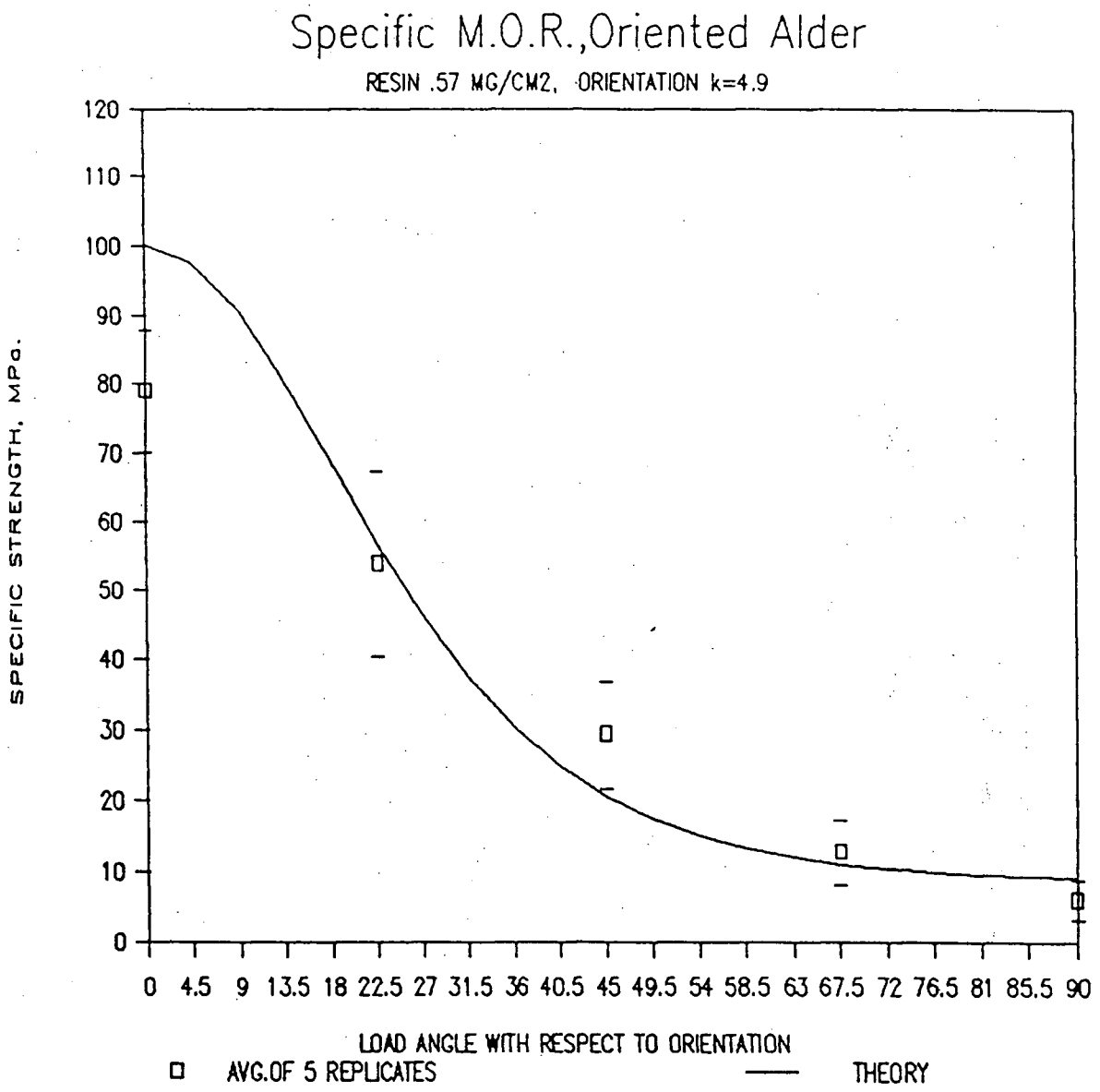

Figure 18. Specific MOR, oriented alder, low resin level

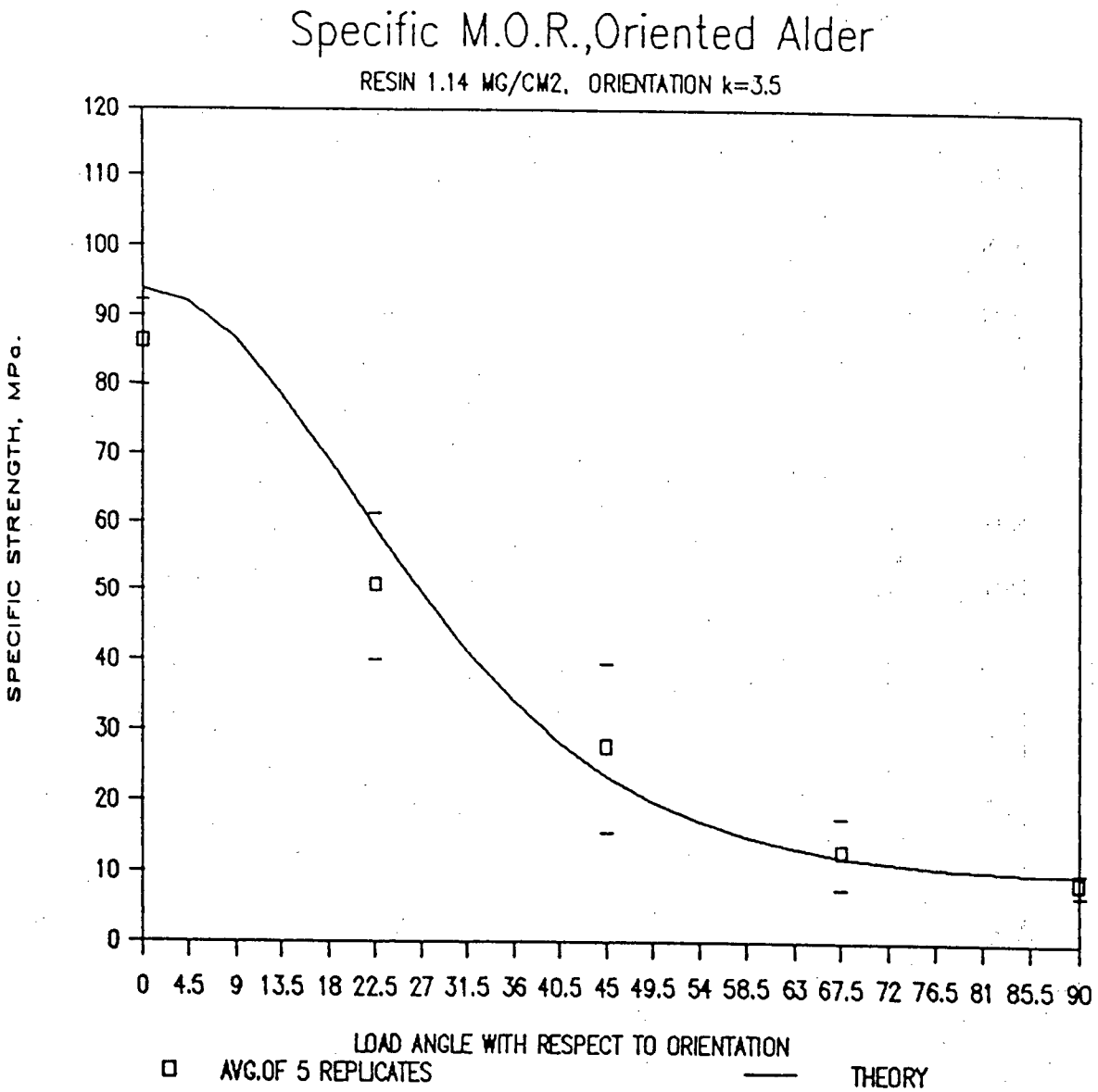

Figure 19. Specific MOR, oriented alder, high resin level.

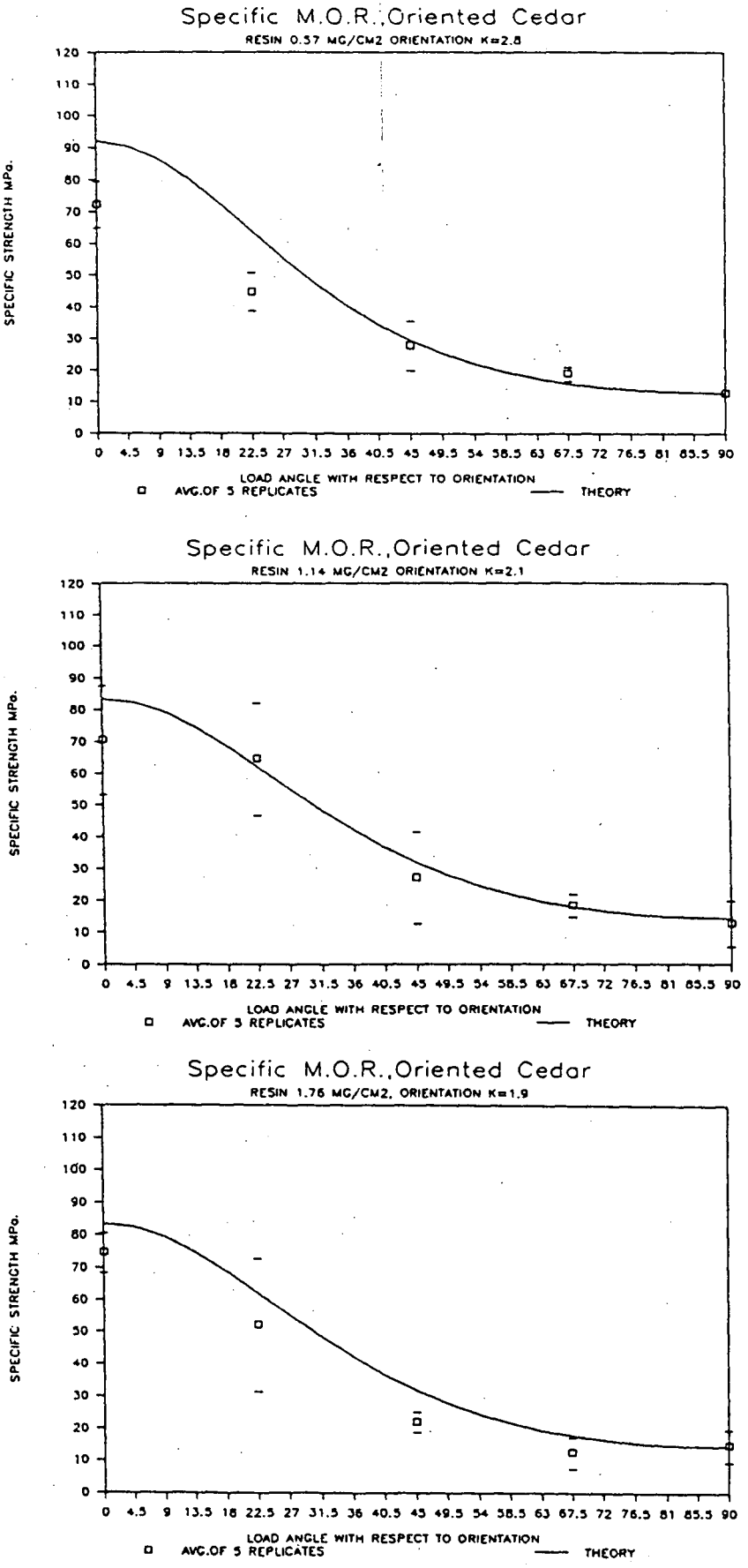

Figure 20. Specific MOR, oriented cedar

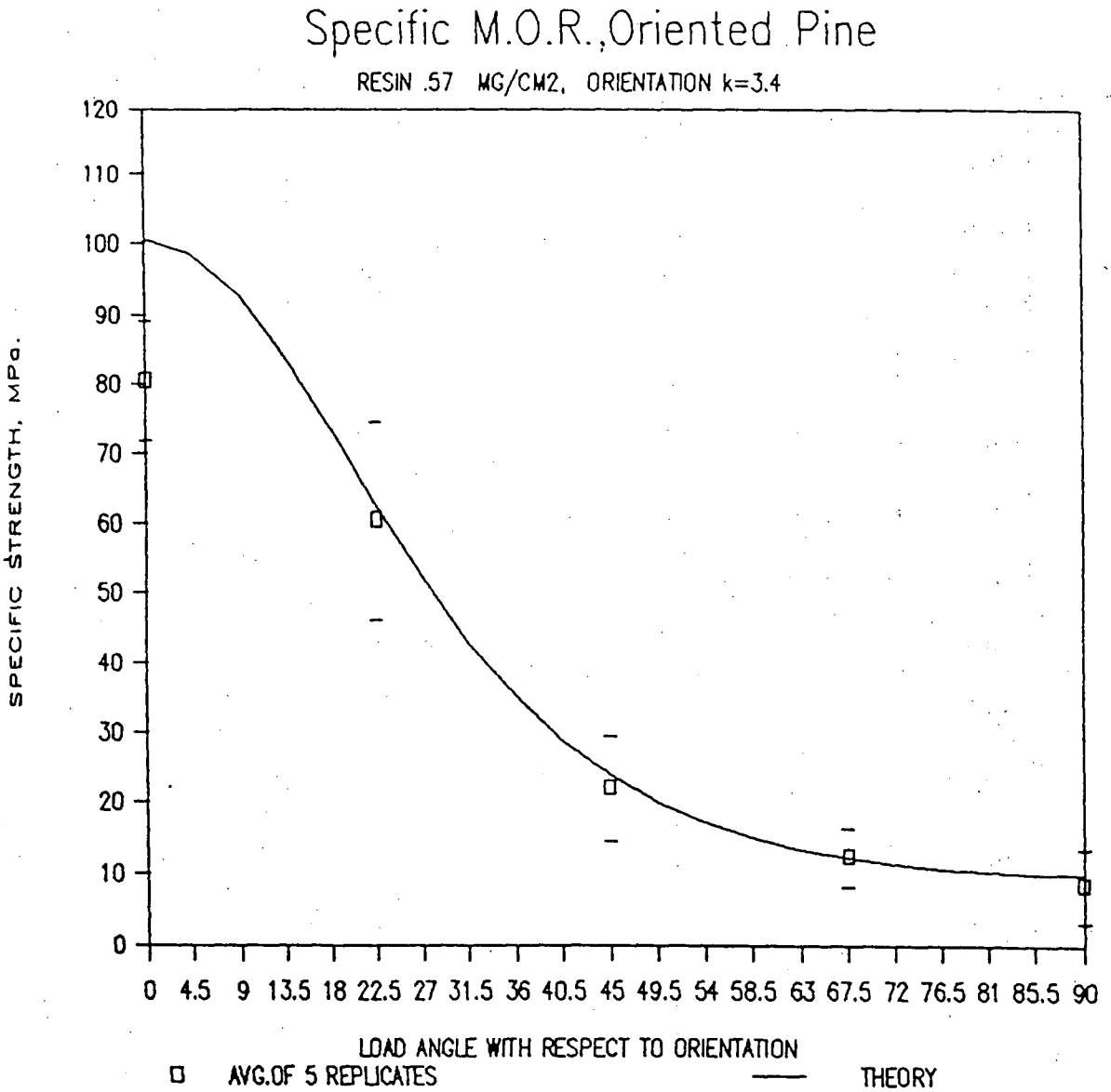

Figure 21. Specific MOR, oriented pine, low resin level

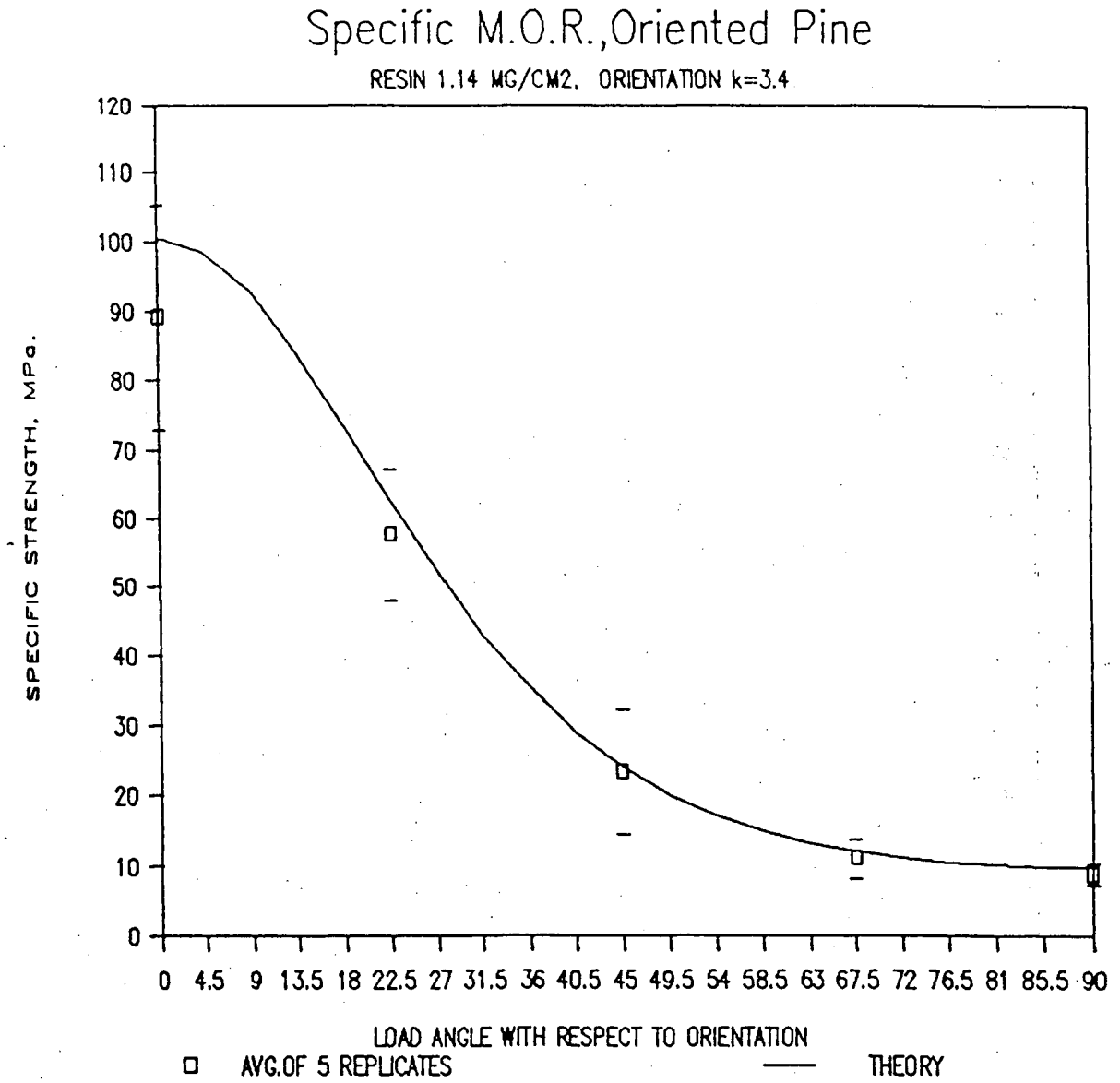

Figure 22. Specific MOR, oriented pine, high resin level

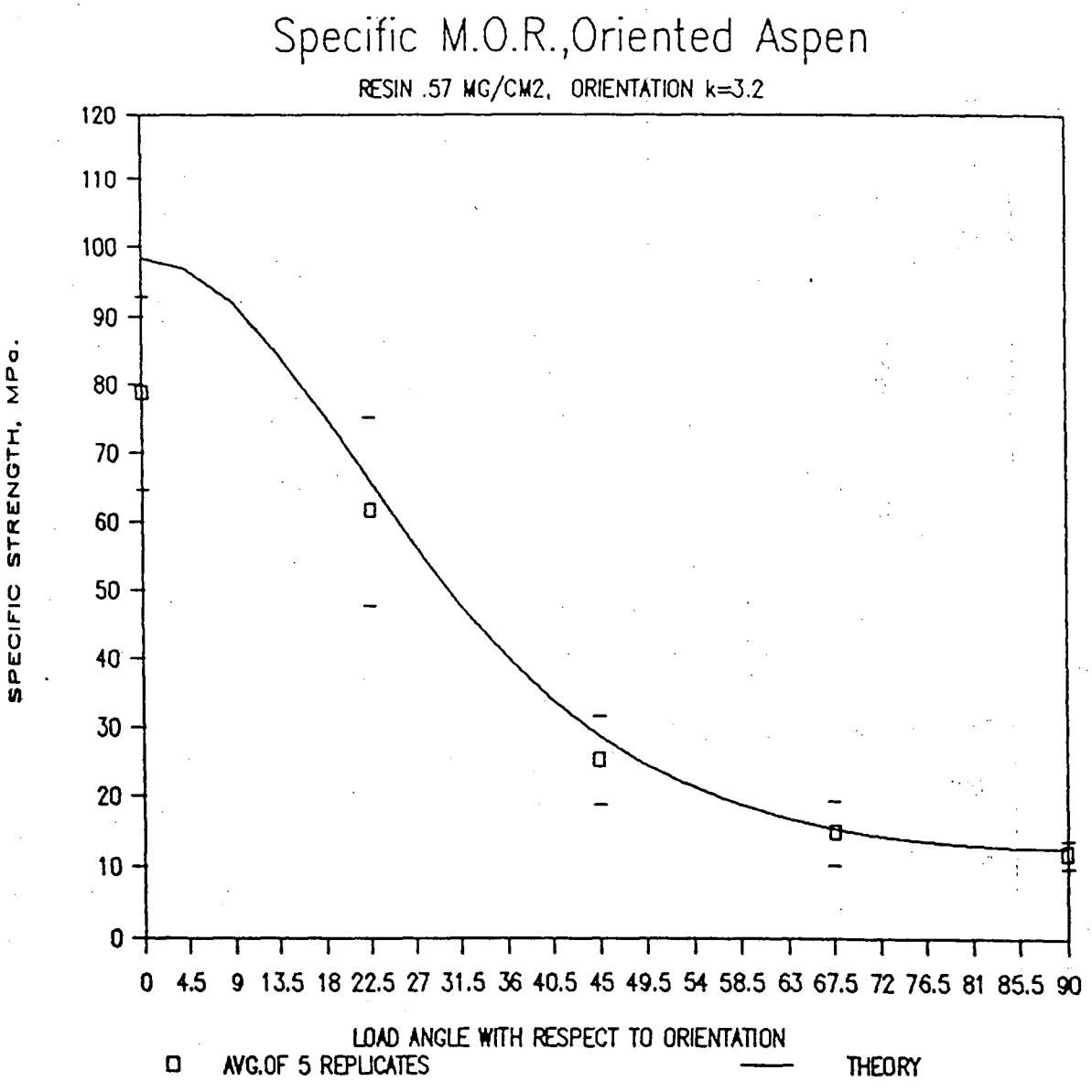

Figure 23. Specific MOR, oriented aspen, low resin level

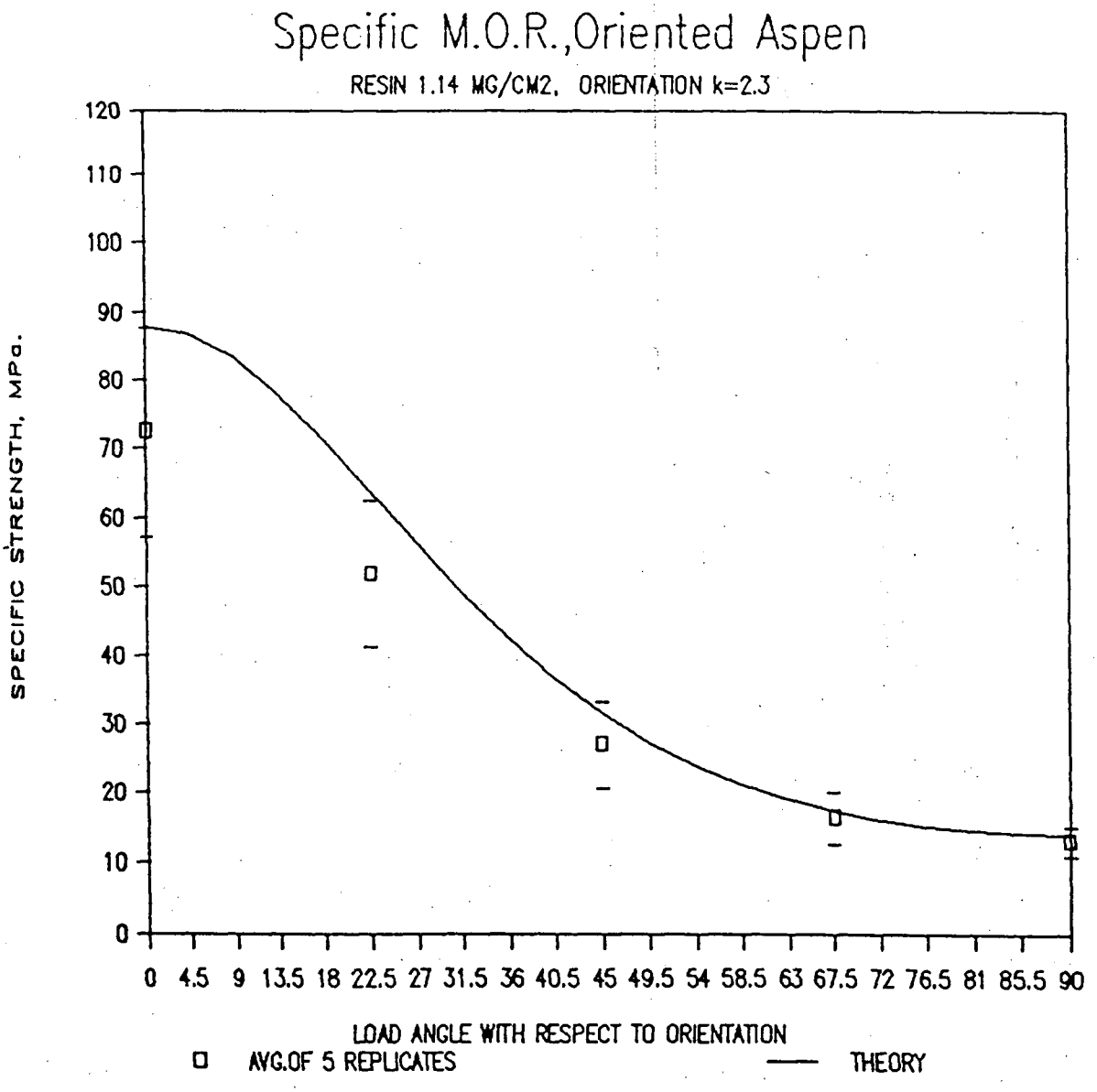

Figure 24. Specific MOR, oriented aspen, high resin level

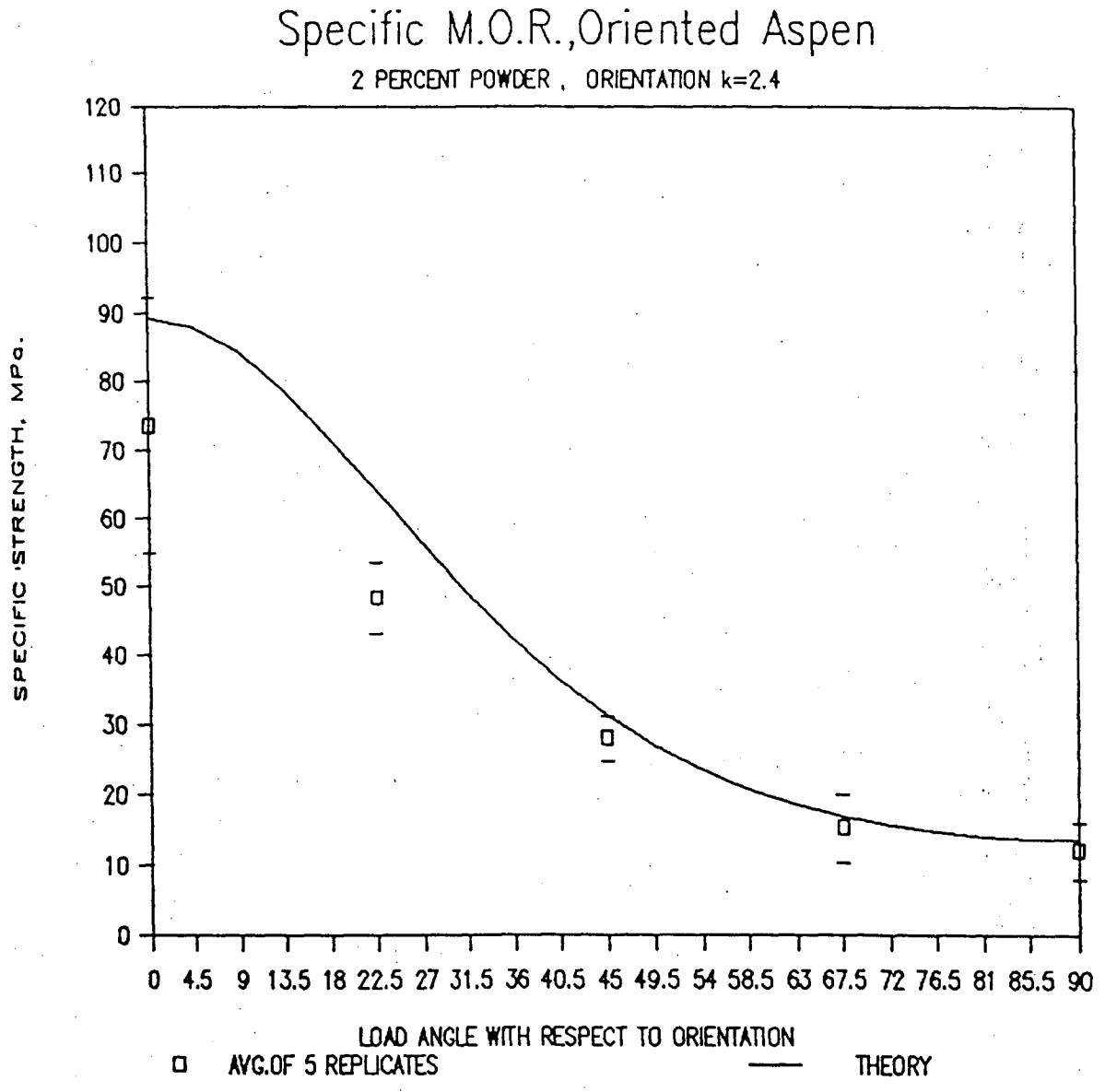

Figure 25. Specific MOR, oriented aspen, powder resin

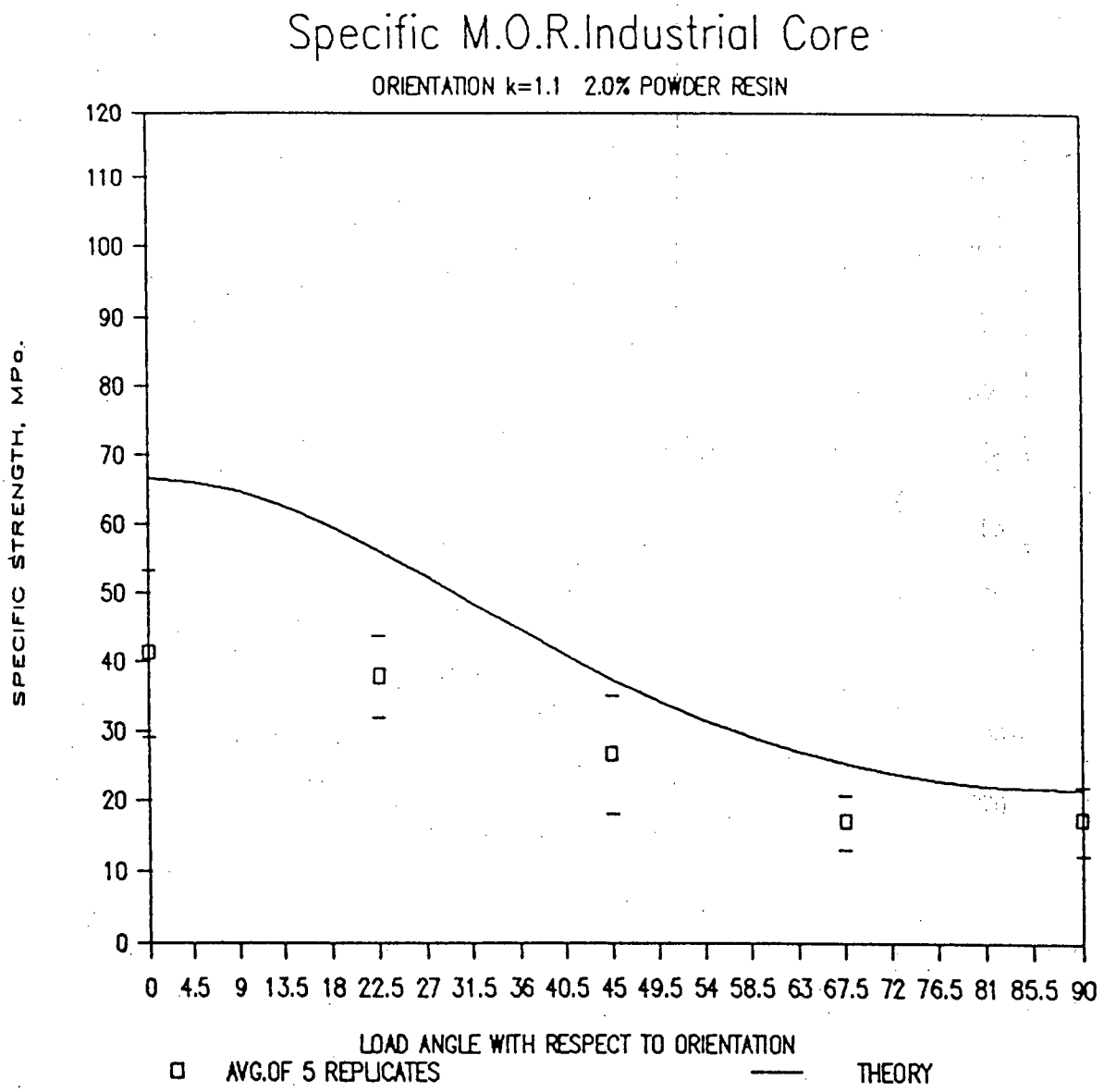

Figure 26. Specific MOR, industrial core

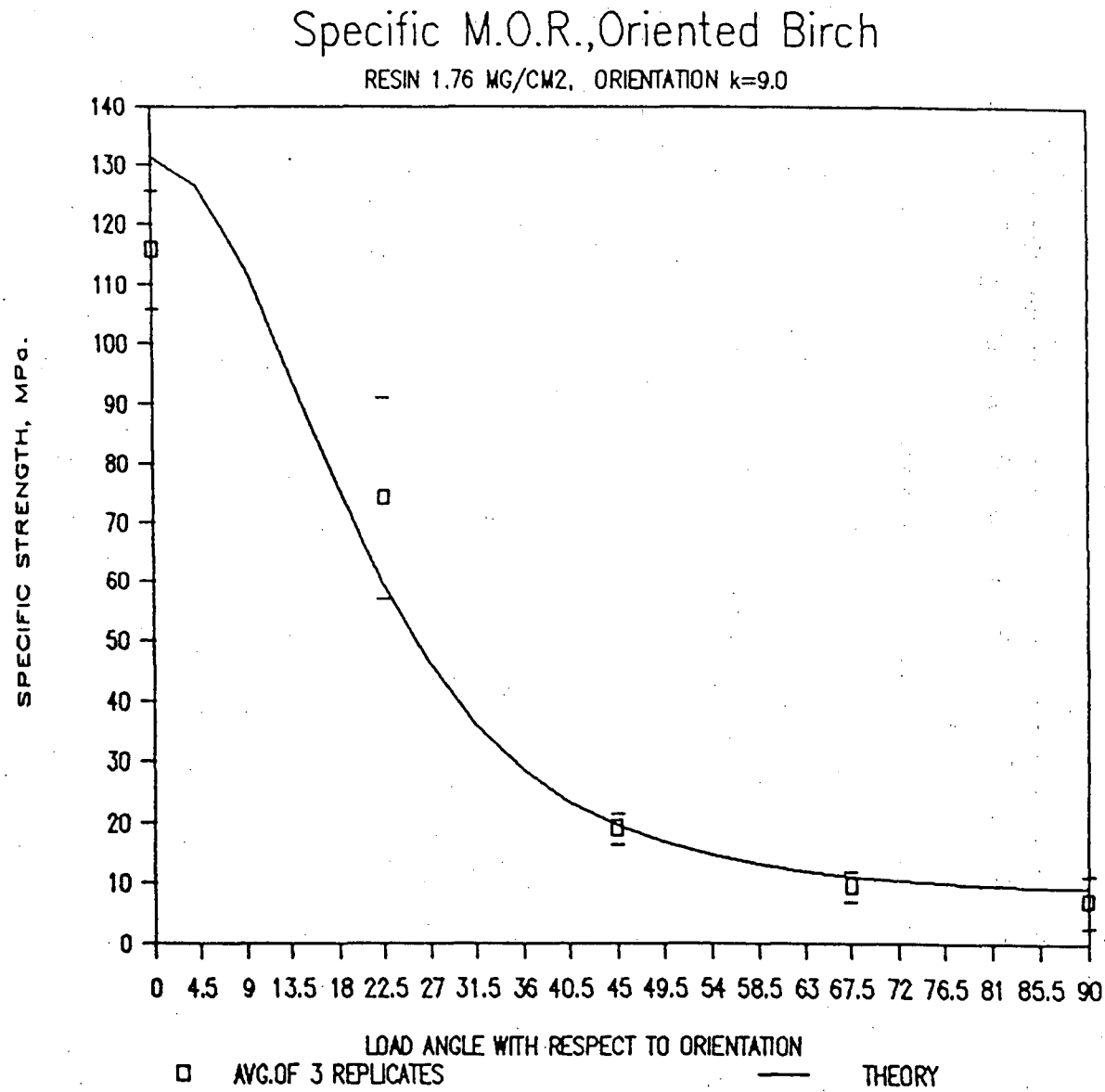

Figure 27. Specific MOR, oriented birch

Table 18 summarizes the tests showing that both resin levels were sufficient to permit strength development close to the model prediction. The data at the higher resin level fit better to the ideal because of the perfect adhesion required of the theory. Contrary to the expectation of some solid woods, the specific MOR was larger than the specific tensile strength in the case of parallel orientation.

The orientation parameters must be similar for direct species comparisons. Results on qualified specimens, also having the same resin levels, are presented in Table 19.

Table 18. Parallel specific flexural strength

Species	Percent of Model Expectation	
	0.57 mg/cm² resin level	1.14 mg/cm² resin level
R. Alder	79.0	92.0
R. Cedar	78.5	84.5
L. Pine	80.1	88.6
T. Aspen	80.1	82.1

		Percent of Model Expectation
T. Aspen	lab board, 2% powder resin	82.5
T. Aspen	industrial core 2% powder resin	61.6
Y. Birch	1.76 mg/cm² liquid phenolic resin	88.3

In Table 19, the results were obtained by applying the t-test statistical significance criterion at the p=0.05 level of confidence.

Table 19. Parallel specific flexural strength: species

Resin Level	Species Compared	Specific MOR
0.57 mg/cm^2	Aspen vs. Pine	no sig. diff.
1.14 mg/cm^2	Aspen vs. Cedar	no sig. diff.
1.14 mg/cm^2	Alder vs. Pine	no sig. diff.

PRACTICAL EXAMPLE

In Fig. 18 through 27, the test data were adjusted to a specific MOR calculated as flexural strength divided by the surface density. The assumption of surface failure is implicit in this data manipulation. If the same assumption is applied in the converse computation then a more practical result is obtained. This is where the strand wood strengths obtained in testing are first adjusted by the surface density and then assigned as input to the model Equation [13]. The model output then becomes the expected ultimate fiber stress MOR of the composite. The expression for linearly adjusting the L and T strengths of the strands to the elevated surface density strength is simply:

$$\text{adjusted input} = \left[\begin{array}{l}\text{tensile test}\\ \text{strength of}\\ \text{the strand}\end{array}\right]\left[\frac{\text{composite surface density}}{\text{average strand density}}\right]$$

The composite surface density is obtained from multiplication of (strand density, Table 3) by (compaction ratio, Table 5) by (density ratio, Table 8).

A demonstration of this is provided in Fig. 28 where comparison of the predicted and actual MOR is presented. The predicted MOR was calculated by the GWBASIC program in Appendix i. This example demonstrates the continuous strand theory to be adequate in predicting the tested MOR. The discrepancy in the parallel direction is because of inadequate stress transfer, as discussed in section 5.1.

It is possible to estimate the test MOR of 3-layer industrial boards on the basis of the network model. When tested with the span parallel to face orientation direction, the test board MOR is approximately equal to the surface adjusted strength calculated as in the example for Fig. 28. As elsewhere in this research, the criterion of first fiber failure at the surface must be accepted in this estimation.

When the span is perpendicular to the orientation of the face strands, in the 3-layer board, then the perpendicular (cross ply) surface layers are ignored as in the case of simple plywood analysis. The parallel oriented, inner core is assumed to carry the load. This would be valid in well oriented composites but not necessarily in the poorly oriented boards of high surface density found in contemporary industry. The density corrected MOR_1 prediction of Equation [13] for the outer fibers of the inner core is then multiplied by the factor (t^2_1/ t^2_2) to yield the expected MOR_2 in the face-perpendicular test direction for the full thickness specimen. The values of t_1 and t_2 are the symmetric thicknesses of the inner core and the full panel thickness, respectively. This reduction factor for the strength is obtained by using the expression $(3Pl/2bt^2)$ for MOR_1 and MOR_2,

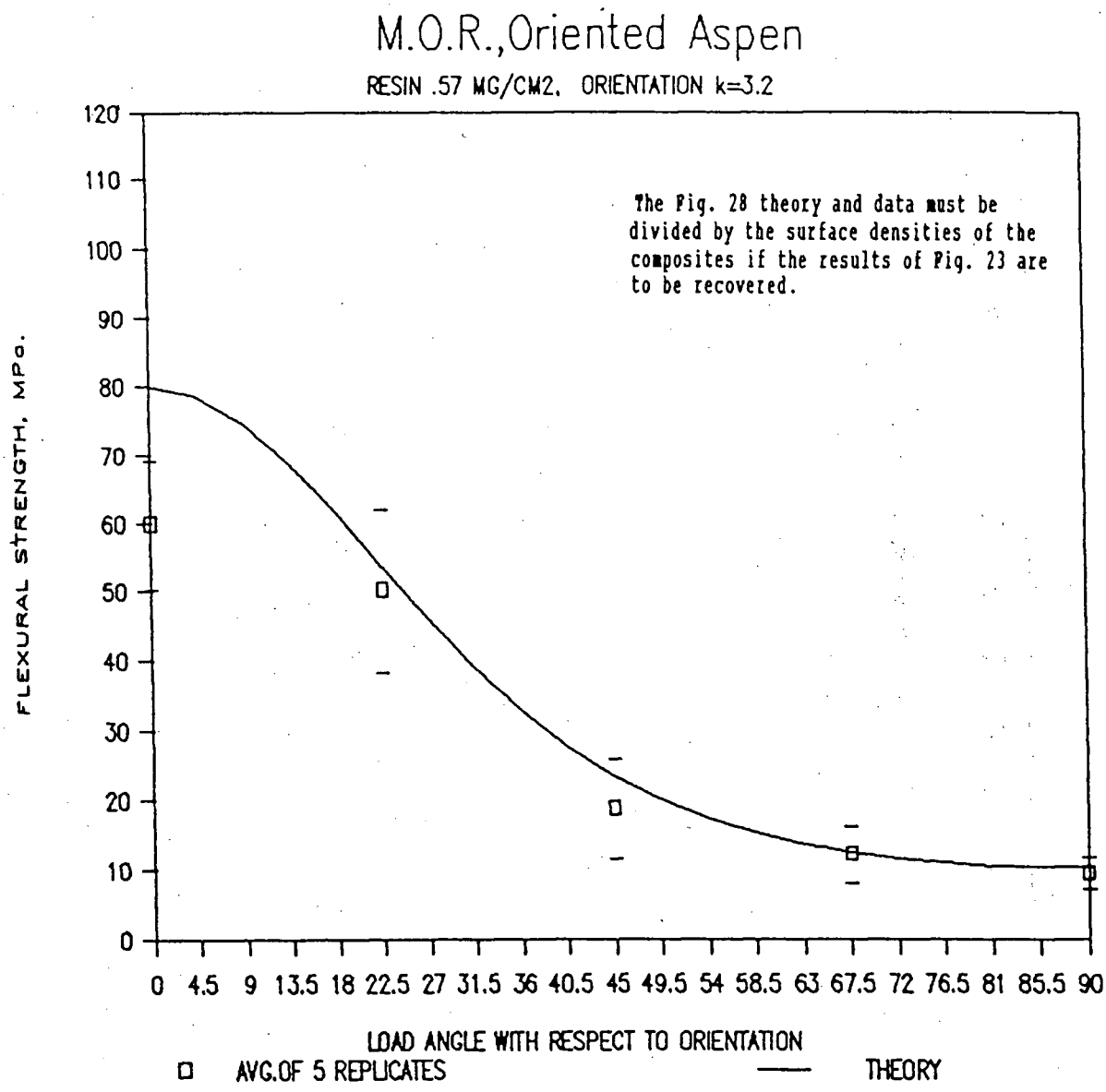

Figure 28 Theory comparison with surface adjusted inputs

with t^2_1 and t^2_2 respectively. MOR_2 is then solved for in terms of MOR_1. P, b, and l are the ultimate load, width, and span of the test beam and are common throughout. This permits the theory, when applied to the inner (core) layer, to be adjusted to estimate the test result MOR_2 for the full thickness board in the cross panel direction.

4.4.3 Flexural Strength, Perpendicular to Orientation

The perpendicular to orientation surface specific MOR's are presented as the 90 degree strengths in Fig. 18 through 27. Comparison of these to the specific tensile strength of the wood strands (Table 7) shows that all the composites had specific MORs which were not greatly different from the cross grain specific strength of the wood itself. The low orientation industrial core was the exception, where low orientation benefits perpendicular strength (see Fig. 10).

Comparing the perpendicular specific MOR strengths to the Equation [13] model prediction showed the model estimate to fit within one standard deviation of the test data mean. This fit is better than the Table 14 comparison of perpendicular specific tensile results to the model. The perpendicular specific MOR's were slightly higher than the perpendicular specific tensile strengths. Compared to the tensile case, there was less improvement in perpendicular specific MOR relative to the model prediction as the resin level was doubled.

4.4.4 Flexural Strength, Random Orientation

The surface specific MOR's were analyzed in a completely randomized design with fixed factors and three replicates (Hicks, 35). The result presented in Table 20 is from analysis of variance on the specific MOR. The independent variable was the test MOR divided by the specimen surface density.

Table 20. Random orientation, specific flexural strength, analysis of variance

Source	d.f.	S.S.	M.S.	F	$F_{.05}$
species	3	145.431	48.477	3.381	3.24 sig.
resin	1	30.623	30.623	2.136	4.47 not sig.
s x r	3	27.693	9.231	0.644	3.24 not sig.
error	16	229.423	14.339		
totals	23	433.169			

As in the tensile test of random boards, species was the only significant factor. Duncan's multiple range test grouped the pine as the lowest in strength, aspen, cedar, and alder, being higher. No other differences were significant at the overall test significance level of p=0.05. The flexural data is presented in Fig. 29 through 33, where each point represents a board replicate. The non-zero k orientation parameter caused by the use of the rectangular forming box was identified as a perceptible rise in the expected theoretical strength as the load angle rotates to the parallel direction. The data for the theoretical strength in Fig. 29 to 33 was produced by the computer program found in the Appendix i. The average strength of the perfectly random composite can be estimated by Equation [21]. In a presentation similar to the tensile case (Table 17) comparisons to the wood strand and the theoretical strengths are

made in Table 21. The results show that the theory predicted the specific MOR of the random boards with slightly better accuracy than it did for the specific tensile strengths.

The relative shortfall in pine strength is thought to be caused by its lower compaction ratio. This can lead to poor bonding as discussed in sections 4.3.2 and 5.1. The random orientation strengths, ranged from 74.5 to 95.5 percent of the model estimates. This is considered to be a good modelling result, given the approximations necessary on both sides of the comparison. The averages of specimens cut at all angles, and the average theoretical strength calculated from Equation [21] were used in Table 21.

Table 21. Comparative flexural strength of random orientations

Species	Surface Specific MOR MPa	Percent of Theoretical Specific MOR	Specific MOR as a Percent of Parallel Grain Strand Strength
R. Alder	34.2	95.5	23.3
R. Cedar	33.9	84.6	22.8
L. Pine	28.1	74.5	16.8
T. Aspen	32.1	78.6	21.1
T. Aspen 2% powder	33.4	81.8	22.8
Y. Birch 1.76 mg/cm^2 resin	37.0	92.4	21.3

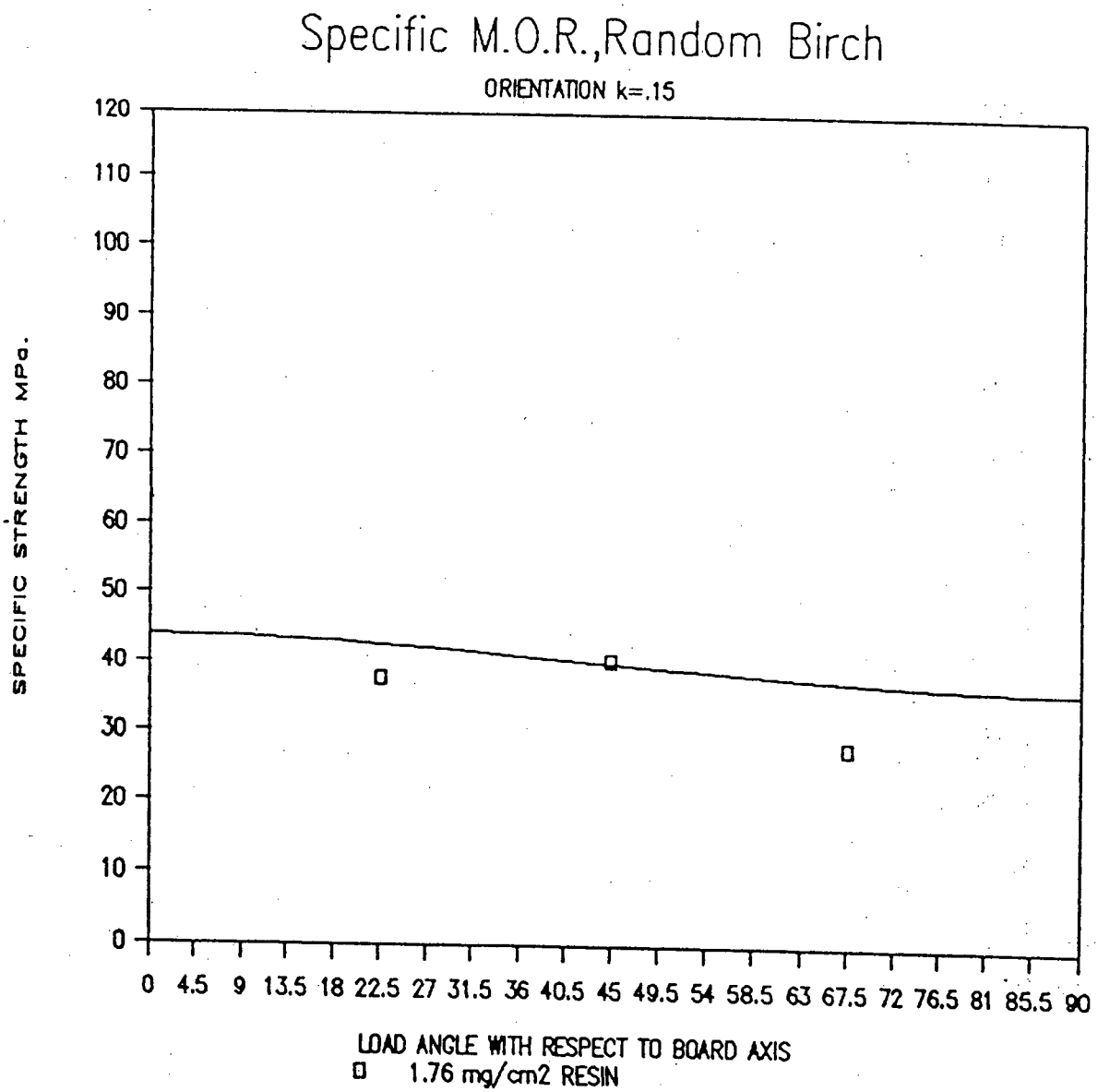

Figure 29. Specific MOR, randomly oriented birch

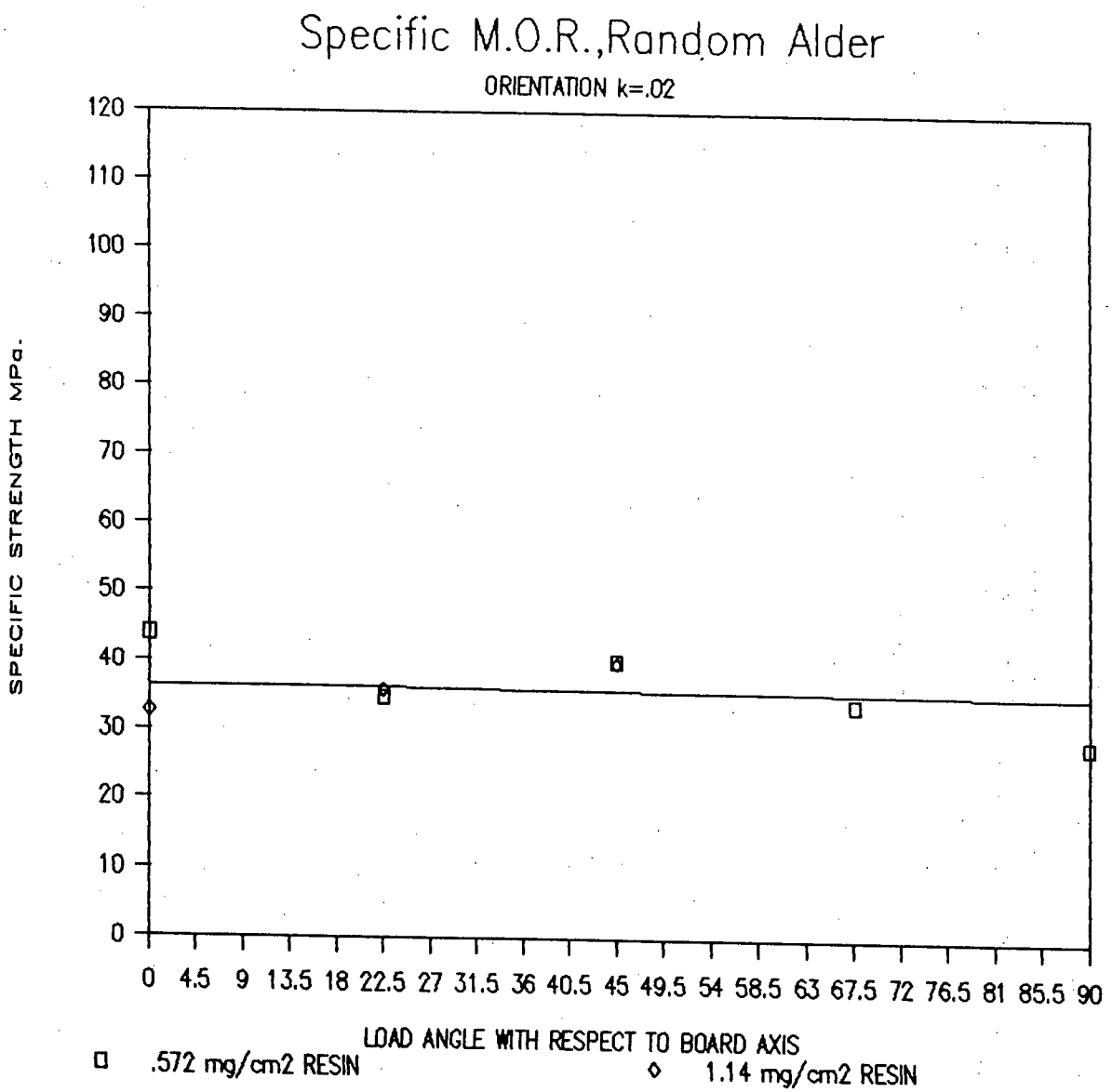

Figure 30. Specific MOR, randomly oriented alder

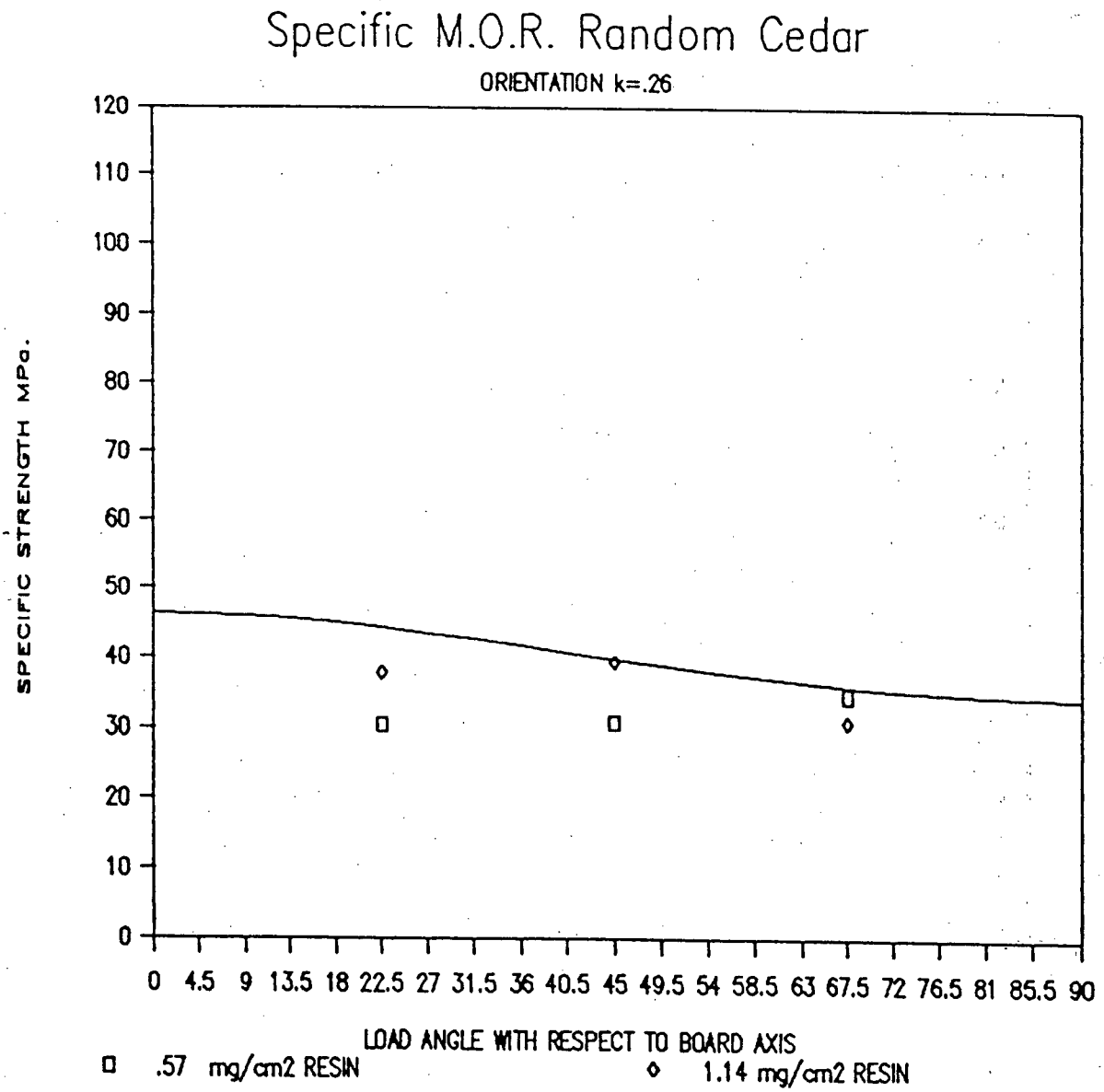

Figure 31. Specific MOR, randomly oriented cedar

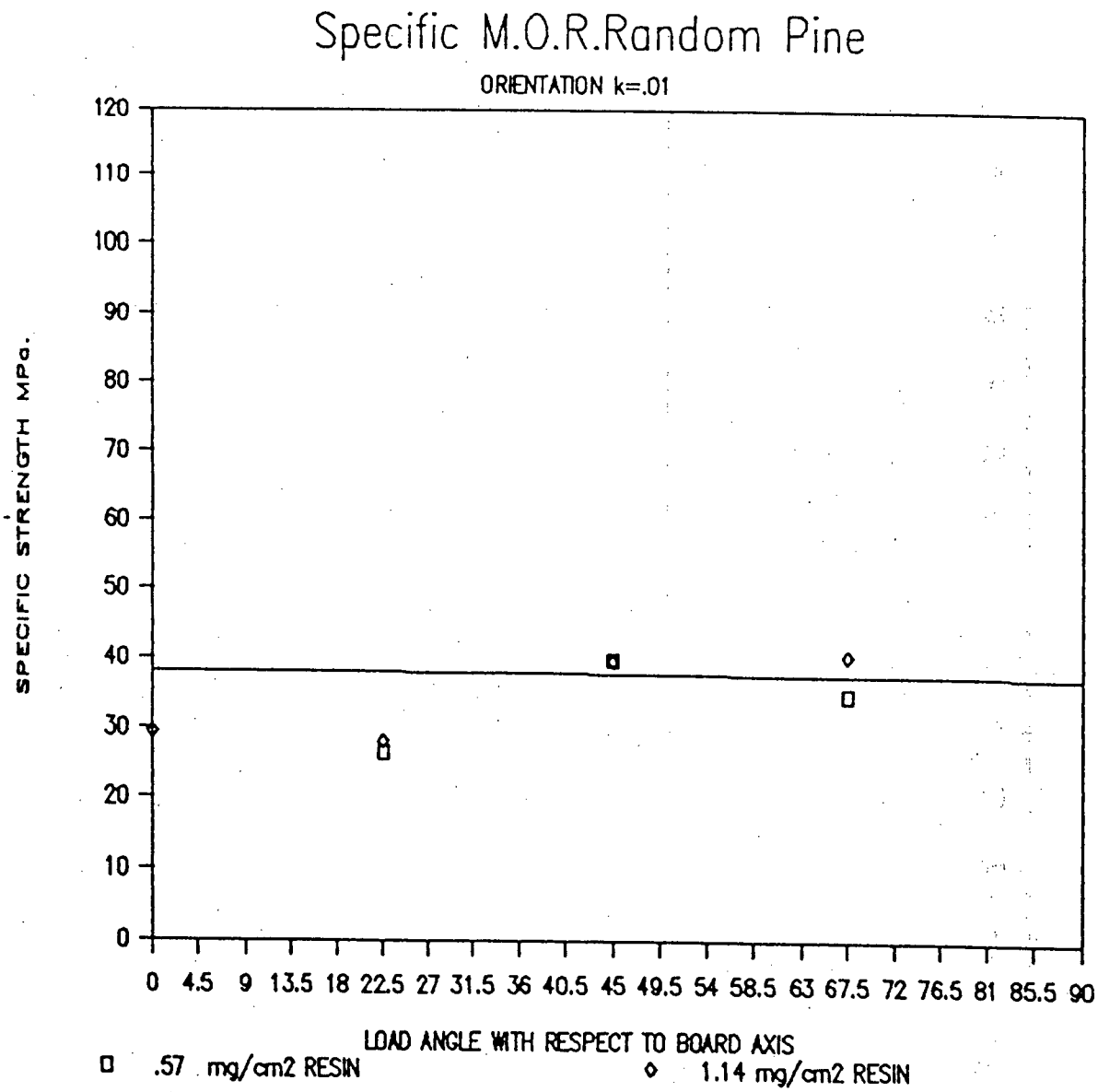

Figure 32. Specific MOR, randomly oriented pine.

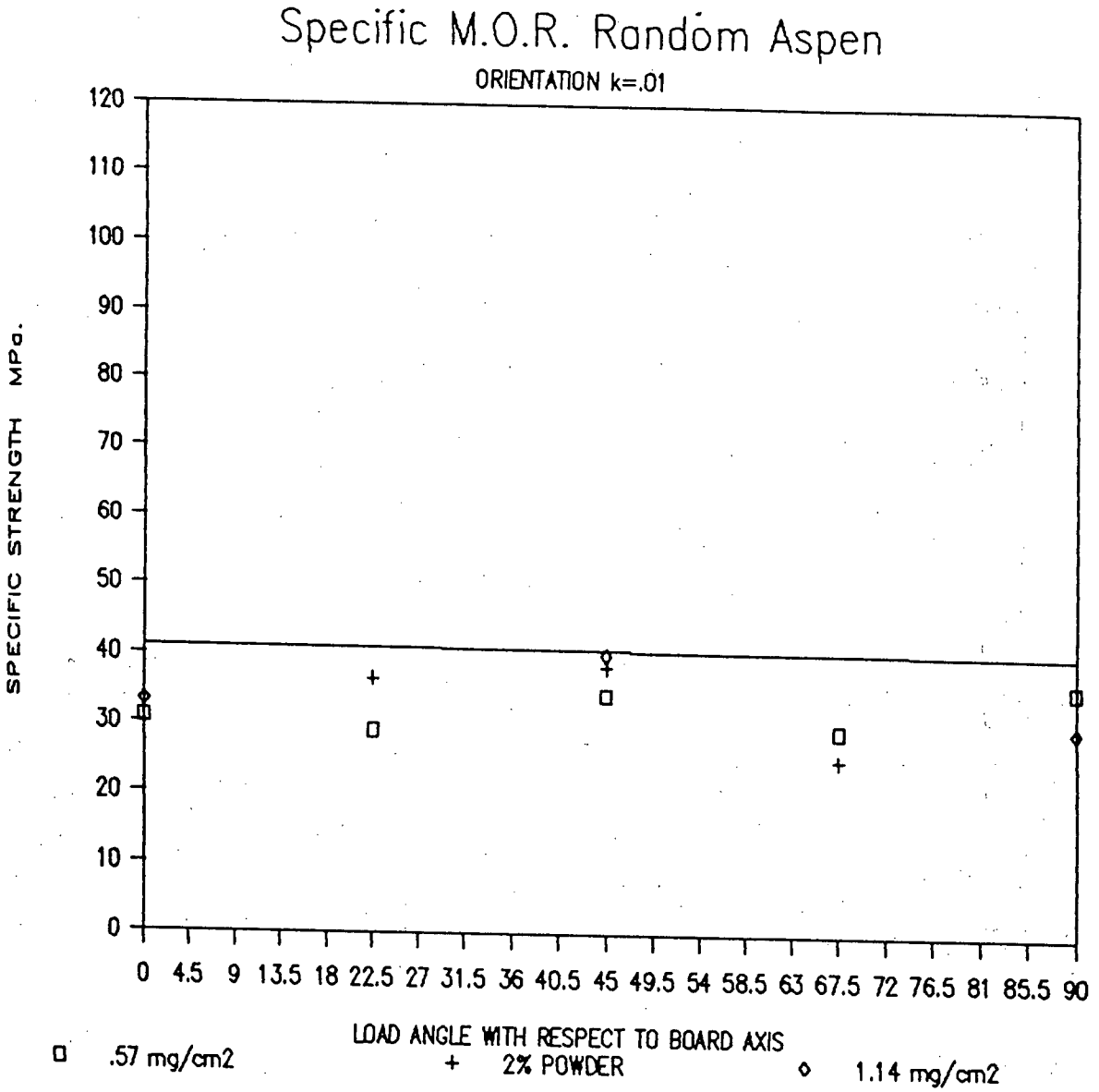

Figure 33. Specific MOR, randomly oriented aspen.

5. DISCUSSION

5.1 Strength Parallel to Orientation

Specific tensile testing was chosen for priority discussion because it is less compromised by the density gradient assumptions than is MOR testing. Testing of MOR for comparison to the theory requires the assumption of first fiber failure at the surface, in addition to knowledge of the surface density.

Red alder formed the strongest of all composites when compared to the expectation of the model. This is thought to be due to a superior wood-adhesive interaction in this species. It is speculated that there exist adhesion factors such as superior wettability, solubility parameter, or acid/base compatibility that improve bonding in alder. These may be founded in the peculiarities of alder's extractive chemistry.

The industrial core was tested for the purpose of placing the results in perspective with the current manufacturing art. Table 11 shows the core reached only 32.6 percent of it's theoretical specific tensile strength (the lowest of all tested). Table 6 shows that the industrial core had a lower estimated compaction ratio. This is a possible cause for poor bonding, and is verified by its density being 0.548 g/cm^3, moderately lower than the other experimental boards. Compaction ratio, rather than resin level, is considered a factor in the case of industrial core because the comparable aspen laboratory control boards reached 41.2 percent of the theoretical specific tensile strength. The lab boards had the same 2 percent powder resin

level, but a higher compaction ratio; the original wood strand densities are assumed equal.

The industrial core could be improved to a higher predicted MOR, without further densification, by orienting the strands to an increased k level. A further optimization, without costly resin increase, is possible by measuring the debonding shear strength, s, and using this to estimate critical strand length l_c. (section 3.10.3). Strength improvement would come with selection of an increased strand length, l, which is much longer than l_c. Methods of testing the bond shear strength of strands which withdraw strands embedded in the composite may prove useful in this study.

Resin effects on specific strengths were studied directly by preparing a series of cedar composites to have approximately the same orientation level but with a sequence of increasing resin levels. Figure 34 was the result. Here, the combination of bonding factors and strand geometry produced a typical asymptotic curve converging to a maximum strength at a resin spread of about 1.76 mg/cm^2 in the case of specific MOR. This convergence required a higher resin spread in the case of specific tensile strength. Laufenberg (50) presented similar results for randomly oriented aspen but with the resin scale increased for the higher bonding level required of shorter, thicker strands having a length/thickness ratio of about 37. The corresponding length/thickness ratios for strands in this thesis ranged from 94 to 134.

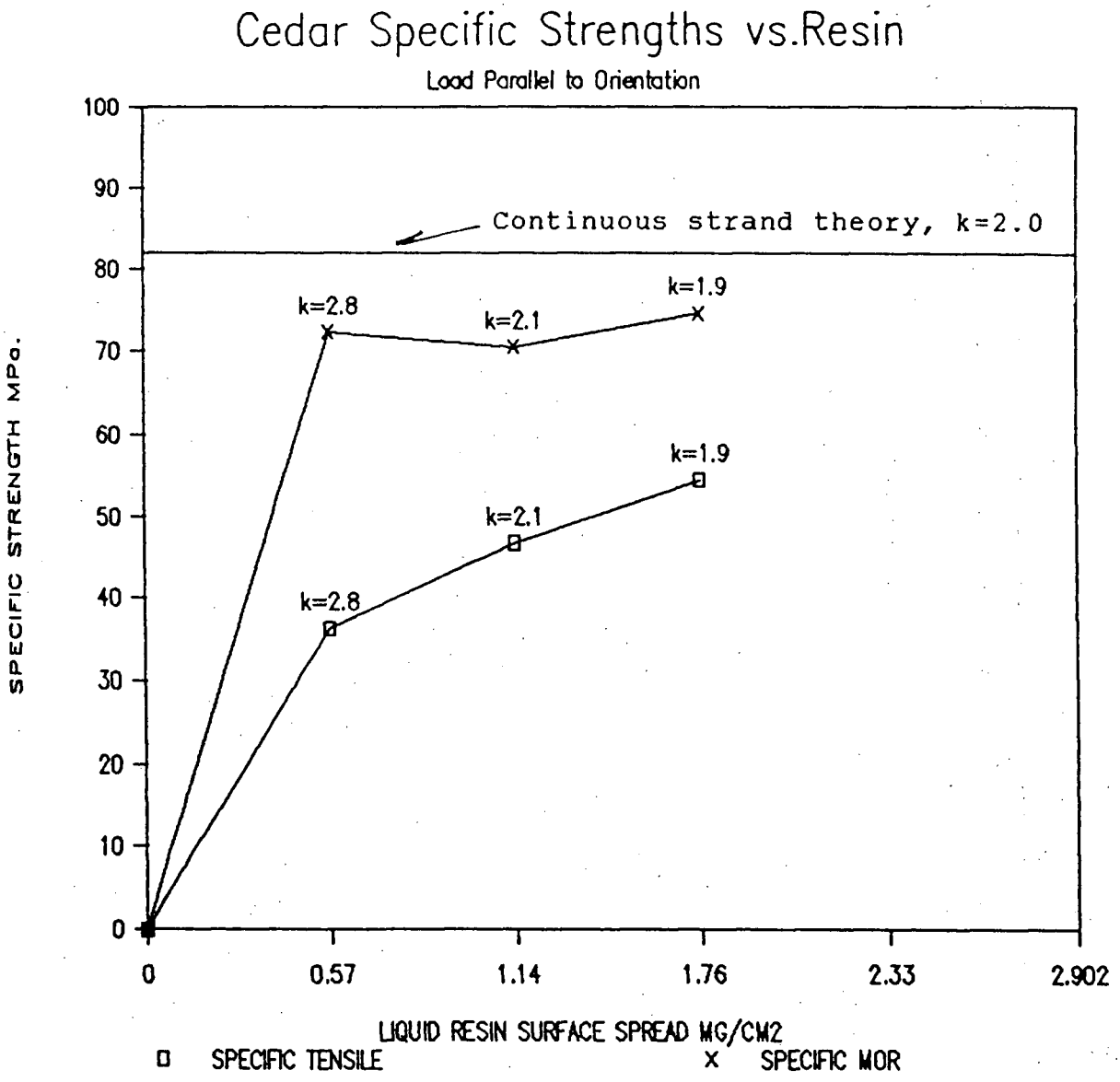

Figure 34. Tensile strength versus resin spread level.

The primary effects of orientation and resin level on strength showed clearly through the superposition of several other factors. Such uncontrolled factors were compaction ratio, intrinsic bonding properties of the species, wood softness roughness, and permeability. When the resin level was high, the parallel specific MOR strengths increased, and approached the theoretical value, reaching it in alder and above 61.6 percent of theoretical in the other species. For optimal strength, the adhesive bonding must be sufficient for transfer of tensile failure stress to strands having parallel orientations within the board. Laufenberg (50) analyzed the failure of strands in OSB using the maximum stress theory. He indicated that highly bonded strands stressed between 2.6 and 17 degrees off parallel to the grain axis, fail in shear, along the parallel grain of the strand. Tensile failure in highly bonded strands dominates at below 2.6 degrees load angle. This force direction is nearly parallel to grain. If the theoretical strength is to be reached, then bonding sufficient to apply failure stress to the strands at their strongest direction is required.

In Table 11 and Table 18 most of the specific strengths are lower than the 100 percent level representing the network theory estimates. The differences are ascribable to inadequate stress transfer. This is confirmed in Fig. 34 where increased resin (adhesion) greatly improved the strength. At the fixed strand dimensions selected for this research, the strength deficits could be restored by augmenting the value of bond shear strength, s, in Equation [16] through additional resin spread. This reduces the value of h_c , so that $h >> h_c$ (section 3.10.3).

The composite strength would expectedly increase when the strand length is large relative to the parallel tensile specimen gage length. This gage length effect, tending to simulate continuous strands, (perfect adhesion) would increase until the zero span equivalence was approached. Thus, a strength advantage (Fig. 34), may go to the MOR specimen due to a smaller peak stress zone. Variance decreases with increased specimen size (Equation [14]).

Pertaining to the Table 11 species bonding differences relative to the theory, it was seen that cedar had a lower specific tensile strength at the 0.57 mg/cm^2 resin level, despite having a higher compaction ratio than alder. All other factors being equal, it is concluded that the resin did not bond the cedar as well as the alder. This discounts other factors such as differing strand damage during compaction, and possible bonding-orientation interaction.

To summarize, it was observed that the parallel strength of an oriented strand composite is a function of how well it is oriented and how well it is bonded. It is clear that the orientation parameter, k, should be maximized for maximum strength in the composite. The strand length to thickness ratio should be made so that the fraction 1-(h/l) is close to 1 (section 3.10.3). This can remedy the condition of $h<h_c$ where the wood or bond shear strength, s, is exceeded and shear failure occurs. The bond or wood shear strength, s, may be exceeded by internal shear stress because of the effects of any of the following factors:

- adhesive level, type, distribution, dispersion, and cure
- strand species, drying history, and surface condition
- compaction ratio and pressing specifications
- short, thick strands rather than long, thin ones

5.2 Strength, Perpendicular to Orientation

Perpendicular to orientation, the tested specific tensile strengths of both the low and high resin level composites were equal or lower in strength compared to the wood strands themselves. A 3 variable analysis of variance was performed, the 3 variable strengths were of the low and the high resin composites and the strands of each species. No significant differences between composites and strands were found in aspen ($p=0.13$) or cedar ($p=0.22$). (reference, Tables 7 and 13). In these comparisons, there are specimen size differences between the strand strengths and the composite strengths that contribute to the strand estimates being relatively large. The lower wood strengths obtained from larger ASTM sized test specimens are presented in Table 7. To remain consistent with the model hypothesis, all perpendicular wood strengths referred to below were from zero span strand tests, not large block tests. All inputs to the model were also zero span strand strengths.

At both resin levels, the composite strengths were expected to be considerably greater than the perpendicular to grain wood strength because of the presence of numerous off-axis strands in the orientation distribution. Evidently, the small perpendicular strength gains available to the composite because of imperfect

orientation were lost because of the effects of poor stress transfer between the off-axis strands, strand damage, or specimen size effect on strength.

Now the comparisons to the theoretical models shall be considered. The percentages of the model specific tensile strengths perpendicular to the orientation axis (Table 14) were significantly increased by increased resin level. Aspen was the exception, having no significant strength response to the resin increase from 0.57 mg/cm^2 to 1.14 mg/cm^2 spread. All comparisons were by "t" statistics at the p=0.05 significance level.

It is noted from Table 14 data that doubling the adhesive spread in aspen did not increase the percentage of the theoretical perpendicular specific tensile strength. This, together with the evidence that the perpendicular specific tensile strengths of the composites were only equal to the wood strand's (Tables 7 and 13) leads to the conclusion that the adhesion at the strand bonding zones was adequate, but that the rolling shear strength of the strands would not support the shear stress necessary to transfer tensile failure load to the perpendicular strands. This means that strand pullout can also be a strength factor in the perpendicular direction. A probable reason for this lies in the strands' effective solid width being much narrower than the apparent 8 mm nominal, measured as unflawed wood. This is summarized in the understanding that the strand's perpendicular tensile strength does not always govern the composite strength in the perpendicular direction.

Parallel to-the-grain cracks in the strands can greatly reduce the effective width. The effect of this on strength is

seen with a low value of shear stress transfer length in Equation [18]. The result of $h < h_c$ can be shear failure at the bond interface. In addition to damage during cutting, it is probable that some strand damage occurs during pressing because the thin, dry strands are quite fragile and easily break parallel to the grain. Further damage can occur in drying, storage, and handling of strands, this produces the detrimental narrow strand fraction seen in Fig. 5. The strength loss explanation is partly based on the substantial narrow strand (fines) portion indicated in the distribution of Fig. 5. The strand tensile strength governs in the wide and unflawed portion of the distribution when adequate adhesion is present. Damage during pressing adds to this width loss.

Cracking is also promoted by the way the wood strands are prepared. They are peeled from the tangential face of wood blocks using the same tangential cutting principle as used in preparing veneer. This produces loose face checks, and often destroys the crack-free width of the strands. The merits of a way of preparing strands without the parallel grain cracks are worthy of further research. A slicing device which peels parallel to grain (longitudinally) may provide improved results, if the strand is produced at low knife angle, using no counter-knife breaker bar. The objective is a strand with minimal micro-damage.

Increasing the perpendicular-to-grain bond strength of highly oriented composites requires a change to a higher strand width/thickness ratio with the shear strength, s, set at the rolling shear strength of the strands. The idealized strength is

reached when the intact strand width, $w >> w_c$ and, with 1-(h/w) approaching 1. The factor w_c is calculated in the perpendicular direction according to $w_c = bt/s$. The resulting improvement in stress transfer would enhance achievement of the strength anticipated by the continuous strand model Equation [13].

Another way of increasing the perpendicular strength of the experimental composites would be to decrease the strand thickness, (factor b), in Equation [16]. This may reduce the stress transfer requirement of shear to less than the rolling shear capacity of the strands thus allowing perpendicular tensile strength to govern. However, increasing the crack-free width is preferable economically, because the weight percent of the costly resin remains constant while the effective resin spread is maintained. Removal of the excessively narrow strand fines seen in the width distribution of Fig. 5 would be a further major contribution to the perpendicular strength.

Weak, low density zones, caused by mat forming artifacts such as voids or by the serial mischance of poor overlapping and interleaving of strands may be causal factors in the low perpendicular to orientation strengths. Such zones could be induced by an orienter having mechanical separation vanes (Fig. 6). These can interrupt stress transfer from strand to strand and create intolerable interface stress levels in a fashion similar to cracked strands. But the comparatively low standard deviation of strengths does not support the presence of these superimposed variables. Such factors are worthy of further

research in a fracture mechanics study of strand composite strength in the perpendicular direction.

5.3 Powdered Vs. Liquid Adhesive

Considering the data in Table 17 it was observed that the aspen composite having either a high or low level of liquid resin on randomly oriented aspen strands yielded a higher percentage of the theoretical model tensile strength (77.6 percent) than the 2 percent powder resin (59.3 percent). This trend was also apparent in the perpendicular to orientation tensile strength as seen in Table 14. Here, the comparison again favours liquid (58.7 percent) over powder resin application (54.0 percent). Contrary to this, in tensile testing aspen parallel to orientation, the powdered resin yielded slightly higher strengths, 41.2 percent of the theoretical strength, as compared to 36.5 percent of the theoretical for the liquid resin (Table 11). Of these 3 comparisons, only the first showed a significant difference between powder and liquid at the $p=0.05$ level of confidence.

A comparison of resin types is more convincing if it meets the following condition:

> To preclude resin type-orientation interaction, the orientation k levels should be the same in both composites compared.

This condition is not met for the comparisons in Table 11 or 14. When species are considered collectively in the analysis of variance in Table 15 it was concluded that the resin level (adhesion) is not significant as a determinant of tensile

strength in random composites at the pertinent resin levels. The insensitivity of strength to resin changes in random orientation weakens the conclusion that the liquid form of resin is superior. This insensitivity is also evident in the MOR results, Fig. 33. However, discounting the extra 0.44 percent of p.f. solids present, the liquid resin performed better in the random orientation in aspen specific tensile strength.

Recent improvements in industrial liquid blenders have reduced droplet size to the 30-40 micron range. This is much smaller than the 138 micron range used in the present research. Therefore, liquids having small droplets may prove equal to powders, if good distribution is also present. The lower cost liquid resins are usually preferred when shipping costs do not dominate.

5.4 Flexural Elasticity

Digressing from the topic of composite strength, a discussion of modelling elasticity, using the orientation distribution function, is worthwhile. The algorithm previously studied, and which had merit as a strength estimator, was thought to have an analogue in a flexural elasticity model. Geimer (27) explored a simple analysis which predicted 74 to 120 percent of the actual tested stiffness of three layer cross ply oriented strand boards. He used a transformed moment of inertia formula for EI estimation. This method is also found in laminated beam and plywood design. EI is the product of the test beam's engineering flexural modulus of elasticity and cross sectional moment of inertia. The present study of this subject used

Geimer's approach to a multi-layer system using strand layers of calculated EI contribution according to their density-related modulus and distance from the neutral axis. First, the tensile stiffness in the board axis direction was estimated for a single strand lamina, oriented at any grain angle, θ, relative to the orientation axis. This required use of an elastic transformation equation in the longitudinal - tangential plane such as presented by Bodig and Jayne (12).

$$\frac{1}{E_{11}} = \frac{\cos^4\theta}{E_L} + \frac{\sin^4\theta}{E_T} + \left(\frac{1}{G_{LT}} - \frac{2\nu_{LT}}{E_L}\right) \sin^2\theta \cos^2\theta \qquad [24]$$

where:
G_{LT} = shear modulus
ν_{LT} = Poisson's ratio
E_T = tangential tensile modulus of the strand layer
E_L = longitudinal tensile modulus of the strand layer

The wood ring angle was neglected and the strands were treated as if they were transversely isotropic (2 dimensionally orthotropic with 4 independent elastic constants). This transformation Equation [24] replaced the Hankinson expression in the Equation [13] integral, numerically producing the expected laminate elasticity for a network of strands under loading at any chosen angle, m, relative to the principal axis of orientation.

Some explanation about how the board's vertical density gradient affects the flexural modulus is offered as follows. The superposition of repeated x-ray density profiles, two elements of which are exemplified in Fig. 16, showed a repeated parabolic decrease in density toward the board center. This is confirmed by Steiner et al. (84). A parabolic equation was used to

describe the vertical density gradient and produce an elastic modulus densification factor for increments in vertical level through the composite. The parabolic shape parameter (focus) was based on these x-ray density profiles. It was assumed that the elastic moduli of wood, E_L and E_T are directly proportional to the density. Text book values (Table 23) of elastic moduli for uncompressed wood (12) were used as the primary elastic constants. The availability of such values in the literature makes this modelling more versatile than the use of elastic constants determined by tests on thin sheets taken from descending positions in the laminate (Geimer, 27). A numerical integration of the modified Equation [13] was computed to estimate the composite stiffness, EI. The parallel axis theorem (22) was used for determination of each lamina's moment of inertia. The composite thickness was subdivided into laminae represented by the individual strands. Thus, the overlapping and interwoven network of strands was perceived by the model as a laminate of graded density laminae.

The cumulative calculation made for the stiffness, EI, assumed that each strand layer was approximately equal in thickness. This uniform thickness introduces the model concept of the densified surface layers as being caused by the void filling deformation and consolidation of strands into intersticial cavities during hot pressing. The void volume is thought to be lower in the surface zones. Finally, the summed EI result was divided by the apparent moment of inertia for the whole thickness to estimate an "effective" E modulus.

Two trials (Table 22) on high resin composites yielded reasonable estimates of MOE relative to actual tests. These results are comparable to some of Geimer's (27) and Woodson's (97) transformed section estimates. The results are also similar to those of Harris (34) who used a layered, serial, spring model for specific tensile modulus in the direction of orientation. His experimental results fell modestly short of his model prediction. The present computations showed, for example, that the density gradient in alder caused an increase from about 6069 MPa (parallel MOE) to the 13883 MPa result when the parabolic gradient was factored into the uncompressed strand network strength. The estimate was within the range of the MOE test average of 9940 MPa. The elastic input moduli are taken at 12 percent moisture content, but the testing was at 8 percent moisture. Therefore, the differences in Table 22 are partially explainable by this inconsistency.

Table 22. M.O.E. in flexure (MPa)

		Network Model MOE		Test Mean Flexural MOE	
Species	K	Parallel	Perpendicular	Parallel	Perpendicular
R. Alder	3.5	13883	966	9940	975
Y. Birch	9.0	14291	885	16933	1066

Table 23. Input elastic constants (MPa)

Species	Tensile E_L	Tensile E_T	Shear G_{LT}	Poisson ratio LT
R. Alder	10427	355.86	452.41	.50
Y. Birch	14629	640.69	721.37	.50

Considering the data of Table 22, one source of modelling discrepancy in the parallel direction is thought to be due to the contribution to stiffness caused by elastic interactions between the wood strands. The parallel ply, (transformed section) estimation of elasticity used for plywood cross ply laminates is even less theoretically rigorous for use with multi-directional, oriented wood strand laminates. The elastic interaction is accommodated in LPT (laminated plate theory) through the required multiplication of the tensor elements of the plate constitutive equation. The interaction is reduced, but not eliminated, because of the statistical symmetry about the midplane of the orientation angles and stack positions of strand laminae having equal thickness and elastic properties. This allows the assumption(s) of zero coupling between extension or bending with twisting of the laminate. (5) In this case, the coupling stiffness matrix $[B_{ij}] = 0$.

Strand interweaving, and overlapping, contribute to the apparent modulus of the practical wood strand composite. Some error in the theoretical modulus is incurred because of the approximation that elastic moduli increase directly proportionately to density. Any damage in pressing is neglected. The conclusion is that the network analysis provides a first approximation estimate of flexural MOE of variable accuracy in the parallel to orientation axis direction and one of good accuracy in the perpendicular direction. The GWBASIC program in

Appendix ii calculates these estimates according to the transformed moment of inertia method and could be used for studying reconstituted wood strand lumber or OSB core layer MOE as functions of orientation, wood species, or density gradient.

An improved model of MOE would include the elastic effects of one strand upon the other. A suggested alternative model would first describe the probability distribution function for orientation, as does the network model. The proposed elasticity model would then randomly choose a sequence of sample strand angles, weighted by the probability distribution for orientation, to represent angular arrangements through the thickness of a model specimen. Density gradient effects on the elastic properties would then be accommodated through parabolic adjustment regressions. Classical laminated plate theory (LPT) would finally be applied to the composite giving a total constitutive equation which includes the effects of elastic interactions between laminae. As a Monte Carlo simulation, this could be calculated multiple times to build a statistical description of the elastic properties of the composite. This stochastic model would produce a random function tensile, flexural, or shear modulus output for each discrete value of k, the orientation parameter.

There is substantial practical merit in the ability to forecast the tensile and bending elastic properties of a unidirectional multiple layer of strands. However, the commodity OSB panelboard is composed of 3 such composites, consisting of densified face and back layers and a low density cross-band core of greater thickness. The MOE calculation for such a panel is

thought to be possible through manipulation of the proposed stochastic - laminated plate theory (LPT) model in an expanded form, using one or more orientation parameters. Such is left to the consideration of those choosing to intensively study wood strand composite elasticity.

If the researcher chooses to use less readily available inputs such as the 4 independent engineering elastic constants required by 2 dimensional orthotropic LPT, then the composite elastic response described above might be modelled. The LPT input difficulty is lack of information on how density affects the constants and sparsity of information, on all species, for the elastic constants themselves.

6. CONCLUSION

This research creates and examines an orientation model for the maximum strength performance of bonded wood strand composites. The ultimate specific tensile and specific bending strengths of wood composites were determined by tests and compared to a mathematical algorithm which estimates the strength of the composites when the stress transfer between strands is close to ideal. The orientation model shows that the use of high orientation will permit industrial evolution of new panel and strand-lumber composites having specific strengths approaching those of wood. The von Mises probability distribution function was found to accurately describe the orientation of industrial and experimental wood strand composites. It was also concluded that the potentials of composite orientation are not fully exploited in contemporary industrial products. A quantitative understanding of the contribution of the strand orientation level to composite strength was verified by studying of the relationship between the experimental results and the orientation models, at different resin levels.

The orientation model was concluded to be accurate when sufficient resin was used to provide adequate stress transfer. The experimental levels of phenolic resin required to produce composites having the orientation model's ideal parallel specific MOR, ranged from 2 to 3 times the 2 percent level of resin typically applied industrially. This factor became 5 to 7 times the resin applied industrially when comparing specific tensile strength to the orientation model. The fashion in which strength

increased with resin in the parallel direction was demonstrated to be asymptotic to a point near the strength prediction of the orientation model. In a core from a contemporary industrial composite, the poor adhesive bond limited the strength parallel to the axis. Bonding was increasingly critical to the parallel strength as the orientation level increased. At the other extreme, in randomly oriented composites, doubling the industrial resin level had no effect on specific tensile strength or MOR.

As the load angle with respect to orientation moved to the perpendicular, a smaller gap between model prediction and test results appeared in both flexure and tension. This is consistent with the conclusion that the stress transfer requirements for strand failure were more easily satisfied by the adhesive when the strands were loaded near perpendicular to the grain axis.

7. SUMMARY

This research is meaningful in guiding progress toward higher strength to weight ratios in industrial wood strand composites. Achieving the intent of high specific strength is dependent on the composite being bonded so that the maximum principal stresses are transferred from one load bearing element to another. Identification of composite bond weakness was made possible by use of the orientation model for an estimate of the composite's potential strength when perfectly bonded. Strength deficits can only be eliminated when the ideal strength is known. For example, in parallel specific MOR, the higher oriented experimental birch composite reached 66.6 percent of the specific tensile strength of the parallel grain wood itself and 88.3 percent of the continuous strand orientation model prediction of ultimate stress.

The adhesive level which is adequate to produce the strength equivalent of a continuous strand orientation model varies with the species, resin type, compaction level, and strand shape. Ideally, the most cost effective bonding is achieved when using strands of high length to thickness ratio.

The research was broad in terms of composite density profile, resin level, resin distribution, and resin dispersion, all of which included ranges used in industrial practice. Certain uniformities in these variables were attained for validation of the strength comparisons.

The analysis presented in this research leaves challenges to equipment designers and forest products manufacturers to make

more strength efficient and profitable wood strand composites. Further research using the von Mises distribution in combination with laminated plate theory would lead to an improved method of assessing the elastic properties of wood strand composites.

REFERENCES CITED

1. Anon. 1978. Proceedings First International Conf. on Wood Fracture, Forintek Publication, 304 pp.

2. Anon. 1981. U.S.D.A., List of Publications: Particleboard and Panel Products, Forest Prod. Lab. Rpt. 81-014, Madison. 12 pp.

3. Abramowitz M. and I.A. Stegun. 1965. Handbook of Mathematical Functions, Dover, New York. 1046 pp.

4. Adams, R.D. 1981. Composite wood utility poles, E.P.R.I., Rpt. E.L.-1745, Michigan Technology Univ., Res. Project 796-1, 107 pp.

5. Agarwal, B.D. and L.J. Broutman. 1980. Analysis and Performance of Fiber Composites. Wiley-Interscience, 355 pp.

6. Alexopoulos, J. and J. Shields. 1982. Structural potential of waferboard made from alternate wood supplies. Can. Waferboard Symp. Forintek SP508E: 145-151.

7. Bacon, M.R. and T.F. Rust. 1973. The determination of caustic phenol formaldehyde resin in wood products. Forest Prod. J. 23(9): 113-114.

8. Barnes, D. 1988. U.S. patent 4,751,131, Waferboard Lumber.

9. Barnes, D. 1986. U.S. patent 4,610,913 Long Wafer, Waferboard Panels.

10. Barrett, J.D. 1974. Effect of size on tension - perpendicular-to-grain strength of Douglas fir. Wood and Fiber, 6(2):126-143.

11. Batschelet, E. 1965. Statistical Methods for the Analysis of Problems in Animal Orientation and Biological Rhythms. Am. Inst. of Bio. Sci., Monograph, 57 pp.

12. Bodig, J. and B. Jayne. 1982. Mechanics of Wood and Wood Composites, Van Nostrand Reinhold Co, 711 pp.

13. Boulay, B., B. Drowin, R. Gagnon, and P. Bernard. 1986. Paper fiber orientation measurement with a submillimeter laser. J. Pulp and Paper Sci. 12(1): 26-29.

14. Chow, Poo. 1988. Oriented strandboard made from six three year old hardwood species. 22nd Particleboard/ Composite Materials Symp., W.S.U., Pullman: 203-233.

15. Corte, H. and O.J. Kallmes. 1961. in F. Bolam, ed. Statistical Geometry of a Fibrous Network. Vol.I Tech. Sec. of the British Vapor and Board Assoc. pp. 13-52.

16. Danielson, R. and S. Steenberg. 1947. Quantitative determination of fiber orientation in paper. Svensk Papperstid. 50(13): 301-305.

17. Dawson, D.H. J.G. Isebrands, and J.C. Gordon. 1975. Growth, dry weight yields, and specific gravity of three year old populus grown under intensive culture. U.S.D.A. Forest Service Res. Paper NC-122, 7 pp.

18. Drake, P. 1982. Waferboard supply and demand balance in North America, Can. Waferboard Symp. SP508E Forintek: 78-81.

19. Easterling, K.E., R. Harrysson, L.J. Gibson, M.F. Ashby. 1982. On the mechanics of balsa and other woods. Proc. R. Soc. Lond. A383: 31-41.

20. Ebewele, E. and B. River. 1979. Tapered double cantilever beam fracture tests of phenolic wood adhesive joints. Wood and Fiber 11(3): 197-213.

21. Einspahr, D.W., M.K. Benson, and M.L. Harder. 1972. Influence of irrigation and fertilization on growth and wood properties of quaking aspen. Growth Acceleration Symposium. Proceedings. Section I, U.S.D.A., Madison. 11 pp.

22. Fitzgerald, R.W. 1967. Strength of Materials. Addison-Wesley. 418 pp.

23. Gatchell, C.J. and B.G. Heebink. 1964. The effect of particle geometry on properties of molded wood-resin blends. Forest Prod. J. 14(10): 501-506.

24. Geimer, R.L. 1986. Mechanical property ratios, a measure of flake alignment. U.S.D.A. Forest Service, Res. Paper. F.P.L. 468, 10 pp.

25. Geimer, R.L. 1979. Predicting flakeboard properties and improvements in bending properties by aligning a mixture of flakes. 13th Wash. State Univ. Particleboard Symp.: 59-75.

26. Geimer, R.L. 1976. Flake alignment as affected by machine variables and particle geometry. U.S.D.A. Forest Service, Res. Paper. F.P.L. No. 275, 16 pp.

27. Geimer, R.L., H.M. Montrey, and W.F. Lehmann. 1974. Effect of layer characteristics on the properties of three - layer particleboards. Forest Prod. J. 25(3): 19-29.

28. Go, T.A. 1988. New developments in waferboard/OSB resin technology. 22nd Wash. State Univ. Particleboard/Composite Materials Symp.: 123-133.

29. Go, T.A. 1982. Lignin binder system for the production of waferboard. Can. Waferboard Symp. SP508E. Forintek: 117-123.

30. Gollob, L. 1985. Relationship between chemical characteristics of P.F. and adhesive performance. Forest Prod. J. 35(3): 42-48.

31. Gunn, J.M. 1963. Wafer dimension control. Forest Prod. J. 13(4): 163-167.

32. Harless, T.E.G. F. Wager, P. Short, R. Seale, P. Mitchell, and D. Ladd. 1987. A model to predict the density profile of particleboard. Wood and Fiber Sci. 19(1): 81-92.

33. Harris, R.A. and J. Johnson, 1982. Characterization of flake orientation in flakeboard by the von Mises probability distribution function. Wood and Fiber 14(4): 254-266.

34. Harris, R.A. 1977. Measuring Particle Alignment in Particleboard and Predicting Selected Mechanical Properties of Oriented Boards. PhD. Thesis, Virginia Polytechnic Inst. 74 pp.

35. Hicks, C.R. 1982. Fundamental Concept in the Design of Experiments, 3rd Edition. C.B.S. College Pub. 422 pp.

36. Hse, C.Y. 1975. Properties of flakeboards from hardwoods growing on southern pine sites. Forest Prod. J. 25(3): 48-56.

37. Hse, C.Y. 1975. Formulation of an economical fast cure P.F. resin for exterior hardwood flakeboard. Proc. 9th Wash. St. Univ. Particleboard Symp. 5 pp.

38. Hse, C.Y. P. Koch, C. McMillin, and E.W. Price 1975. Laboratory scale development of a structural exterior flakeboard from hardwoods growing on southern pine sites. Forest Prod. J. 25(4): 42-50.

39. Jessome A.P. 1961. Strength and related properties of woods grown in Canada. Eastern F.P.L., Forestry Tech. Rpt. 21. 37 pp.

40. Jozsa, L.A., J.E. Richards, and S.G. Johnson. 1987. Calibration of Forintek's direct reading densitometer. Rpt.I C.F.S. No.36a. 27 pp.

41. Kaminski, B.E. and T. Lantz. 1969. Strength theories of failure for anisotropic materials. Composite Materials Testing and Design. ASTM, STP 460: 160-169.

42. Kasper, J. and S. Chow. 1980. Determination of resin distribution in flakeboard using x-ray spectrometry. Forest Prod. J. 30(7): 37-40.

43. Keller, H.A. and R.J. Saunders. 1975. Orienter for wood strands. U.S. patent 3,896,536.

44. Kelly, M. 1977. Critical literature review of relationships between processing parameters and physical properties of particleboard. Forest Prod. Lab. Gen. Tech. Rpt. F.P.L. - 10, U.S.D.A., Madison. 64 pp.

45. Kieser, J. and E.F. Steck. 1978. The influence of flake orientation on MOR and MOE of strandboards. 12th Wash. State Univ. Particleboard Sym.: 99-122.

46. Kim, K.Y. 1986. A note on the Hankinson formula. Wood and Fiber Science 18(2) 345-348.

47. Klauditz, W.K. 1960. Manufacture and properties of wood chip materials with directed strength. Holz Roh Werkstoff 18(10): 377-385.

48. Lau, P.W.C. 1981. Numerical approach to predict the modulus of elasticity of oriented waferboard. Wood Sc. 14(2): 73-85.

49. Laufenberg, T.L. 1986. Using gamma radiation to measure density gradients in reconstructed wood products. Forest. Prod. J. 36(1): 59-62.

50. Laufenberg, T.L. 1984. Flakeboard fracture surface observations and correlation with orthotropic failure criteria. J. of Wood Sc. 10(2):57-65.

51. Law, K.N. and Z. Koran. 1979. Microtensile strength of white spruce wood - A new approach. Wood Sc. 11(4): 221-226.

52. Law, K.N., J.J. Garceau and Z. Koran. 1977. Measurement of intra-increment tensile strength using a zero-span technique. Wood Sci. 10(1): 42-48.

53. Lehman, W.F. 1965. Improved particleboard through better resin efficiency. Forest Prod. J. 15(4): 155-161.

54. Lei, Y. and J. Wilson. 1981. A model for predicting fracture toughness of flakeboard. Wood Sc., 13(3): 151-156.

55. Lyon, D. 1988. Structural wood composites, new technologies for expanding markets. F.P.R.S. Conference Proceedings, Memphis. 14pp.

56. Maloney, T.M. 1985. Utilization of lodgepole pine forest and forest products residuals for composition board. Lodgepole Pine Symposium, Proceedings, Wash. State Univ., May 8-11.

57. Maloney, T. and E. Huffaker. 1984. Fundamentals and analysis of a short retention time blender. Proc. of 18th Wash. St. Univ. Particleboard Symp.: 310-343.

58. Mardia, K.V. 1972. Statistics of Directional Data. Academic Press. 357 pp.

59. McIntosh, J.A. and M. Carroll. 1979. Utilization of western Canadian hardwoods. Proc. of Forintek Canada Symp. SP-2. Prince George B.C. 1979.

60. Meinecke, E. and W. Klauditz. 1962. Physics and technology of glue application and mutual bonding of wood particles in the manufacture of particleboards. Inst. Wood Res. Forschungeber Landes Nordheim-Westfalen Rpt. 1052, Koln and Opladen, W. Germany. Transl. from U.S. Dept. of Commerce. 81 pp.

61. Musial, M.W. 1988. A nondestructive method for determining the degree of flake orientation in OSB. Wood Sci. and Technology 22(4): 371-378.

62. Nadeau, J., R. Bennett, and E. Fuller. 1982. An explanation for the rate of loading and the duration of load effects in wood in terms of fracture mechanics. J. Materials Sci. 17: 2831-2840.

63. Nalimov V. 1963. The Application of Mathematical Statistics to Chemical Analysis. ed. M. Williams. Oxford Permagon. 251 pp.

64. Niskanen, K.J. and J.W. Sadowski. 1987. Critical evaluation of some methods used to determine fiber orientation in paper. TAPPI. International Paper Physics Conference, 5 pp.

65. Norris, C.B. 1950. Strength of orthotopic materials subjected to combined stresses. U.S.D.A., Forest Prod. Lab. Rpt. No.1816. 35 pp.

66. Olson, J.R. and D.G. Arganbright. 1981. Prediction of mass attenuation coefficients of wood. Wood Sc. 14(2): 86-90.

67. Pellicane, P. J. Bodig, and J.R. Goodman. 1982. Simulation of the tensile strength-fracture toughness relationship. Wood Sc. 14 (4):168.

68. Perkins, R.W., R.E. Mark, J. Silvy, H. Anderson, and A.R.K. Eusutzai 1983. Effects of fiber orientation distribution on the mechanical properties of paper. TAPPI. International Paper Physics Conference, 5 pp.

68. Perkins, R. 1967. Mechanics of wood deformation: strength and plastic behavior. Forest Prod. J. 17(4): 57-62.

70. Porter, A.W. 1964. On the mechanics of fracture in wood. Forest Prod. J. 14(8): 325-331.

71. Post, P.W. 1961. Mechanical and dimensional properties of flakeboard. Forest Prod. J. 11(1): 34-37.

72. Price, E.W. 1974. Analysis of Southern Hardwoods As Furnish For A Wood Flake-Resin Composite Structural Material. Ph.D. Thesis Univ. of Illinois Urbana Champaign. 149 pp.

73. Pronin, D. and C. Vaughan. 1968. A literature survey of populus species with emphasis on P. tremuloides. Forest Prod. Lab. Rpt. No.0180, Madison. 65 pp.

74. Rautakorpi, H. 1971. An analysis of constructional plywood. The State Institute For Technical Res., Julkaisu Finland Publication. 165 64 pp.

75. Samson, M. 1984. Measuring general slope of grain with the slope of grain indicator. Forest Prod. J. 34(7): 27-32.

76. Schniewind, A.P. and T. Ohgama, T. Hoki, T. Yamada. 1982. The effect of specific gravity, moisture content and temperature on fracture toughness of wood. Wood Sc. 15(2): 101-109.

77. Schuler, A.T. 1982. Resource potential for waferboard production in Canada. Canadian Waferboard Symp. Forintek. SP508E: 179-185.

78. Scop, P. and A. Argon, 1967. Statistical theory of laminated composites. J. Composite Materials (1): 92-99.

79. Simpson, W. 1977. Model for tensile strength of oriented flakeboard. Wood Sci. 10(2): 68-71.

80. Singh, T. 1987. Wood density variation in thirteen Canadian tree species. Wood and Fiber Sc. 19(4): 362-369.

81. Stamm, A.J. 1964. Wood and Cellulose Science, Ronald Press, New York. 549 pp.

82. Stegmann, G. and J. Durst. 1965. Particleboard from beech wood. Holz-Zentrabl. 90(153): 313-318.

83. Steiner, P.R. L.A. Jozsa, M.L. Parker, and S. Chow. 1978. Application of x-ray densitometry to determine density profile in waferboard. Wood Sc. 11(1): 48-55.

84. Steiner, P.R., S. Chow and D. Nguyen. 1978. Improving mill wafer properties by x-ray densitometer evaluation methods. Forest Prod. J. 28(12): 33-34.

85. Stephans, R.S. and N. Kutscha. 1987. Effect of resin molecular weight on bonding flakeboard. Wood and Fiber Sc. 19(4): 353-361.

86. Stevans R.R. 1978. Slicing apparatus aids in the determination of larger-density of particleboard. Forest Prod. J. 28(9): 51-55.

87. Strickler, M.D. 1959. Properties of Douglas-fir flakeboard. Forest Prod. J. 9(7): 203-215.

88. Suchsland, O. 1960. An analysis of the particleboard process. Michigan Quarterly Bulletin, Dept. of Forest Products, Article 42-31, 42(2): 370-371

89. Suchsland, O. 1959. The strength of glue joints in wood obtained with minimum glue spread. Quarterly Bulletin, Mech. Agric. Expt. Sta., Mich. State Univ. 41(3) p. 577.

90. Talbot, J.W. and E.K. Stefanakos 1972. Aligning forces on wood particles in an electric field. Wood and Fiber, 4(3): 193-203.

91. Tsai, S. 1968. Strength Theories of Filamentary Structures, presented In: Fundamental Aspects of Fiber Reinforced Plastic Composites, ed. R.T. Schwartz. Wiley Interscience N.Y.

92. Turner, H.D. 1954. Effect of particle size and shape of strength and dimensional stability of resin bonded wood particle panels. Forest Prod. J. 4(5): 218-233.

93. Wellwood, R.W. 1962. Tensile testing of small wood samples. Pulp and Paper Mag. Canada Feb., T61-T67.

94. Wilson, J.B. 1984. Durability as affected by resin type. Southern Forest Experiment Sta., U.S.D.A., Technical Rpt. 50-53: 53-57.

95. Wilson, J.W. 1967. Some points of organization within growth zones of coniferous woods. Faculty of Forestry publication, Univ. of B.C., Vancouver. 15pp.

96. Winistorfer, P.M. W.C. Davis, and W. Moscher. 1986. A direct scanning densitometer to measure density profiles in wood composite products. Forest Prod. J. 36 (11/12): 82-86.

97. Woodson, G.E. 1976. Properties of Fiberboard from Southern Hardwoods. PhD. Thesis, Colorado State Univ. 126pp.

98. Yurgartis, S.W. 1987. Measurement of small angle fiber misalignments in continuous fiber composites. Composites Science and Technology 4(30) 279-293.

Appendix i

STRENGTH

```
LIST
2 PRINT"                    CONTINUOUS STRAND NETWORK MODEL"
4 REM     Inputs are strand specific L and T strengths,yielding output as
          composite specific strength    OR    strand L and T strengths which have
          been adjusted to the strength equivalent of the composite surface ,
5 REM     this option yields the flexural M.O.R. estimate.
6  DIM X(200) :DIM RG(200) : DIM XP(200)
7 INPUT"longitudinal str. L";L: INPUT"transverse str. T";T:INPUT"orientation par
ameter,k";K
8 PRINT "longitudinal str. L=";L,"transverse str. T=";T,"orientation k=";K :PRIN
T" "
9 Q=K/3.75:I=0:OPEN "AL.PRN" FOR OUTPUT AS #1
10 OPEN "GAL.PRN" FOR OUTPUT AS #2
11 REM I=Bessel function
12 IF K<=3.75,THEN I=1+3.51562*Q*Q+3.08994*(Q^4)+1.20674*(Q^6):GOTO 20
15 Q=1/Q :I=0 :F1=0
16 I=(EXP (K)/SQR(K))*(.39894+(.01329*Q)+.00225*(Q*Q)-.00158*(Q*Q*Q))
18 I=I+(EXP (K)/SQR(K))*(.00916*(Q^4)-.02058*(Q^5)+.02635*(Q^6)-.01647*(Q^7))
20 W=1/(3.14159265#*I)
22 PRINT"angle deg.  von Mises p.d.f."
25 FOR N=0 TO 20:M=(1.570796327#/20)*N
99 REM Simpsons Rule integration
100 D=0:E=3.14159265#:F=50
120 B=(E-D)/2/F
130 A=0:X=D:GOSUB 500
140 A=Y+A:X=X+B:GOSUB 500
150 A=Y*4+A:X=X+B:GOSUB 500
160 A=Y+A:F=F-1
170 IF F<>0 GOTO 140
180 C=A*B/3
182 C=W*C
185 IF N=0,THEN GOSUB 600
188 M=M*57.29577951#
190 PRINT C,M:WRITE #1,AL,C,M
198 NEXT N
500 G=(EXP(K*COS(2*(X-M)))):RG=G*W
501 IF N=0,THEN  X(F1)=X:RG(F1)=RG:F1=F1+1
502 Z=SIN(X)
505 H=L/(1+(L/T-1)*Z*Z)
508 Y=G*H
510 RETURN
600 M1=50
610 FOR NX=0 TO M1
620 XP(NX)=(X(NX)-1.5707963#)*90/1.5707963#   :NG=M1-NX
630 PRINT XP(NX),RG(NG):WRITE #2,GAL,XP(NX),RG(NG)
640 NEXT NX
650 M1=50
660 FOR NX=0 TO M1
670 XP(NX)=X(NX)*90/1.5707963#
680 PRINT XP(NX),RG(NX):WRITE #2,GAL,XP(NX),RG(NX)
690 NEXT NX
691 PRINT" " :PRINT"     model          load":PRINT"composite str.  angle deg."
700 RETURN
701 REM This program files the p.d.f. output as C:\DOS\GAL.PRN and strength
          output as C:\DOS\AL.PRN for file import to LOTUS or other graphics.
0
```

Appendix ii

ELASTICITY

```
LIST
1   PRINT"FLEXURAL ELASTICITY OF WOOD STRAND NETWORK:PARABOLIC DENSITY GRADIENT"
2  PRINT"The von Mises p.d.f. concentration parameter,k, characterizes the
        orientation"
3 DIM X(200):DIM RG(200):DIM XP(200):DIM C(30):DIM M(30)
4 PRINT"Inputs are elastic constants for an uncompressed strand layer,units in
MPa.":PRINT     "Strands assumed transversely  isotropic in the cross grain dire
ction"
5 INPUT"parallel grain MOE";EPA:INPUT"transverse grain MOE";EPE:INPUT "parallel
shear modulus";S:INPUT"parallel grain poissons ratio";P
6 PRINT"  parallel grain MOE.";EPA,"transverse grain MOE.";EPE,"  parallel shear
 modulus";S,"parallel-transverse poissons ";P
7  INPUT"strand orientation k parameter";K
8 PRINT "strand population orientation parameter,k";K
9 Q=K/3.75:I=0:OPEN "AL.PRN" FOR OUTPUT AS #1
10 OPEN "GAL.PRN" FOR OUTPUT AS #2
12 IF K<=3.75,THEN I=1+3.51562*Q*Q+3.08994*(Q^4)+1.20674*(Q^6):GOTO 20
15 Q=1/Q :I=0 :F1=0
16 I=(EXP (K)/SQR(K))*(.39894+(.01329*Q)+.00225*(Q*Q)-.00158*(Q*Q*Q))
18 I=I+(EXP (K)/SQR(K))*(.00916*(Q^4)-.02058*(Q^5)+.02635*(Q^6)-.01647*(Q^7))
20 W=1/(3.14159265#*I)
21 PRINT"Composite E ,without correction for the parabolic density gradient
        is output at 4.5 degree intervals of loading angle."
25 FOR N=0 TO 20:M=(1.570796327#/20)*N
100 D=0:E=3.14159265#:F=10
120 B=(E-D)/2/F
130 A=0:X=D:GOSUB 500
140 A=Y+A:X=X+B:GOSUB 500
150 A=Y*4+A:X=X+B:GOSUB 500
160 A=Y+A:F=F-1
170 IF F<>0 GOTO 140
180 C=A*B/3
182 C=W*C:C(N)=C
188 M=M*57.29577951# :M(N)=M
190 PRINT N,C,M
198 NEXT N
200 GOTO 705
500 G=(EXP(K*COS(2*(X-M)))):RG=G*W
501 REM  To view pdf,type line 501 if n=0,then print x ,rg
502 Z=(SIN(X))*(SIN(X)): ZZ=(COS(X))*(COS(X))
505 H=1/((ZZ*ZZ/EPA)+(Z*Z/EPE)+((1/S)-(2*P/EPA))*Z*ZZ)
508 Y=G*H
510 RETURN
705 INPUT"centre density,g/cm3";DC
707 INPUT"uncompressed strand density,g/cm3";DS:INPUT"total composite thickness,
mm";TB
710 INPUT"nearest odd number of gradient strands in total thickness";NL
712 PRINT "uncompressed strand density g/cm3";DS,"total composite thickness,mm";
TB
713 PRINT "nearest even number of strands in total thickness";NL+1  :TH=TB/(NL+1
)
```

```
714 DIM L(100):DIM DF(100):DIM EII(30):DIM EFF(30):DIM Y(100)
715 PRINT "average thickness of strands,mm";TH
716 INPUT "shape constant (focus) of parabolic density gradient";CF
717 REM As CF increases from just above the value of the centre density,it
      yields decreasing E and decreasing average density in the composite.
718 NL2=NL/2:SU=0
720 FOR L= 0 TO NL
725 Y(L)=((NL2-L)^2)/50/CF+DC:PRINT"pressed strand density was"; Y(L):DF(L)=Y(L)
/DS:SU=SU+Y(L):WRITE #2,L,Y(L)
732 PRINT "for lamina number,";L,"with packing densification factor";DF(L)
735 NEXT L
736 PRINT" ": PRINT"centre density,g/cm3";DC
737 PRINT"surface density,g/cm3";Y(0)
738 AD=SU/(NL+1):PRINT"average density,g/cm3";AD:PRINT" "
739 PRINT"Load Angle  Eff.Flex.E,MPa
740 FOR N2=0 TO 20
745 FOR L=0 TO  NL
746 REM Parallel axis theorem,with elasticity weighted for density(df(1)*c(n2))
747 EII=EII+DF(L)*C(N2)*((((NL+1-L)*TH)^3)-((NL-L)*TH)^3)/12
750 NEXT L
755 EII(N2)=EII
760 IA=((TB)^3)/12
765 EFF(N2)=EII(N2)/IA
770 PRINT M(N2),EFF(N2):WRITE #1,M(N2),EFF(N2)
772 EII=0
775 NEXT N2
780 END
```

Appendix iii

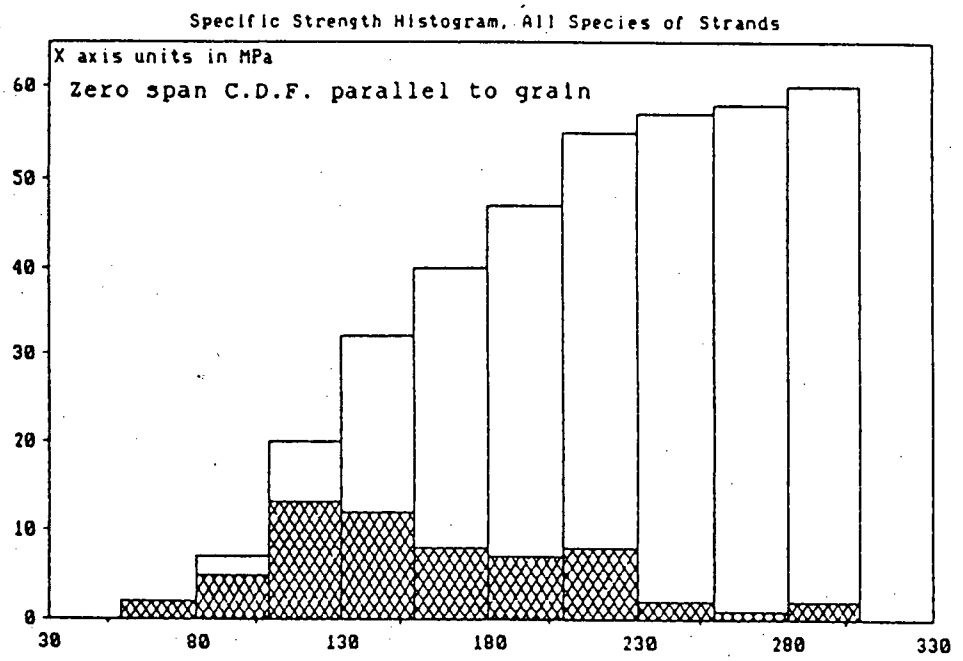

Mean = 160.54 Variance = 2647
Standard Deviation = 51.45 Skewness = .5314

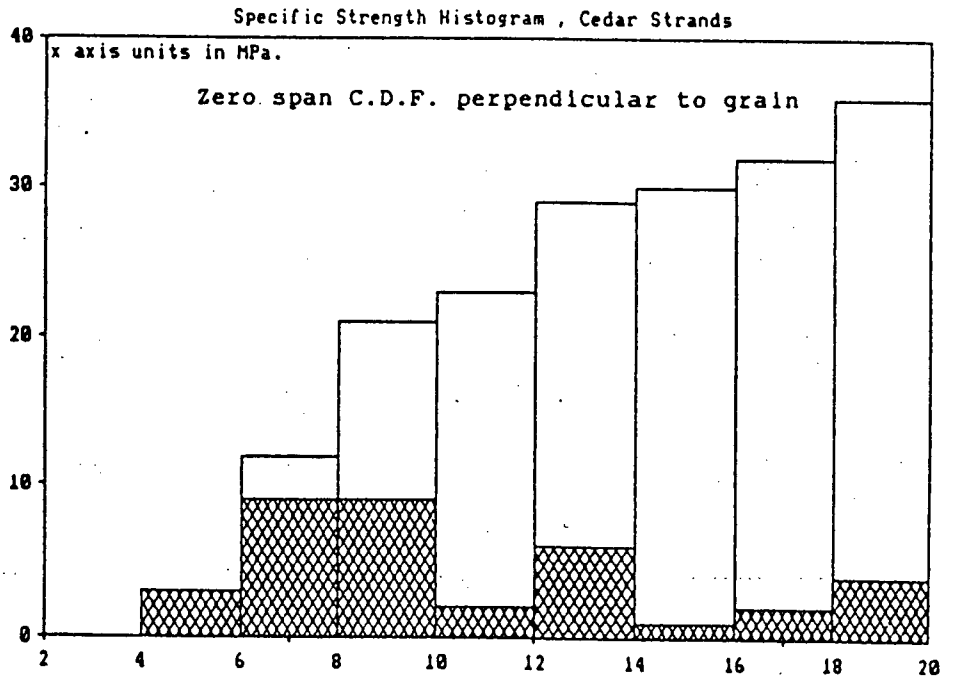

Mean = 10.795 Variance = 20.56
Standard Deviation = 4.534 Skewness = .6362

Appendix iv

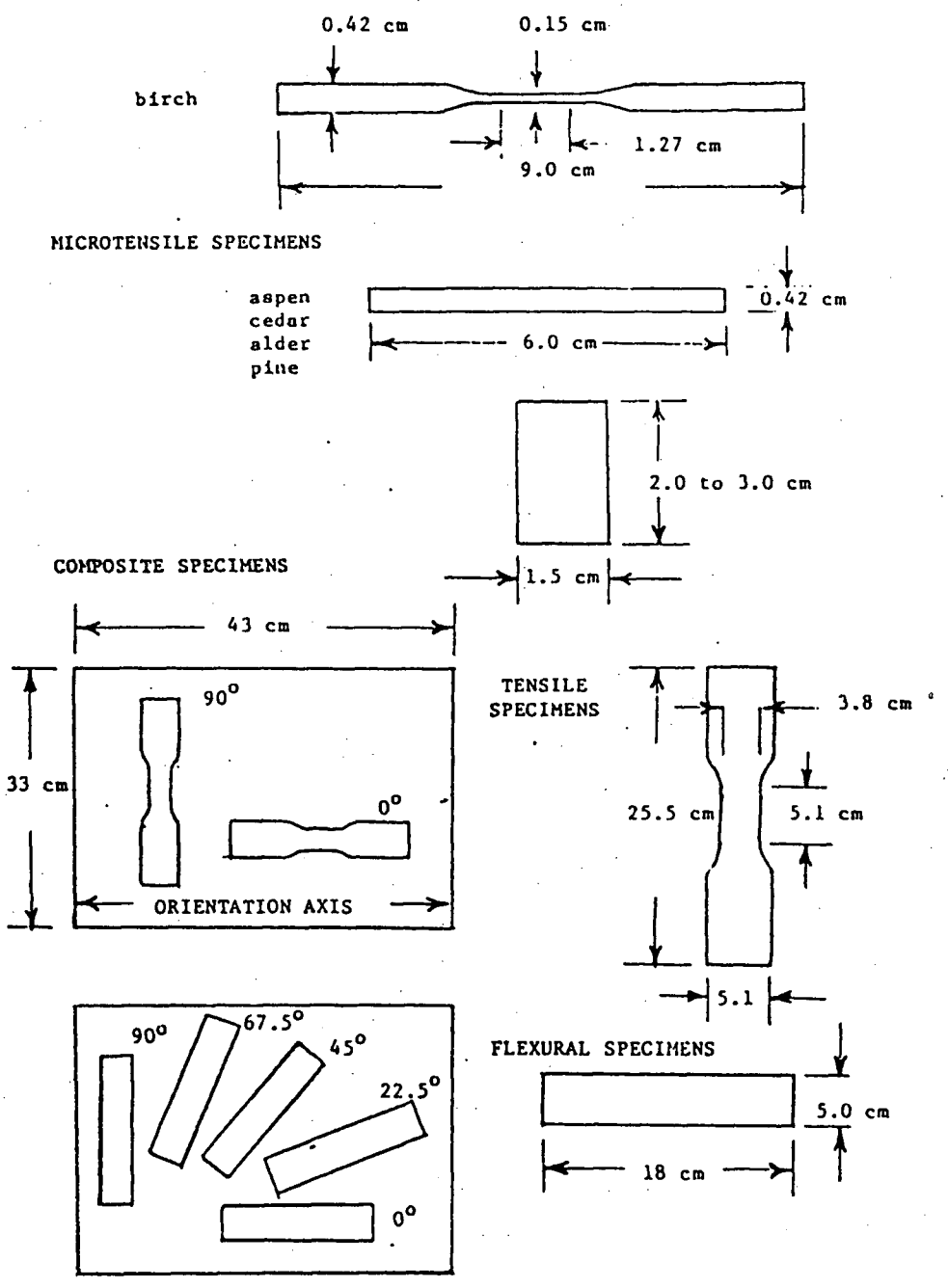
0.42 cm
0.15 cm
birch
1.27 cm
9.0 cm
MICROTENSILE SPECIMENS
aspen
cedar
alder
pine
0.42 cm
6.0 cm
2.0 to 3.0 cm
1.5 cm
COMPOSITE SPECIMENS
43 cm
33 cm
90°
0°
ORIENTATION AXIS
TENSILE
SPECIMENS
3.8 cm
25.5 cm
5.1 cm
5.1
90°
67.5°
45°
22.5°
0°
FLEXURAL SPECIMENS
5.0 cm
18 cm